ABSTRACT PROCEEDINGS

from the

ASPET
Transforming Discoveries Into Therapies

aD₂C academic **DRUGDISCOVERY** consortium

3rd ADDC/ASPET Academic Drug Discovery Colloquium

Introducing the Next Generation of Drug Hunters

May 19 - 20, 2024
Hyatt Regency Crystal City, Arlington, VA

3rd ADDC/ASPET ACADEMIC DRUG DISCOVERY COLLOQUIUM
Poster Index

Poster Presentations - Sunday, May 19, 2024, 5:15 pm - 7:15 pm

	BOARD	Company Name
SPONSORED POSTERS	A	**Agilent Technologies**
	B	**Cube Biotech Inc.**
	C	**Life Chemicals Inc.**
	D	**Promega**
	E	**Schrödinger**

Scientific Peer Reviewed Posters

Board #	Author First Name	Author Last Name	Author Affiliation	Abstract Title
800	Rola	Abdallah	American University of Beirut	Anti-cancer and Anti-inflammatory Properties of *Ziziphus Nummularia* Ethanolic Extract in Triple Negative Human Breast Cancer Cells MDA-MB-231
801	Mai	Abouzeid	Al Azhar Univ	Poly (ADP) Ribose Polymerase (PARP)-1 as a novel therapeutic target for alleviating the manifestations of Atopic Dermatitis
802	Tauseef	Ahmad	University of Tasmania	Fucoidan extracts from *Undaria pinnatifida (UPF)* and *Fucus vesiculosus* (FVF) mitigate DSS-induced acute colitis in Mice: A Preclinical Investigation
803	Niousha	Ahmari	Cincinnati Children's Hospital	C5aR-antagonism alone or in combination with MEK inhibition durably alters the plexiform neurofibroma tumor micro-environment
804	Oluwatobi	Akinsanya	Rosalind Franklin Univ	IER3 Paucity Inhibits oxLDL-induced Foam Cell Formation in ApoE-deficient macrophages via Promoting an Alternative Phenotype
805	S M Sabbir	Alam	Borch Department of Medicinal Chemistry and Molecular Pharmacology, Purdue University, IN, USA	Dynamic fluorescent cyclic AMP biosensors (cAADis) to study recombinant and endogenous adenylyl cyclase 1 (AC1) signaling in HEK 3/6KO and SH-SY5Y cellular models
806	Laxminarayan	Bhat	Reviva Pharmaceuticals, Inc.	Brilaroxazine Displays Limited Interaction with Clinically Relevant Drug Transporters
807	Laxminarayan	Bhat	Reviva Pharmaceuticals, Inc.	Absorption, Metabolism, and Excretion of Brilaroxazine in Rats
808	Abigail	Brewer	Univ of Minnesota	cFOS expression following rimonabant precipitated withdrawal from WIN 55212-2 in the rat brain
809	Lauren	Bystrom	University of Miami	Inhibition of Parabrachial CGRP Neurons Reduces Morphine Reinforcement and Withdrawal
810	Karina	Cantu	University of Texas HSC at San Antonio	Identifying Berberine's Mechanism of Action to Enhance Social Behavior
811	Ting-chao	Chou	PD Science LLC	MAL-PD Theory/Algorithm Guided Clinical Protocol Design for Computerized Data Analysis and Digital Conclusions in Drug Evaluations for Single Drugs and Combinations
812	Tim	Chow	Sanofi, Cambridge, Massachusetts, USA	Population Pharmacokinetic/Pharmacodynamic Modeling and Simulation of a Flat Quarterly Riliprubart Dosing Regimen for Patients With Cold Agglutinin Disease
813	Benjamin	Clements	University of Michigan	Enhancement of Opioid Analgesia by Positive Allosteric Modulation of the µ-Opioid Receptor in a Rat Model of Chronic Neuropathic Pain
814	Kristan	Cleveland	University of Washington	Beta2-Adrenergic receptor agonism as a therapeutic strategy for the treatment of Cushing's syndrome
815	Sydney	Cobb	University of Virginia	Design, Synthesis, and Biological Evaluation of Substituted Hydroxyquinolinone Compounds as 20S Proteasome Enhancers
816	Daniel	Colombani-Garay	University of Virginia	Development of *N*-acyl Fluspirilene 20S Proteasome Enhancers for the Treatment of Neurodegenerative Diseases
817	James	Cornwell	Queen's University	Interaction between hERG and the Fc Domain of IgG Leads to the Phosphorylation of a C-terminal ITIM by Src which Induces Chronic Channel Internalization
818	Joseph	Cronin	University of California, Davis	Efficacy of Biologic let-7-5p Isoforms in the Modulation of Target Gene Expression in HCC Cells
819	Ivana	Daniels	Indiana Univ School of Medicine	A Treatment to Eliminate Respiratory Viral Infections Associated with Asthma Exacerbations
820	Sayantap	Datta	University of Houston	Contribution of High Mobility Group Box 1 to Nicotine-Induced Podocyte Injury and Glomerular Sclerosis
821	William	Davis	Johns Hopkins School of Medicine	Associations Between Proinflammatory Cytokines, Laboratory-evoked Pain, and Opioid Response Profiles in Healthy Human Subjects

Board #	Author First Name	Author Last Name	Author Affiliation	Abstract Title
822	Francesco	De Pascali	Thomas Jefferson University	Diverse pathways in GPCR-mediated activation of Ca2+ mobilization in HEK293 cells
823	Roxane	Domain	CEPR	Activation of neutrophil elastase-related serine proteases in myelomonocytic cells
824	Lin	Du	National Cancer Institute	Structure-Based Design and Synthesis of Potent and Selective Serine/threonine Kinase Inhibitors from a Marine Natural Product Pharmacophore
825	Tiffany	Dwyer	Purdue University	Targeting Adenylyl Cyclase 1 for Development of Non-Opioid Pain Therapeutics
826	Lee	Eiden	NIMH, NIH	PACAP(6-38) Deletants as Peptide-based PACAP Antagonists
827	Inga	Erickson	University of Washington	Intestinal Dysbiosis Alters Seizure Burden and Antiseizure Medicine Activity Profile in the Theiler's Virus Model of Acute Encephalitis
828	Maaike	Everts	Critical Path Institute	C-Path's Translational Therapeutics Accelerator: A Unique Solution to Successfully Bridge the Valley of Death in Academic Drug Discovery and Development
829	Amanda	Fakira	Cooper Medical School of Rowan Univ	The neuropeptide receptor GPR83 regulates anxiety-like behavior
830	Daniel	Foster	University of South Carolina School of Medicine	Pharmacological potentiation of M4 muscarinic acetylcholine receptors suppresses excessive grooming in SAPAP3 knockout mice
831	Pradip	Gadekar	Northeastern University	Optimizing positive allosteric modulators to selectively target the high sensitivity (α4)2(β2)3 nicotinic acetylcholine receptor
832	Khalid	Garman	National Institute of Arthritis and Musculoskeletal and Skin Diseases	CDK Inhibition Impairs RNA Splicing: A Novel Therapeutic Approach for Merkel Cell Carcinoma
833	Samaneh	Goorani	University of Arkansas for Medical Sciences	Novel compounds that target epoxyeicosanoids protect rat kidney epithelial cells in organ transplant solution during cold storage
834	Adithya	Gopinath	University of Florida	Neuroimmune Circuitry of Midbrain Dopamine Neurons
835	Said	Goueli	University of Wisconsin and Promega Corp	Monitoring G-Protein Coupled Receptors using a Bioluminescent, Homogenous, and High Throughput Formatted Assay for cAMP, cGMP, and IP3
836	Yanjing	He	Shenzhen Baoan Shiyan People's Hospital	The H2S-releasing donor N-acetylcysteine may attenuate myocardial ischemia reperfusion induced acute lung injury via upregulating pulmonary Neuregulin-1
837	Eric	Hoffman	Binghamton Univ - State University of New York	THE VENTURE PHILANTHROPY MODEL OF DRUG DEVELOPMENT - WORKING WITH NON-PROFIT FOUNDATIONS AND GOVERNMENTS FROM CONCEPT TO DRUG APPROVAL
838	Kimberly	Holter	Wake Forest University School of Medicine	EEG studies reveal estradiol-dependent differences in GluN2A-containing NMDAR function
839	Kylie	Hornaday	University of Calgary	G-protein coupled receptors expressed in human uterine tissues: Novel targets for labour management
840	Jingzhu	Huang		Effects of total flavone of Litchi Semen on the hepatocellular carcinoma cell proliferation and apoptosis
841	Michael	Ippolito	Temple University	GPR55 Antagonist KLS-13019 Prevents and Reverses Chemotherapy-Induced Peripheral Neuropathy (CIPN) in Rats
842	Kenneth	Jacobson*	NIDDK/NIH	2-Substituted (N)-Methanocarba A3 Adenosine Receptor Agonists: In silico, in vitro and in vivo Characterization
843	Anel	Jaramillo	University of Kentucky	The Parabrachial Nucleus Modulates Anxiety in Alcohol Withdrawal and Abstinence Following Repeated Stress
844	Huiting	Jia	University of Pittsburgh, School of Pharmacy	Fatty Acid Metabolizing Cytochrome P450 4F11 as a Novel Drug Target for Lung Cancer Treatment
845	Nathan	Jones	Univ of Wisconsin-Madison	Psilocybin-induced anxiolytic effects supported by transient elevation of corticosterone.
846	Ram	Kandasamy	California State University, East Bay	Simultaneous Inhibition of Soluble Epoxide Hydrolase and Fatty Acid Amide Hydrolase Prevents Nitroglycerin-induced Hypersensitivity in Female Rats
847	Jack	Keady	University of Kentucky	Developmental Impacts of Adolescent Intermittent Nicotine Vapor Exposure on the Murine Hippocampus
848	Rhema	Khairnar	St. John's University	High Fructose - High-Fat Diet Accelerates Non-Alcoholic Fatty Liver Disease Possibly Mitigating Hepatic Nuclear Lipocalin Prostaglandin D2 Synthase
849	Kristopher	Knight	Aflac Cancer and Blood Disorders Center, Department of Pediatrics, School of Medicine, Emory	Utilizing Ancestral Sequence Reconstruction to Generate a Novel Recombinant Humanized L-Asparaginase with Enhanced Chemotherapeutic Properties
850	Harshita	Kondeti	Loyola Univ Chicago	TARGETED DRUG DELIVERY OF LEUKOMIMETIC NANOPARTICLES TO ALLEVIATE PERIPHERAL NEUROPATHY IN CHARCOT-MARIE-TOOTH 1X

Board #	Author First Name	Author Last Name	Author Affiliation	Abstract Title
851	Samuel	Krug	University of Maryland, Baltimore	Utilizing Orthogonal Mass Spectrometry Approaches to Understand Metallodrug Pharmacokinetic Parameters for *in vitro* Lead Compound Optimization
852	Siva Hariprasad	Kurma	National Institute of Diabetes and Digestive and Kidney Diseases, National Institutes of Health, USA	P2Y14 Receptor Antagonists: Heteroaromatic Piperidine Bioisosteres in 4-Phenyl-2-Naphthoic Acid and Aryl-Triazolyl-Biphenyl Series
853	Zhijun	Li	Saint Joseph's Univ	Developing 2-Aminothiophene Derivatives as Positive Allosteric Modulators of Glucagon-Like Peptide 1 Receptor
854	Mengchu	Li	University of Michigan	A New Class of Drug-like Negative Allosteric Modulators of Mu-Opioid Receptor
855	Vanessa	Lopez	University of Washington	Elucidating the Disposition and Metabolism of Benzalkonium Chloride compounds in C57BL/6 mice
856	Irwin	Lucki	Uniformed University of the Health Sciences	Reversal of Mechanical Hypersensitivity by 2R,6R-Hydroxynorketamine by Activation of Group 2 Metabotropic Glutamate Receptors
857	Frank	Mao	University of California, Davis	In Vivo Production of Novel RNA Molecules and Computational Modeling of Their 3D Structures
858	Vitoria	Mattos Pereira	University of Wyoming	Inhibition of the Cysteine Protease Cathepsin K Attenuates Diabetic Neuropathic Pain
859	David	McFall	Georgetown University	The Effect of Senolytic Therapy in a Mouse Model of Post-Traumatic Epilepsy
860	Eric	Miller	Emory University	Tetrahydroisoquinoline-Based Small Molecule Inhibitors of the Chemokine Receptor CXCR4
861	Catherine	Moore	West Center for Computational Chemistry and Drug Design, SJU, Philadelphia PA	Leveraging a Novel GPCR ITIM Motif that Drives Gradient Signaling for Targeted Antibody Design and Peptide Inhibitor Development
862	Amy	Moritz	Molecular Neuropharmacology Section, NINDS/NIH	Regulation of Dopamine Receptor Subtypes by G Protein-Coupled Receptor Kinase Isoforms
863	Ryan	Murphy	University of Texas Medical Branch	Extracellular Loop 2-Dependent Mechanism of Action for Orphan Receptor GPR52 Allosteric Agonists
864	Martin	Ng	NIH	Discovery of Natural Product ITPK1 Inhibitors using a Luciferase-Based High-Throughput Screen
865	Ashley	Nilson	Molecular Neuropharmacology Section, National Institute of Neurological Disorders and Stroke, NIH	Characterization of NCGC1360 and NCGC1366 as Highly-Selective D2 Dopamine Receptor Antagonists and Lead Candidates for the Treatment of Neuropsychiatric Disorders
866	Michael	Ofori	Dr. Hilla Limann Technical Univ	Betulin, a Compound Isolated from *Crinum asiaticum* Bulbs Exerted Anti-Silicosis and Pulmonoprotective Effects Through the Inhibition of NF-κB activation in Rat model
867	Frank	Ogundolie	Baze University, Abuja, Nigeria	Green Silver Nanoparticles Synthesized from *Moringa Oleifera* Stem Bark Elicits Effective Antidiabetic Effect in Alloxan-Induced (Type I) Diabetic Wistar Rats
868	Paola	Oliva	NIDDK/NIH	Structure-Activity Relationship of 5-Arylethynyl Derivatives of (2-Aminothiophen-3-yl)(phenyl)methanones as A1 Adenosine Receptor Positive Allosteric Modulators
869	Ogochukwu	Orabueze	Western University of Health Sciences	A Gαs and Gαi Chimera Alters cAMP Kinetics and Appears to Inhibit GRK Function
870	Karim	Pajazetovic	California Northstate University	A GPT4-based Patient Simulation to Enhance the Integration of Pharmacology with Clinical Decision Making in a PharmD Program
871	Hua	Pan	Washington Univ School of Medicine	NF-κB Inhibition Mitigates Colorectal Cancer Lung Metastasis
872	Yingxian	Pan	Rutgers New Jersey Medical School	Targeting Exon 7-associated 7TM C-Terminal Variants of the Mu Opioid Receptor Gene for Mitigating Adverse Effects of Mu Opioids Without Altering Analgesia in Pain Management
873	Amit	Pandey	Univ of Bern	Nanoencapsulation of Curcumin-Piperine Complex for Targeting CYP17A1 in Castration-Resistant Prostate Cancer
874	Eleni	Papadopoulos	Rowan-Virtua School of Translational Biomedical Engineering and Sciences	Low Dose Methylphenidate Modulates Risky Decision Making and Prefrontal Catecholamine Regulation in a Sex-Dependent Manner Following Repeated Mild Traumatic Brain Injury
875	Matteo	Pavan	NIDDK/NIH	Identification and characterization of extrahelical allosteric binding site for 1*H*-imidazo[4,5-c]quinolin-4-amine A3 adenosine receptor positive allosteric modulator
876	Stevan	Pecic	California State University, Fullerton	Multitarget-Directed Ligands with Soluble Epoxide Hydrolase and Fatty Acid Amide Hydrolase Inhibitory Activities for Treatment of Chronic Pain

Board #	Author First Name	Author Last Name	Author Affiliation	Abstract Title
877	Jingdan	Pei	Tulane University	The Effects of Taurine on Alcohol-Associated Liver Disease are Dose-Dependent Associated with Alterations of Taurine-Conjugated Bile Acids and FXR-FGF15 Signaling
878	Anh	Pham	Pennsylvania State Univ	Inhibitors of the Gram-negative cell envelope stress response as anti-infectives and antibiotics
879	Leah	Phan	University of Florida	Comparative Analysis of Dopamine Neuron Activity in Pavlovian Versus Non-Contingent Methamphetamine Exposure
880	Satyanarayana	Pondugula	Auburn University	The KRAS-G12C Inhibitor Sotorasib Induces Cancer Therapy Resistance by Activating Human Pregnane Xenobiotic Receptor
881	Kenneth	Jacobson	NIDDK/NIH	Lipid Trolling to Optimize A3 Adenosine Receptor Positive Allosteric Modulators (PAMs)
882	Mohammad Atiqur	Rahman	University of Houston	Membrane Raft Redox signalling pathway in Nicotine-Induced NLRP3 Inflammasome Activation and Podocyte Injury
883	Katelyn	Reeb	Drexel University College of Medicine	EAATs for stroke: to modulate or not to modulate
884	Genesis	Rodriguez	San Juan Bautista School of Medicine	Blockade of Brain Angiotensin II AT1 Receptor Ameliorates Inflammation, YKL-40, and ROS Production from Astrocytes
885	Suchismita	Roy	University of California, San Diego	Phosphorylation of Gαi shapes canonical Gα(i)βγ/GPCR signaling
886	Shubhra	Saha	National Institutes of Health	Activation of PTH1 receptor using chimeric peptide templated in situ click reaction of nanobody conjugates
887	Shatha	Salameh	Children's National Hospital	Preclinical model to assess the impact of myocardial maturity on drug responsiveness
888	Paul Victor	Santiago Raj	The University of Arizona	MARY1 Promotes Recovery from Acute Kidney Injury through Induction of Mitochondrial Biogenesis
889	Dana	Selley	Virginia Commonwealth University School of Medicine	Sphingosine-1-phosphate receptor 1 (S1PR1) modulators acutely reverse paclitaxel-induced neuropathic pain signs in mice without downregulating S1PR1 in the CNS
890	Sushrut	Shah	Thomas Jefferson University	Biased Allosteric Modulation of β2-adrenergic Receptor Signaling and Bronchodilation by different β-agonists
891	Jocelyn	Smith	Ohio Northern Univ	Novel RGS2-Gaq Interaction Inhibitors Show Anti-Cancer Activity
892	Hudson	Smith	The Univ of Texas Medical Branch	Discovery of agonists for orphan GPR52 using a ligand-based pharmacophore model and virtual screening
893	Kirsten	Snyder	NIH	Discovery, Characterization, and Optimization of a Novel Positive Allosteric Modulator-Antagonist of the D3 Dopamine Receptor
894	Mehonaz	Sultana	St. Johns Univ	Dissecting the novel anti-obesity mechanism of prostaglandin D2 via DP1 receptor agonism utilizing mouse 3T3-L1 adipocytes as well as primary human subcutaneous adipocytes
895	Alexis	Surtel	Molecular Neuropharmacology Section, NINDS/NIH	Neuroprotection in C. Elegans Parkinson's Disease Models: Discovering Therapeutic Insights via RNAi and Small Molecule High Throughput Screening.
896	Shwetal	Talele	University of California-Irvine	Impact of RGS10 on Microglial Cell Migration and Proliferation
897	Prerna	Tiwari	Creighton Univ	STRUCTURE ACTIVITY RELATIONSHIP (SAR) OF GJ079 COMPOUND TO DEVELOP NOVEL TREM-1 INHIBITORS IN THE MANAGEMENT OF GLOBAL-ISCHEMIA AND RELATED NEUROINFLAMMATION
898	Julia	Tobacyk	University of Arkansas for Medical Sciences	Deuterated Buprenorphine Mitigates Fentanyl Effects in Pregnant Rats.
899	Alicja	Urbaniak	University of Arkansas for Medical Sciences	Monensin and its derivatives increase MHC Class I and II presentations in breast cancer
900	Yue	Wen	University of Washington	Novel Mechanistic Physiologically Based Pharmacokinetic Model to Predict Renal Clearance and CYP2D6 Activity Across Pregnancy
901	Paul	Whiteaker	Virginia Commonwealth University	Analogs of α-conotoxin PnIC are selective for α7β2 over α7-only subtype nicotinic acetylcholine receptors
902	Mary	Wilkerson	Ohio Northern University	Pharmacologic Factors and Their Impact on Drug Elimination Half-Life
903	Molly	Woodson	Saint Louis Univ	Metabolism and clearance characterization of novel HBV RNase H inhibitors
904	Weiyi	Xia	Department of Health Technology and Informatics, The Hong Kong Polytechnic University	Enhancement of ANGPTL4 exacerbates post-ischemic myocardial ferroptosis and cellular injury in diabetic conditions via impairing AKT/AMPK signaling
905	Alexander	Zestos	American Univ	Chemical Analysis of Neuropeptide Y and Glutamate using Carbon Fiber Microelectrodes and Fast-Scan Cyclic Voltammetry
906	Huiliang	Zhang	University of Arkansas for Medical Sciences	SS-31 Attenuates Doxorubicin-induced Cardiomyoblast H9C2 Cell Senescence

* Poster to be presented by Dilip Tosh

800

Anti-cancer and Anti-inflammatory Properties of *Ziziphus Nummularia* Ethanolic Extract in Triple Negative Human Breast Cancer Cells MDA-MB-231

Rola Abdallah[1], Joelle Mesmar[1], Elias Baydoun[1]

American University of Beirut[1]

Breast cancer continues to be one of the most diagnosed cancers in women worldwide with triple-negative breast cancer (TNBC) that makes up approximately 15% to 20%. TNBC is challenging to treat because it does not respond to hormonal therapies and often develops resistance to chemotherapy. Natural products have long been utilized in traditional medicine as remedies to improve health and treat illnesses. Importantly, they have a key role in modern drug discovery. Recently, there has been an increasing interest in the search for bioactive agents from natural sources as alternative or complementary modalities to conventional treatments and synthetic medicines; especially for treatment of cancer which incidence and mortality rates have been on the rise worldwide. *Ziziphus nummularia*, a small bush belonging to the Rhamnaceae family, has been widely used in traditional medicine for the treatment of various diseases. Its traditional therapeutic uses may be attributed to its richness in bioactive compounds and the wealth of its pharmacological properties, including antioxidant, anti-inflammatory, anti-cancerous activities. However, its phytochemical composition or chemo-preventive effects against the aggressive TNBC are still poorly explored. In the present study, an ethanolic extract of leaves of *Z. nummularia* (ZNE) was prepared and chromatographically fractionated. ZNE reduced the viability of MDA-MB-231 cells, a TNBC cell line, with the ZNE Fraction 6 (F6) exhibiting the strongest activity. ZNE and F6 are rich in phytochemicals and HPLC-PDA-MS/MS analysis identified several compounds with F6 being particularly rich in Caffeoyl-benzene. Both ZNE and F6 showed potent antioxidant activities in the DPPH assay but promoted reactive oxygen species (ROS) production in MDA-MB-231 cells; an effect which was blunted by the antioxidant N-acetyl cysteine (NAC). NAC also blunted ZNE- and F6-induced reduction in TNBC cell viability. We also demonstrated that ZNE and F6 induced an arrest of the cell cycle at G1, and triggered apoptosis- and autophagy-mediated cell death. This was confirmed by the decrease in Ki67 and BCL-2 protein levels and the increase in P38, P21, P27, Rb, caspase 3, BAX and LC3B. ZNE and F6 inhibited metastasis-related cellular processes as well. Namely, ZNE- and F6- treated MDA-MB-231 cells had a reduced cell migration, invasion, and adhesion to collagen. This was supported by the decrease in MMP-9 and integrin β1 levels. In addition, ZNE and F6 also reduced the production of inducible nitric oxide synthase (iNOS) and inhibited in-ovo angiogenesis. It was also found that ZNE has potent anti-inflammatory properties by suppressing the LPS-stimulated inflammatory responses in RAW 264.7 macrophage cells. It significantly reduced the mRNA and protein expression of iNOS, cyclooxygenase-2 (COX-2) by targeting the NF-κB pathway. Taken together, our findings reveal that *Z. nummularia* is rich in phytochemicals that can attenuate the malignant phenotype of TNBC and may offer innovative avenues for the discovery of new drug leads for treatment of TNBC and other cancers.

801

Poly (ADP) Ribose Polymerase (PARP)-1 as a novel therapeutic target for alleviating the manifestations of Atopic Dermatitis

Mai Abouzeid[1], Mohamed A. Ghonim[1], Kusma Pyakurel[2], Jeffrey Wang[2], Hamid Boulares[2]

Al Azhar University[1] LSUHSC[2]

Background: Atopic dermatitis (AD) is a multifaceted and multifactorial chronic inflammatory skin disorder. Patients with AD have few treatment choices. Therefore, understanding the main molecular pathways involved in the development of the illness would improve the chances of developing effective

therapies to prevent or treat the disease. AD is driven by immune system abnormalities, including dysregulated Th2 responses and excessive synthesis of IgE. Mounting data indicates that the extracellular matrix (ECM) protein periostin has a significant function in AD. Our group has thoroughly investigated the involvement of PARP-1 in the development of several chronic inflammatory conditions, such as allergic asthma. We reported that PARP-1 inhibition, either by genetic means or with Olaparib, effectively protects against the development of AD. Such protection is achieved by preventing the generation of Th2 cytokines, IgE, and other associated components.

Objective: To assess whether PARP-1 inhibition by gene deletion or Olaparib would be effective in mitigating the progression of AD in both *n vitro* and the *in vivo* model of the diseases.

Method: Wild-type and PARP-1−/− mice were subjected to epicutaneous exposure to ovalbumin (OVA) three times per week for a duration of three weeks, with each week being followed by a two-week resting period. WT mice were administered Olparib at a dosage of 5mg/kg. Following the protocol's completion, the degree of dermatitis was assessed utilizing a clinical skin scoring (CSS) technique. The mice were euthanized, and skin biopsies were examined by IHC. Serum samples were obtained and analyzed for levels of OVA-specific IgE and cytokines. Cells obtained from the spleen were evaluated using flow cytometry. WT or PARP-1−/− skin fibroblasts were exposed to LPS or IL-13 for varying durations and subsequently analyzed using RT-PCR or immunoblot techniques.

Results: Utilizing the Eczema Area and Severity Index (EASI) clinical scoring system, we found that PARP-1 inhibition by gene deletion or pharmacologically by Olaparib effectively reduced the disease manifestations, including redness, thickness, itching, and lichenification. Such effects may be achieved by altering Th1/Th2 cytokine production. PARP-1 inhibition effectively reduced the production of Th2 cytokines (such as IL-4, IL-5, and GM-CSF) and allergen-specific IgE ewithout any effect on the production of the anti-inflammatory cytokine IL-10 or the Th1 cytokine, IFN-γ. These differential effects resulted in a statistically significant increase in the number of T-regulatory cells and a downregulation in the expression of periostin protein. These findings suggest that inhibiting PARP-1 might potentially affect the function of T cells to generate Th2 cytokines, as well as control the formation of extracellular matrix (ECM) proteins such as periostin.

Conclusion: Our findings provide evidence for the potential of PARP-1 inhibitors as a novel therapeutic approach and Olaparib as a likely candidate to be tested in human clinical trials for the treatment of Atopic Dermatitis.

802

Fucoidan extracts from *Undaria pinnatifida* (UPF) and *Fucus vesiculosus* (FVF) mitigate DSS-induced acute colitis in Mice: A Preclinical Investigation

Tauseef Ahmad[1], Muhammad Ishaq[2], Samual Karpiniec[3], Ahyoung Park[3], Corinna Dwan[3], Darren Henstridge[2], Vanni Caruso[2], Rajaraman Eri[4], Helen Fitton[5]

Univ of Tasmania[1] University of Tasmania[2] Marinova Biotech[3] RMIT University[4] RDadvisor, Hobart[5]

The escalating global prevalence of inflammatory bowel diseases (IBDs), comprising ulcerative colitis and Crohn's disease, poses a considerable burden on public health. Despite therapeutic advances, persistent inflammation and associated complications underscore the limitations of current medical approaches. Fucoidans, fucose-rich sulfated polysaccharides found in edible brown algae, exhibit promising anti-inflammatory properties. However, variations in bioactivities and efficacy among fucoidans from distinct seaweeds warrant comprehensive investigation.

Methods
This study systematically assessed the therapeutic potential of fucoidan extracts from Undaria pinnatifida

(UPF) and Fucus vesiculosus (FVF) in a murine model of Dextran Sulfate Sodium (DSS)-induced acute colitis. Daily monitoring of colitis severity, coupled with macroscopic evaluation of collected colons and spleens, provided a comprehensive understanding. Histological scrutiny, utilising Hematoxylin and Eosin (H&E staining), and quantification of cytokines via enzyme-linked immunosorbent assay (ELISA) were integral components of our rigorous methodology

Results

Oral administration of UPF and FVF over seven days significantly mitigated body weight loss, improved the Disease Activity Index (DAI), and reduced colon and spleen weight compared to their DSS-treated counterparts. DSS-induced mice exhibited notable histological abnormalities, including loss of crypt architecture, goblet cells, immune cell infiltration, and edema, all of which were effectively reversed by UPF and FVF supplementation. Importantly, the macroscopic improvements correlated with a substantial reduction in the production of 18 pro-inflammatory cytokines in distal colon (DC) tissues. The findings propose the potential of orally administered UPF and FVF as a nutraceutical alternative for IBD treatment
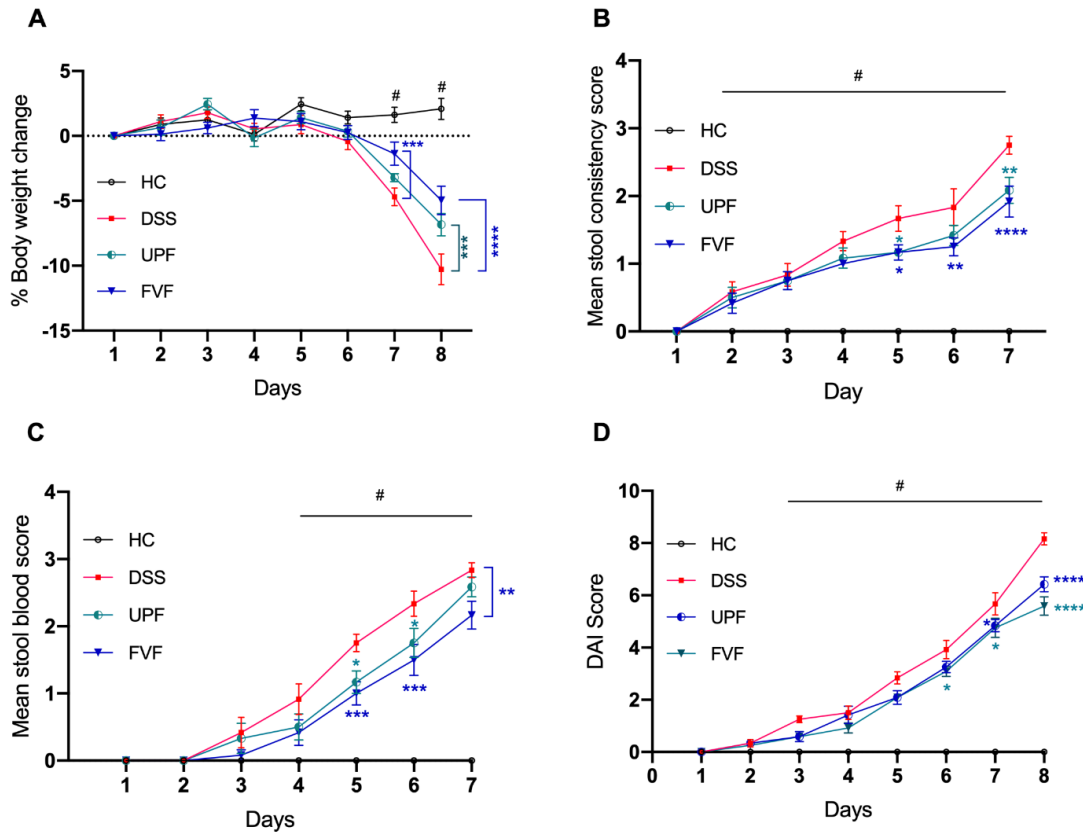
Figure 1. Effect of UPF and FVF on the pathology of acute colitis. (A) % body weight change in C57BL/6 mice between the groups receiving fucoidan treatment and without fucoidan treatment. Change in the body weight was calculated by dividing the body weight each day by the initial body weight before the start of the DSS treatment. (B) Stool samples were scored daily for stool consistency. (C) Stool samples were checked daily for occult blood. (D) Disease activity index (DAI) is a combined score of daily body weight change, stool consistency score, and occult blood score. Data are represented as the percentage or mean ± SEM (n = 12/group). Two-way ANOVA followed by Tukey's post-test was used to calculate the statistically significant values. # Significant effect HC vs DSS; *Significant effect treatment vs DSS (DSS vs UPF) or (DSS vs FVF). A p-value of <0.05 was considered significant. *p < 0.05, **p < 0.001, ***p < 0.0001 and ****p < 0.00001. Healthy control (HC), DSS treated (DSS), *Undaria Pinnatifida* fucoidan treated (UPF), and *Fucus vesiculosus* fucoidan treated (FVF).

803

C5aR-antagonism alone or in combination with MEK inhibition durably alters the plexiform neurofibroma tumor micro-environment

Niousha Ahmari[1], Melissa Perrino[2], Jay Pundavela[1], Sara Szabo[1], Trent Woodruff[3], Eva Dombi[4], Mi-Ok Kim[5], Jörg Köhl[6], Jianqiang Wu[1], Nancy Ratner[1]

Cincinnati Children's Hospital[1] St. Jude Children's Hospital[2] The University of Queensland[3] National Cancer Institute[4] University of California San Francisco[5] The Institute for Systemic Inflammation Research[6]

Mutations in the NF1 tumor suppressor gene, which encodes a negative regulator of RAS signaling cascades, predispose affected individuals to manifestations including development of benign nerve tumors (neurofibromas). The formation and growth of plexiform neurofibroma (PNF) tumors depend on the interplay between tumor cells and the surrounding tumor microenvironment (TME), which is marked by chronic inflammation, myeloid cell expansion, and remodeling of local and systemic immune compartments. Although inhibiting mitogen-activated protein kinase (MEK) signaling downstream of RAS shrinks most established plexiform neurofibromas (PNF), not all patients respond to MEK inhibition and even in those that do the response is not durable. Our aim in this study was to identify and test a druggable target to synergize with MEK inhibitor treatment to promote efficacy and durability of treatment. Using flow cytometry and single cell anlaysis of two murine models and histological examination of human tumors, we discovered an increase in the C5a-C5a receptor (C5aR) system in PNF as characterized by an increase in C5aR1 expressing macrophages, the predominant cell in PNF tumors, which is not normalized by MEK inhibition. Thus, to test the hypothesis that C5aR can synergize with MEK inhibition to modulate inflammatory responses in PNF we treated immunocompetent PNF-bearing Nf1f/f; DhhCre mice, a model which has historically demonstrated robust translational importance, for 60 days with either a MEK inhibitor, a C5aR1 inhibitor, or a combination of the two. We found that therapeutic reduction of C5aR1 activity induced cell death in tumor macrophages and enhanced the engulfment of dying Schwann cells by macrophages but did not affect neurofibroma number or size. Complete or partial genetic depletion of C5aR1 in Nf1f/f; DhhCre mice confirmed these results, suggesting stronger therapy would not increase efficacy of response.We next tested if the combination of MEK and C5aR1 inhibition would improve durability of response. To test this idea, we treated mice for 1 month, and then maintained mice off therapy for one month. Tumors regrew in all groups, but only mice treated with a combination of MEK and C5aR1/2 inhibitors showed altered tissue cellular architecture, expansion of dendritic cells, and increased macrophage MHCII expression. We conclude that C5aRA in combination with MEK inhibition is tolerable and causes durable immunosuppressive effects on the neurofibroma microenvironment.

804

IER3 Paucity Inhibits oxLDL-induced Foam Cell Formation in ApoE-deficient macrophages via Promoting an Alternative Phenotype

Oluwatobi Akinsanya[1], Davontae Cocroft[1], Mohd Shahid[1]

Rosalind Franklin University[1]

INTRODUCTION: Atherosclerosis is a chronic inflammatory disorder and the central cause of ischemic heart disease and stroke. It is characterized by the narrowing of large arteries due to the accumulation of fatty and fibrous plaque. The early stages are defined by subendothelial aggregation of foam cells—lipid-

filled macrophages, lacking the ability to migrate as a result of cholesterol engorgement. The accumulation of these foam cells ultimately leads to the buildup of cholesterol, and atherosclerotic plaque formation. The Immediate early response gene 3 (IER3) is a stress inducible gene that is highly expressed in macrophages and regulates their phenotype. We hypothesize that IER3 in macrophages is required for foam cell formation and thereby contributing to atherosclerosis pathogenesis.

METHODS: To investigate a cell autonomous role of IER 3 in foam cell formation, we harvested bone marrow (BM) cells from mice lacking Apolipoprotein-E (ApoE-/-) or ApoE and IER3 (ApoE-/-IER3-/-). These cells were first treated with macrophage-colony stimulating factor (M-CSF) to differentiate into mature macrophages and next with LPS (10 ng/ml) or IL-4 (10 nM) for 24 hours to transform them into pro- or anti-inflammatory phenotypes. Macrophage phenotypes were determined by quantifying the mRNA levels of pro- and anti-inflammatory marker genes using qRT-PCR and flow cytometry. In another experiment, macrophages were treated with oxLDL (10 µg/ml) for 24 hours to induce foam cell formation, which was subsequently quantified using Oil-Red-O staining.

RESULTS: LPS increased mRNA levels of TNF-α (15±3-fold, p<0.05) and iNOS (2.4± 0.2-fold, p<0.05) in ApoE-/- cells, an effect which was inhibited in ApoE-/-IER3-/- cells. Conversely, IL-4-induced increases in mRNA levels of Arg-1 (675±131-fold) and MRC-1 (3.2±0.2-fold) were markedly potentiated in ApoE-/-IER3-/- cells as compared to ApoE-/- control. Likewise, LPS-induced activation of proinflammatory state as determined by flow cytometry was attenuated in ApoE-/-IER3-/- cells as compared to ApoE-/- control. Moreover, ox-LDL-induced foam cell formation and accumulation of intracellular oil droplets were also suppressed in ApoE-/-IER3-/- macrophages as compared to ApoE-/- cells. Collectively, this data suggests that IER3 paucity hinders foam cell formation by inhibiting the proinflammatory state of macrophages.

CONCLUSION: IER3 contributes to foam cell formation in macrophages and may promote atherogenesis.

805

Dynamic fluorescent cyclic AMP biosensors (cAADis) to study recombinant and endogenous adenylyl cyclase 1 (AC1) signaling in HEK 3/6KO and SH-SY5Y cellular models

S M Sabbir Alam[1], Emily K. Davidson[1], Kayla Johnson[2], Camryn Fulton[1], Amanda Klein[3], Val Watts[1]

Borch Department of Medicinal Chemistry and Molecular Pharmacology, Purdue University, IN, USA[1]
Department of Pharmacy Practice and Pharmaceutical Sciences, University of Minnesota, MN, USA[2]
Department of Pharmacology and Toxicology, University at Buffalo, NY, USA[3]

Adenylyl cyclases mediate the production of cyclic AMP (cAMP) and plays a pivotal role in regulating important physiological processes. Adenylyl cyclase 1 (AC1) is robustly activated by Ca^{2+}/calmodulin (CaM), highly expressed in the central nervous system, and has been implicated in chronic pain modulation, alcohol behaviors, and memory and learning processes. However, the absence of a robust neuronal cell model along with technological limits for measuring cAMP have posed challenges in studying AC1, and potential therapeutic interventions. Specifically, most cell-based methods lack essential neuronal properties necessary for mimicking native cellular conditions, leading to limitations in assessing endogenous AC activity and inhibitor responses in a neuronal model. To address this gap, we aimed to establish a neuronal model utilizing SH-SY5Y neuroblastoma cells expressing genetically encoded cAMP biosensors to study endogenous adenyl cyclase activity and evaluate potential inhibitors of AC1 signaling. The initial studies used our novel HEK AC3/6 KO cells stably expressing AC1 (ACΔ3/6KO-AC1) to assess cAMP signaling with several dynamic cAMP biosensors (cAADis). Progress to date includes significant advancements in successful expression of all cAADis sensors in HEK ACΔ3/6KO-AC1 cells and subsequent stimulation of AC activity by forskolin, calcium ionophore (A23187), isoproterenol, and capacitive calcium entry. Both a Neo2 plate reader and Cytation 3-based imaging were utilized for fluorescent measures across different plate configurations, including 96-well and 384-well formats. Studies with constitutively active Gs and Gi-linked receptors (u-opioid and D2 dopamine

receptors) were also conducted. Additionally, cAMP overshoot or heterologous sensitization experiments using cAADis cAMP biosensors were successfully executed in the ACΔ3/6KO-AC1 cells. A second series of experiments used the best performing cAADis cAMP biosensors in SH-SY5Y neuroblastoma cells to investigate endogenous AC1 activity and explore potential inhibitors of AC1. SH-SY5Y cells express high levels of AC1 mRNA, however, significant Ca^{2+}/CaM-stimulated cAMP accumulation is not readily observed. We hypothesized that cell-selective analysis of cAMP using the targeted cAADis biosensors in SH-SY5Y cells would improve our overall signal to noise window of AC1 activity. Stimulation of SH-SY5Y cells with calcium ionophore, A23187 revealed a significant increase in the endogenous cAMP response of approximately 20% versus the maximal forskolin response. This study presents promising advancements towards establishing a robust neuronal model expressing genetically encoded cAMP biosensors, to study endogenous AC1 activity and explore potential AC inhibitor responses pertinent to chronic pain treatment.

Keywords: *Adenyl Cyclase*; *cAMP Signaling*; *cAMP Biosensors*; *Chronic Pain*; *Neuronal Models*; *HEK 293 Cells*; *SH-SY5Y Cells*; *Calcium Ionophore*.

806

Brilaroxazine Displays Limited Interaction with Clinically Relevant Drug Transporters

Laxminarayan Bhat[1], Seema R. Bhat[2], Palaniappan Kulanthaivel[2]

Reviva Pharmaceuticals, Inc.[1] Reviva Pharmaceuticals Holdings Inc.[2]

Background: Transporters influence drug absorption, distribution, and elimination, leading to pharmacokinetic and pharmacodynamic drug-drug interactions (DDIs) with co-administered inhibitors and/or inducers. Drug regulators have recommended that sponsors evaluate their investigational drugs as substrates and/or inhibitors of clinically relevant transporters.
Brilaroxazine, a $D_{2/3/4}$ and 5-$HT_{1A/2A}$ partial agonist, a 5 $HT_{2B/7}$ antagonist with binding affinity for 5-HT_{2B} > D_2, and a mediator of inflammatory cytokines, offers a differentiated pharmacological and safety profile over other antipsychotics. Clinical trial experience established its efficacy, safety, and pharmacokinetic profile. Currently, brilaroxazine has completed phase 3 for schizophrenia.

Methods: This *in vitro* study investigated this agent's interaction potential with clinically relevant drug transporters. P-gp and BCRP substrate/inhibitor studies involved Madin-Darby canine kidney (MDCKII) epithelial cells (Sigma-Aldrich, St. Louis, MO). OATP1B1, OATP1B3, OAT1, OAT3, OCT1, OCT2, MATE1, and MATE2-K evaluation involved HEK293-derived human BSEP membrane vesicles, mock HEK-293 cells, and Corning® TransportoCell™ cryopreserved transporter cells (Corning Life Sciences, Bedford, MA). Brilaroxazine concentrations tested were 3, 10, and 30 µM. Standard inhibitors and positive controls used were specific to these transporters.

Results: Brilaroxazine inhibited OATP1B1, OATP1B3, OAT1, OAT3, OCT1, OCT2, MATE2-K, BSEP, P-gp and BCRP with IC_{50} values ranging from 5.7 mM to >100 mM. MATE1 was the only transporter with an IC_{50} of <1 mM. Brilaroxazine showed defined concentration-dependent inhibitions with P-gp, BCRP, OATP1B1, OATP1B3, OAT3, OCT1, OCT2, MATE1, MATE2-K and BSEP, and a weak inhibition withOAT1. Brilaroxazine showed low to moderate permeability in MDR1-transfected MDCKII cell monolayers expressing P-gp at all concentration levels tested, with efflux ratios of 9.18, 3.54, and 1.71 at 3, 10 and 30 µM, respectively. P-gp inhibitor ketoconazole (50 µM) showed low permeability, with efflux ratios < 2 at all brilaroxazine concentrations. Brilaroxazine showed low to moderate permeability in BCRP-expressed MDCKII cell monolayers at all concentration levels tested, with efflux ratios of 4.33,

1.52, and 1.42 at 3, 10, and 30 μM, respectively. The BCRP inhibitor Ko-143 (10 μM) reduced brilaroxazine from 3 to 2.5 μM.

All other transporter evaluations failed to demonstrate any significant evidence of substrate interactions. These included concentration-dependent inhibitions (OATP1B1, OATP1B3, OCT1 and OCT2), uptake activity vs. mock cells (OAT1, OAT3, OATP1B1, OATP1B3, OCT1, OCT2, MATE1, MATE2-K), lack of inhibition by known blockers (MATE1, MATE2-K), ATP-dependent uptake with S/N ratios ~1 (BSEP), and inhibition of activity in human hepatocytes BSEP). No differences appeared in all these evaluations vs. positive controls.

Conclusions: Brilaroxazine did not interact with most transporters. It did not display substrate interactions with OATP1B1, OATP1B3, OAT1, OAT3, OCT1, OCT2, MATE1, MATE2-K, or BSEP. Thus, one should not expect DDIs with inhibitors or inducers of these transporters. Brilaroxazine appears to be a defined P-gp and weak BCRP substrate. Co-administration with strong inhibitors or inducers of these transporters may affect systemic exposure, although such interactions need confirmation within the clinic.

Reviva Pharmaceutical Holdings, Inc.

807

Absorption, Metabolism, and Excretion of Brilaroxazine in Rats

Laxminarayan Bhat[1], Seema R. Bhat[2], Palaniappan Kulanthaivel[2]

Reviva Pharmaceuticals, Inc.[1] Reviva Pharmaceuticals Holdings Inc.[2]

Background: Brilaroxazine, a novel multimodal neuromodulator, belongs to a class of next-generation treatments for schizophrenia and comorbid conditions. It functions as a $D_{2/3/4}$ and 5-$HT_{1A/2A}$ partial agonist and a 5 $HT_{2B/7}$ antagonist with binding affinity for 5-HT_{2B} > D_2. It also mediates inflammatory cytokines. With defined efficacy, safety, and pharmacokinetics from clinical trials, it offers a differentiated profile over other antipsychotics.

Brilaroxazine's development involved rats, mice, and dogs for nonclinical toxicological evaluations. This study evaluated the absorption, metabolism, and excretion of brilaroxazine in rats after a single ^{14}C-brilaroxazine dose to qualify rats as a suitable toxicology species.

Methods: This study involved 12 male Sprague Dawley rats divided equally into three groups. These animals received a single [^{14}C]-brilaroxazine 20 mg/kg (200 mCi/kg) oral dose. Group 1 rats had a bile-duct cannula (BDC) surgically implanted for bile and feces collection. Group 2 rats had blood collected for metabolite evaluation. Group 3 rats had urine and feces collected to determine the mass balance. Maximal post-dose collection times for bile samples were 72 hours (Group 1), serial blood samples were 72 hours (Group 2), and urine and feces samples were 168 hours (Group 3).

Sample analysis included liquid scintillation counting (LSC) or a combustion/ LSC combination (blood, plasma, and excreta), validated liquid chromatography–mass spectrometry/mass spectrometry (unlabeled brilaroxazine and RP5081 plasma concentrations), and mass spectral analysis or direct comparison with authentic standards for metabolite structures (brilaroxazine, and metabolite RP5081).

Results: Bile or feces of BDC rats or intact rats were the predominant routes for dose radioactivity excretion. The percent of the administered dose recovered in Group 1 BDC rat bile, feces, and urine accounted for 79.52%, 13.02%, and 5.60%, respectively. Bile and urine in Group 3 intact rats showed at least 85% dose absorption, with 81.51% of the administered dose recovered in feces and 8.89% in urine.

Brilaroxazine represented ~31% of the circulating radioactivity exposure with three primary metabolites-

M641a (oxidation + glucuronidation), RP5081 (O-dealkylated acid), and M219 (N-[2,3-dichlorphenyl]-glycine)- accounting for ~29%,~16%, and ~16%, respectively. In Group 1 rat bile, the analysis did not detect brilaroxazine but identified M641a, accounting for 70% of the bile radioactivity or 56% of the dose. In Group 3 intact rat feces, the mono-hydroxylated compound, M465a, was the major metabolite, accounting for 86% of the fecal radioactivity or 71% of the dose. The gut microflora likely converted the glucuronide metabolite, M641a, observed in Group 1 rat bile, to the mono-hydroxylated metabolite M465a, which underwent fecal elimination in Group 3 rats. Glucuronidase hydrolysis of M641a, producing M465a in a near quantitative yield, confirmed this supposition.

Conclusions: Following oral administration, brilaroxazine in rats underwent rapid absorption, extensive metabolism, and elimination via hepato-biliary excretion. The primary human metabolites, RP5081 and M219, were among the most commonly circulated in rats. Both humans and rats utilize 465a formation as the major metabolic pathway. These findings confirm that rats are a suitable rodent species for the toxicological evaluations of brilaroxazine.

Reviva Pharmaceutical Holdings, Inc.

808

cFOS expression following rimonabant precipitated withdrawal from WIN 55212-2 in the rat brain

Abigail Brewer, Sade M. Spencer

University of Minnesota[2]

Abrupt cessation of cannabinoid use commonly results in symptoms of withdrawal in humans. In animals, cannabinoid withdrawal is characterized by quantification of somatic behaviors following either abrupt cessation of cannabinoid administration or precipitation of withdrawal with an antagonist/inverse agonist such as rimonabant. c-Fos expression is frequently used to quantify neuronal activity in the central nervous system following external simulation because it is rapidly activated. c-FOS expression following acute cannabinoid administration in naïve subjects invokes different activation patterns versus chronic cannabinoid administration. Precipitation of cannabinoid withdrawal with rimonabant greatly increases the levels of neuronal activation in brain regions critical in mediating negative affect and stress response. We aimed to compare the pattern and levels of c-FOS expression in male and female rats following rimonabant administration following either vehicle or chronic cannabinoid administration. Rats were given escalating doses of WIN 55212 or vehicle twice per day over four days. On the fifth day, four hours after the final dose of WIN or vehicle, a dose of rimonabant (3 mg/kg for females and 10 mg/kg for males) was administered ip to precipitate withdrawal with behavior observed for 30 minutes. These doses were chosen due to our recently published work showing 10 mg/kg rimonabant precipitated withdrawal from WIN in males without causing increased somatic behaviors in cannabinoid naïve rats but in females 3 mg/kg rimonabant was sufficient to see this same effect (Brewer., et al., 2024). One hour after withdrawal, animals were sacrificed by administration of an overdose of pentobarbital and immediately perfused with paraformaldehyde. After 24 hours post fixation, brains were mid-sagitally sectioned and one hemi section underwent cFOS antibody labeling followed by tissue clearing via polyethylene glycol-associated solvent systems (PEGASOS) passive immersion procedures. Whole intact hemi sections were imaged on a 3i cleared tissue light sheet microscope. Imaged hemi sections were then processed by mapping activated cell coordinates in atlas space following the Waxholm Space Atlas to quantify the number of cFOS active cells by region in the hemi brain. Preliminary data analysis (Male n=5; Female n=2 per group) show that cFOS expression is higher in females compared to males in many regions of the brain. WIN withdrawal did increase expression of cFOS in the hemibrains of female rats while expression decreased or remained stable in male brains. These preliminary results show that expression of cFOS during WIN withdrawal is dependent upon brain region as well as sex. Furthermore, sex differences in cFOS expression following administration of rimonabant in vehicle treated rats demonstrate potential sex differences in baseline activation of CB1 receptors in the brain. Importantly, the use of tissue

clearing will allows us to map the pattern of cFOS expression across an entire hemisphere of the brain and elucidate functional networks associated with cannabinoid withdrawal or dependence.

809

Inhibition of Parabrachial CGRP Neurons Reduces Morphine Reinforcement and Withdrawal

Lauren Bystrom[1], Nicole Kujas[2], Luis M. Tuesta[2]

Univ of Miami Department of Psychiatry[1], University of Miami Miller School of Medicine[2]

Opioid Use Disorder (OUD) is a chronic, relapsing disease that, despite our best research efforts, has become a worsening public health crisis. Currently, the medications to treat OUD belong to the opioid class of drugs and, therefore, continue to interact directly with opioid receptors. While these medications are safe and effective for the cessation of opioids with higher abuse potentials, there is still a need for effective non-opioid receptor-targeting therapeutics. Exploring novel non-opioid targets is necessary to overcome this barrier. One such non-opioid target we are currently investigating is the calcitonin gene-related peptide (CGRP) system, particularly CGRP-expressing neurons in the parabrachial nucleus (CGRP^{PBN}). These neurons have been well studied in itch and pain and are known to project to brain regions implicated in opioid reward and withdrawal. Previous studies in our lab have found that CGRP^{PBN} activity decreases during opioid taking and increases during opioid withdrawal. To further characterize the behavioral role of CGRP^{PBN} neurons in opioid withdrawal, Calca-Cre transgenic mice received viral injections into the PBN containing an inhibitory DREADD (hm4Di), and two weeks later, mice were implanted with 2x25 mg morphine pellets. After five days, morphine withdrawal was induced by removing the pellets. Mice were administered either clozapine-N-oxide (CNO) (3 mg/kg, I.P.) or vehicle (saline, I.P.) 5.5 hours post pellet removal, and behavior was recorded at 6 and 24 hours post pellet removal. Two experimenters scored videos for jumping and wet dog shakes. Those mice injected with CNO showed fewer wet-dog shakes at the 6-hour time than vehicle-injected controls. We next sought to characterize the behavioral role of CGRP^{PBN} neurons in opioid taking. In this experiment, morphine intravenous self-administration (IVSA) was used. Calca-Cre transgenic mice received viral injections into the PBN containing either an inhibitory DREADD (hm4Di) or a control mCherry vector and, two weeks later, were implanted with jugular catheters. Subsequently, operant responding for intravenous morphine was established. After 12 daily sessions, mice were administered CNO (3 mg/kg, I.P.) or vehicle (saline, I.P.) and allowed to respond for morphine. CGRP^{PBN} inhibition reduced morphine intake in hm4Di-injected animals, while those with a control virus maintained their previous levels of morphine intake. Decreases in morphine intake were maintained 24 hours after CNO administration but returned to previous baseline levels at 48 hours. These results suggest that CGRP^{PBN} neurons play a role in the behavioral consequences of both opioid reinforcement and withdrawal. CGRP receptor inhibitors are FDA-approved for the treatment of migraine and exist in both short and long-lasting formulations. By leveraging these available medications for the off-label purpose of treating OUD, we may be able to determine the translational potential of these preclinical findings and, therefore, expand our therapeutic arsenal for long-term maintenance of opioid abstinence and relapse.

810

Identifying Berberine's Mechanism of Action to Enhance Social Behavior

Karina Cantu[1], P. Bridgette Stewart[1], Anja C. Shakocius[1], Juliet Garcia-Rogers[2], Sophia Torres[2], Riley McDaniel[2], Ruben Vasquez[2], Matthew Salizar[2], Ian Pak[2], Brett C. Ginsburg[3], Georgianna G. Gould[2]

University of Texas Health Science Center at San Antonio Cellular & Integrative Physiology[1], University of Texas Health Science Center at San Antonio Psychiatry[3], University of Texas Health Science Center at San Antonio[3]

Social withdrawal is a debilitating and treatment-resistant symptom of psychiatric disorders such as autism and schizophrenia. In preclinical studies in mice, we found acute intraperitoneal (i.p.) injection of the isoquinoline alkaloid berberine at 5 mg/kg enhances social sniffing during social interaction preference tests in female mice, and social dominance in male mice relative to vehicle control treatment. Prior publications indicate that berberine has antidepressant-like properties that may be due to changes it induces in the kynurenine-serotonin pathway. Kynurenine is a product of tryptophan metabolism and may direct tryptophan away from serotonin (5-HT) production. Berberine was reported to disrupt several enzymes along this pathway to favor 5-HT synthesis in brain, ultimately enhancing brain derived neurotrophic factor (BDNF) expression to produce antidepressant-like effects. Given this we hypothesized that both acute and chronic berberine administration would enhance social behaviors by increasing brain 5-HT and BDNF levels. To test this, mice were treated with either berberine or vehicle control for 50 min (acute, via i.p. injection) or 3-4 weeks (chronic, via 0.5 - 4 g/L dissolved in drinking water), tested for social behaviors in social preference and social dominance tasks and were then humanely euthanized to measure blood glucose and collect serum and brain. Blood glucose levels averaged 100 – 126 mg/dl and did not differ among treatments. Brains were immediately frozen on a bed of powdered dry ice and stored at -80°C until use. Homogenates from 3 mm hippocampal and frontal cortex punches were made to measure 5-HT using enzyme-linked immunosorbent assay kits and each protein level was measured by Bradford assay. We found brain 5-HT levels of around 3 ng/mg protein and BDNF levels of around 100 fg/mg protein did not significantly differ after either type of berberine treatment. To investigate further, we measured whole brain 5-HT, 5-hydroxyindole acetic acid (5-HIAA), and kynuric acid levels by gas-chromatography-mass spectroscopy and observed they were unaffected by the berberine treatment, in agreement with our brain punch ELISA findings. Frozen serum was used to measure serum concentrations of the stress hormone corticosterone, and we found that berberine treatment significantly reduced ($p < 0.05$) the corticosterone levels relative to vehicle controls (N = 8). Taken together our findings indicate that the mechanism of action for berberine to reduce social behavior is unlikely to involve 5-HT metabolism or BDNF levels in brain but instead may correspond with attenuation of the stress response. A future direction will be to examine the effect of the chronic treatment on brain 5-HT2 receptor expression, as this receptor is targeted by atypical antipsychotics that are used in the treatment of autism and schizophrenia.

811

MAL-PD Theory/Algorithm Guided Clinical Protocol Design for Computerized Data Analysis and Digital Conclusions in Drug Evaluations for Single Drugs and Combinations

Ting-chao Chou[1], Jianing Fu[2], Joseph H. Chou[3], Shu-Fu Lin[4], Imourana Alassane-Kpembi[5], Taitsung Chang[6], Xiao Wan[7], Richard J. Wong[8], Yuman Fong[9], Gudrun S. Ulrich-Merzenich[10], Theresa A. Shapiro[11]

PD Science LLC[1] Columbia University Medical Center[2] Massachusetts General Hospital[3] Chang Gung Memorial Hospital[4] Université de Montréal[5] Kaohsiung Medical University[6] NATA - Nucleic Acid Therapy Accelerator[7] Memorial Sloan Kettering Cancer Center[8] City of Hope[9] University Clinic Center Bonn, Medical Clinic III, Center for Internal Medicine[10] Johns Hopkins University School of Medicine[11]

Mathematical system analysis on mass-action law (MAL) and enzyme model resulted in the derivation of over 300 reaction-rate equations, which can be deduced into unified general MAL-dynamics theories/algorithms for computer simulation of *diagnostic plots*: **i.** The Median-Effect Eq. (MEE) & (MEP) for "*action*" determines Dm (Median-effective-dose) for the potency of drugs or mass-entities and its dynamics (m value) for the shape of dose-effect-curve (DEC). **ii.** The Combination Index Eq (CIE) & (CIP) for "*interactions*" allows digitalization of synergism (CI<1), additive-effect (CI=1), and antagonism (CI>1), and **iii.** The Dose-Reduction Index Eq. (DRIE) & (DRIEP) for the "*consequences of interactions*". The

unified MAL-dynamics theory/algorithm of pharmacodynamics/bioinformatics **(MAL-PD/BI)** and the Minimum Two-dose Data Point Theory (MTDPT) of MAL-PD automatically add two default dose-data points (Dose zero and Dm) to all MAL-dynamics analysis, thus the basis for efficiency and cost-effectiveness for R&D. MEE/MEP allows the projection of *optimal* dose range, dose density, and protocol design in vitro, in vivo, and in clinical trials. The universal/unlimited applicability is due to *all* terms of Equations i-iii being *dimensionless relativity ratios.* (i.e., canceled out with ratio), thus independent of unit physical state, structure, and mechanism. All Equations i-iii are based on One, thus leading to the Unity of One Theory (UOT). To date, this MAL-PD/CI/BI dynamics/informatics has garnered over 25,000 citations in 23,000 papers, in 1,541 journals and 1,341 patents internationally, which attests to the significance and importance in all spectrum of R&D. This MAL-theory/algorithm allows a simple, efficient, Econo-green, and unified drug evaluations R&D. For single drugs, each requires about 6, 4, and 3 *doses* in vitro, in animal, and in clinical protocol design, respectively (at MAL-PD/MEE/MEP guided/designed dose range and density) for effects (at selected end-points and target/surrogate measurements). The drug combination evaluation follows the *same* guidelines, with the MAL-PD/CI being the most efficient diagonal constant-ratio combination scheme for all dose-dependent dynamic analyses, with automated quantitative computer simulation. This paper will illustrate specific MAL-PD/CI/BI examples for experimental planning, protocol design, data analysis, data entries, computer simulations, and computer printout reports. It is demonstrated that using two anticancer agents against xenograft tumors in nude mice (e.g., Taxotere, T-607, and their Combination) and anti-HIV agents in clinical trials (e.g., AZT, IFN, AZT+IFN), using only 10 dose-data-points (<70 mice and 36 patients, respectively), the **MAL-PD/CI/BI** method quantitatively determined potency of each drug and Combinations, and quantitatively determines synergism (CI<1) with PD-automated computer simulation. It is concluded that the MAL theory/algorithm-based Top-Down R&D approach is complimentary alternative to the traditional/conventional observation/statistics-based Bottom-Up R&D approach. However, using the same MAL fundamental principles, the MAL theory/algorithm provides unified and streamlined guidance to scientific R&D in biomedical sciences and beyond, including environmental, agricultural, marine, and food sciences.

812

Population Pharmacokinetic/Pharmacodynamic Modeling and Simulation of a Flat Quarterly Riliprubart Dosing Regimen for Patients with Cold Agglutinin Disease

Tim Chow[1], Marek Wardecki[2], Shirley D'Sa[3], Josephine Vos[4], Wilma Barcellini[5], Alexander Röth[6], Michael Storek[1], Nancy Wong[1]

Sanofi, Cambridge, Massachusetts, USA[1] Sanofi, Warsaw, Poland[2] University College London Hospitals NHS Foundation Trust, London, UK[3] Amsterdam UMC, University of Amsterdam, LYMMCARE, Cancer Center Amsterdam, Amsterdam and Sanquin[4] Fondazione IRCCS Ca' Granda Ospedale Maggiore Policlinico, Milan, Italy[5] West German Cancer Center, University Hospital Essen, University of Duisburg-Essen, Essen, Germany[6]

Introduction: Riliprubart is a humanized immunoglobulin G4 monoclonal antibody that inhibits the active form of C1s, preventing activation of the classical complement pathway (CP), whilst leaving the lectin and the alternative pathways functionally intact. Riliprubart is currently in development for the treatment of complement-mediated diseases, including cold agglutinin disease (CAD).

Aim: To determine a dosing regimen for patients with CAD using population pharmacokinetic/ pharmacodynamic (popPK/PD) modeling and simulations.

Methods: The PKs of riliprubart in healthy subjects was characterized by a two-compartment model with linear elimination and first order absorption. Typical clearance was 2.12 mL/h, and body weight was the primary source of PK variability on peripheral volume of distribution. The riliprubart PK/PD relationship with Wieslab® CP or 50% hemolytic component (CH50) in healthy subjects was adequately described by a direct non-linear effect model.

Based on the popPK/PD model developed using data from healthy subjects, riliprubart PK and PD were evaluated in patients with CAD after a single intravenous (IV) dose of 30 or 15 mg/kg. Using a Bayesian approach with pre-defined quality criteria, the PK characteristics of riliprubart in CAD patients was consistent with healthy subjects. Hemoglobin (Hb) response to riliprubart exposure in patients with CAD was adequately described by an indirect PK/PD model, including a zero-order rate constant for Hb production, and a first-order constant for Hb elimination, which is inhibited by riliprubart in the central compartment.

The popPK and popPK/PD models were used to simulate a virtual population of 1,000 patients dosed with a quarterly IV regimen, with an additional dose on Day 29, at 3 dose levels: 30 mg/kg, 50 mg/kg and 3.5 g. Evaluation criteria included safety margins and efficacy (as informed by reduction of CH50 values to complement deficient states and >2 g/dL Hb increase from baseline).

Results: A quarterly IV regimen with an additional dose on Day 29 for both 50 mg/kg and 3.5 g were projected to achieve the CH50 and Hb efficacy targets for >90% of the population, including patients with extreme low and high body weights.

For the flat dose approach, there was a trend in area under the curve at steady state (AUC_{ss}) decreasing from extreme low body weights (35–54 kg) to extreme high body weights (130–200 kg); this decrease was ~2.8-fold. For the body weight-based dose regimen, there was an increase in AUC_{ss} with increasing body weight over the same range; this increase was ~1.2-fold. For 65–105 kg, the exposure between flat and weight-based approaches were comparable. The greatest difference was observed for the low (35–54 kg) and high (130–200 kg) body weights; however, the exposure difference between flat and weight-based approaches were <2-fold at both low and high body weights. The flat dose approach had a greater than 3-fold safety margin in all body weight groups and >90% of patients were predicted to have $C_{trough,ss}$ above 300 µg/mL, achieving complement deficient states (based on CH50) leading to improvements of Hb in patients with CAD.

Conclusion: Using a popPK/PD modeling and simulation approach to examine the relationship between clinical and PD efficacy markers for riliprubart, a flat quarterly dose of 3.5 g IV with an additional Day 29 dose was proposed to maximize the likelihood of therapeutic benefits for patients with CAD.

813

Enhancement of Opioid Analgesia by Positive Allosteric Modulation of the µ-Opioid Receptor in a Rat Model of Chronic Neuropathic Pain

Benjamin M. Clements, Kelsey Kochan, Stephen Kemp, John Traynor

University of Michigan

Chronic pain severely impacts the lives of Americans, affecting more that 40% of the U.S. population. Of this group, certain pain conditions like neuropathic pain are inadequately treated by current pharmacotherapies. Opioids are a powerful tool for pain treatment, but adverse effects limit their use. In addition, these drugs show limited efficacy in neuropathic pain. Therefore, development of adjuvants to enhance pain relieving effects of opioids while reducing negative side effects could greatly improve outcomes for these patients. Positive allosteric modulators (PAMs) interact with receptors at a distinct location from the orthosteric binding site to increase the activity and/or affinity of an agonist. Use of PAMs

at opioid receptors could increase opioid-mediated analgesia in chronic pain patients and limit unwanted effects. Administration of an opioid PAM (BMS-986122) in the mouse enhances the analgesia of clinically used opioids in acute models of pain. In addition, BMS-986122 administration at doses effective for pain did not enhance opioid-induced constipation, conditioned place preference, nor respiratory depression. These studies, however, were performed in uninjured animals. The opioid PAM has shown efficacy in carrageenan-induced inflammatory pain, as demonstrated by a reversal of tactile hypersensitivity. The utility of BMS-986122 in neuropathic pain, or its efficacy in the rat, is unknown. Our objective is to assess the activity of this PAM alone or in combination with a clinically used opioid on preclinical pain behaviors acutely in mouse and rat, and in a rat model of mononeuropathy.

To determine the activity of BMS-986122 in chronic neuropathic pain, male and female Sprague-Dawley rats underwent spared nerve injury (SNI) to induce a nerve-injury induced pain state. After establishment of the chronic neuropathic pain, animals received a pre-treatment of BMS-986122 (10 mg/kg, i.p.) or vehicle, followed by a low dose of methadone (1 mg/kg, i.p.) or saline. Tactile hypersensitivity was determined using von Frey measurements 30 minutes after PAM pre-treatment and 15 minutes after opioid administration. BMS-986122 alone did not reverse SNI-induced tactile hypersensitivity alone, but 10 mg/kg BMS-986122 was able to enhance the reversal of tactile hypersensitivity by 1 mg/kg methadone. Our data suggests opioid PAMs may be effective as opioid adjuvants in chronic neuropathic pain, but future studies remain to be done to fully characterize their activity in this state.

814

Beta2-Adrenergic receptor agonism as a therapeutic strategy for the treatment of Cushing's syndrome
Kristan Cleveland, John Scott

University of Washington

Cushing's syndrome is an endocrine disorder caused by chronically elevated cortisol levels. Patients often present with weight gain, chronic fatigue, and hypertension. In turn, this disorder is known to induce high blood glucose levels and changes in renal function. A-Kinase anchoring proteins (AKAPs) direct local signaling events by sequestering protein kinase A (PKA) and other signaling enzymes to defined subcellular compartments. AKAP signaling plays important roles in key cellular responses including gene transcription, ion channel regulation and hormone-mediated insulin secretion. Mutations in the catalytic subunit of PKA (PKAc) drive hypercortisolism in adrenal Cushing's syndrome. Defective local PKA signaling through AKAPs signaling has also been implicated in this endocrine disorder. Current therapies for treating Cushing's syndrome rely on surgery, radiation, or steroids to control cortisol production in the adrenal glands. Unfortunately, these therapies are either invasive, or do not completely alleviate all symptoms and comorbidities. Thus, the identification and development of new therapeutics to treat Cushing's syndrome is important. Recent studies have demonstrated that beta2-adrenergic receptor (AR) agonists can improve renal function after both acute and chronic kidney injury. Based on these findings, we investigated the relationship between Cushing's syndrome, renal function, and the effect of beta2-AR agonists on corticosterone levels in adrenal cells. Our laboratory developed the first mouse model of PKAc-derived adrenal Cushing's syndrome. The PKAc$^{WT/W196R}$ mouse model which expresses an adrenal specific pathogenic allele of the PKAC W196R mutant was used to characterize the kidney disease. We demonstrate that renal dysfunction in PKAc$^{WT/W196R}$ mice, as measured by serum creatinine and the proximal tubule-specific injury marker, kidney injury molecule-1 (KIM-1). PKAc$^{WT/W196R}$ mice also display elevated serum glucose levels. We used an RII overlay, or far Western Blot, to determine global PKA-RII binding as means to assess differences in AKAP expression. Global AKAP expression was increased in the renal cortex of PKAc$^{WT/W196R}$ compared to controls. To test the effect of beta2-AR agonists on corticosterone levels, we used wildtype PKAc, L205R, and W196R Cushing's mutants, which are characterized by elevated corticosterone. Treatment of adrenal cells expressing either PKAc L205R ot

PKAc W196R with the beta2-AR agonists formoterol and salmeterol restored high corticosterone back to control levels in a concentration-dependent manner. In contrast, application of salbutamol had no effect on corticosterone levels, indicating that the property is not shared among all beta2-AR agonists. These data provide evidence that both kidney damage and altered AKAP expression are present in the kidneys of mice with Cushing's syndrome, and that the beta2-AR agonists formoterol and salmeterol decrease elevated corticosterone and may serve as potential therapies for hypercortisolism.

815

Design, Synthesis, and Biological Evaluation of Substituted Hydroxyquinolinone Compounds as 20S Proteasome Enhancers

Sydney G. Cobb[1], Evan D. Savelson[1], Jetze Tepe[1]

University of Virginia[1]

The 20S proteasome is a key component in cellular proteostasis and assists the cell in maintaining proper levels of intrinsically disordered proteins (IDPs). Dysregulation of 20S proteasome-mediated proteolytic degradation often results in the accumulation and aggregation of these IDPs, which are involved in the pathogenesis of neurodegenerative diseases, such as Parkinson's disease. Here, it is hypothesized that using small molecules to enhance the 20S proteasome's degradation of IDPs may prove a viable strategy to combat this toxic protein accumulation. A hydroxyquinolinone compound (MSU-8) was recently identified as a potential lead, and this work focuses on expanding its structure-activity relationship (SAR).
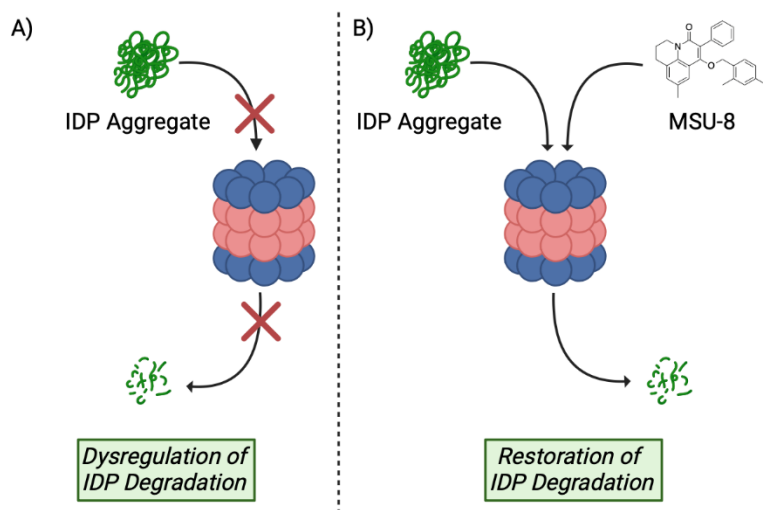
(A) With an abundance of intrinsically disordered protein (IDP) aggregates, 20S proteasome-mediated degradation of IDPs becomes dysregulated, leading to toxicity and further IDP accumulation and aggregation. (B) Treatment with a small molecule enhancer (MSU-8) may lead to the restoration of proteolytic degradation.

816

Development of *N*-acyl Fluspirilene 20S Proteasome Enhancers for the Treatment of Neurodegenerative Diseases

Daniel J. Colombani-Garay[1], Jetze Tepe[1]

University of Virginia[1]

Currently, there are limited therapeutic treatments to slow, prevent, or cure neurodegenerative diseases such as Alzheimer's Disease or Alzheimer's-related Dementias.[1] These diseases are characterized by an accumulation of oligomerized intrinsically disordered proteins (IDPs) and impairment of 20S proteasome-mediated protein degradation.[2–4] In 2021, our group conducted a high-throughput screen of the NIH Clinical Collection and Prestwick libraries and identified FDA-approved drug fluspirilene and its analogue *N*-acyl fluspirilene as a class of small molecules capable of enhancing 20S proteasome-mediated IDP degradation, overcoming IDP-induced 20S proteasome impairment, and degrading intrinsically disordered proteins.[5] This project aims to expand on the published computational, synthetic, and biological efforts to (1) identify the pivotal structural features of the *N*-acyl fluspirilene class necessary for 20S proteasome activation, (2) rationally develop improved 20S proteasome enhancers, and (3) overcome 20S proteasome impairment induced by IDP oligomers.

Successful completion of this work will enable the rapid design, development, and identification of 20S proteasome activators, and elucidate the role of 20S proteasome modulation in neurodegenerative diseases as a novel therapeutic strategy for disease treatment.

Bibliography
(1)   Institute on Aging, N. NIH Scientific Progress Report, 2022. Advancing Alzheimer's Disease and Related Dementias Research for All Populations. **2022**.
(2)   Zondler, L.; Kostka, M.; Garidel, P.; Heinzelmann, U.; Hengerer, B.; Mayer, B.; Weishaupt, J. H.; Gillardon, F.; Danzer, K. M. Proteasome Impairment by α-Synuclein. *PLoS One* **2017**, *12* (9).
(3)   Keller, J. N.; Hanni, K. B.; Markesbery, W. R. Impaired Proteasome Function in Alzheimer's Disease. *J Neurochem* **2000**, *75* (1), 436–439.
(4)   Thibaudeau, T. A.; Anderson, R. T.; Smith, D. M. A Common Mechanism of Proteasome Impairment by Neurodegenerative Disease-Associated Oligomers. *Nature Communications 2018 9:1* **2018**, *9* (1), 1–14.
(5)   Fiolek, T. J.; Keel, K. L.; Tepe, J. J. Fluspirilene Analogs Activate the 20S Proteasome and Overcome Proteasome Impairment by Intrinsically Disordered Protein Oligomers. *ACS Chem Neurosci* **2021**, *12* (8), 1438–1448.
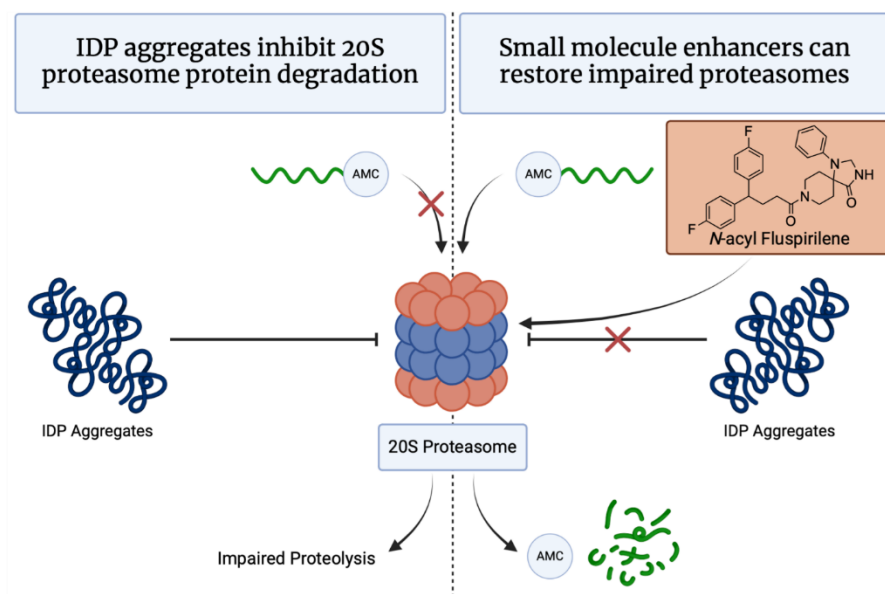
817

Interaction between hERG and the Fc Domain of IgG Leads to the Phosphorylation of a C-terminal ITIM by Src which Induces Chronic Channel Internalization

James D. Cornwell[1], John Szendrey[1], Jun Guo[1], Wentao Li[1], Tonghua Yang[1], Shetuan Zhang[1]

Queen's University[1]

The *human ether-a-go-go related gene* (*hERG*) encodes the Kv11.1 channel which makes up the pore-forming subunit of the rapidly activating delayed rectifier potassium current (I_{Kr}). hERG has been implicated as a likely cause for the abnormally higher incidence of long QT syndrome (LQTS) observed in autoimmune patients. More recently, hERG has been identified to interact with the anti-Ro52 IgG autoantibody leading to endocytosis from the plasma membrane. The exact mechanism for this internalization is not well characterized, but one potential cause may be an immunoreceptor tyrosine-based inhibitory motif (ITIM) located within hERG's C-terminus.

Western blot analysis and whole-cell patch clamping were used in this study to analyze hERG expression and channel activity in hERG-HEK cells. hERG was found to interact with several antibodies to varying degrees, inducing a marked reduction in hERG expression from the surface of cells following culturing with IgG. The Fc domain of IgG in particular was identified to bind to the S5-pore linker of hERG, and not the antigen-binding Fab domain. In this study, we proved that the addition of a Src tyrosine kinase inhibitor (Src I1) significantly attenuated IgG-mediated hERG reduction, while adversely, vSrc overexpression mimicked this reduction of hERG. Here we demonstrate that the substitution of Y827 with an alanine (Y827A), thereby disabling hERG's ITIM, renders hERG completely resistant to the effects of IgG and vSrc.

Thus, our results indicate that not only does hERG interact with antibodies other than anti-Ro52 IgG, but that it behaves as a novel Fc receptor with a functioning ITIM that can mediate its own internalization. This is the first evidence of a mechanistic role for the ITIM found within hERG and provides clear insight into not only hERG's role in autoimmune-induced LQTS but also its potential role in immunity.

818

Efficacy of Biologic let-7-5p Isoforms in the Modulation of Target Gene Expression in HCC Cells

Joseph Cronin[1], Aiming Yu[2], Meijuan Tu[1]

Univ of California, Davis[1] UC Davis School of Medicine[2]

Advancing our understanding of epigenetic regulation in drug metabolism and pharmacokinetics (DMPK) is critical to designing the next generation of safe and effective therapeutics. Multidrug resistance (MDR) is a major barrier in the treatment of hepatocellular carcinoma (HCC) and other cancers and is characterized by the overexpression of efflux transporters such as ABCC1/MRP1, ABCC2/MRP2, and ABCC5/MRP5 that are critical to the absorption, distribution, metabolism, and excretion (ADME) processes of chemotherapeutic drugs. Endogenous microRNA (miRNA) are small noncoding RNAs that are critical posttranscriptional regulators of a wide variety of cellular processes, capable of targeting multiple mRNA transcripts to modulate drug transport and disease progression. The let-7-5p miRNA family consists of several unique isoforms (let-7a, b, c, d, e, f, g, and i) that have demonstrated potential

in previous experiments inhibiting HCC viability and negatively regulating the expression of ADME genes implicated in MDR. To further elucidate the therapeutic potential and efficacy of individual let-7-5p isoforms against HCC, the current study utilized a novel *in vivo* fermentation based, RNA bioengineering approach to produce unique biologic let-7-5p miRNAs (BioRNA/let-7-5p) in high yield. When analyzed by Western blot, three human HCC cell lines (Hep3B, Huh7, and HepG2) showed high basal protein expression of several potential let-7-5p targets (ABCC1-5, Lin28B) and were selected as suitable *in vitro* models for future study. HCC cell lines were transfected with individual BioRNA/let-7-5p agents for 48-h or 72-h using Lipofectamine 3000 reagent. Stem loop RT-qPCR was utilized to confirm that all BioRNA/let-7-5p treatments were selectively processed to their mature let-7-5p isoforms in all HCC cell lines. Western blot analysis revealed that all BioRNA/let-7-5p isoforms similarly downregulated protein level of oncogene Lin28B, with BioRNA/let-7d-5p demonstrating the strongest and most consistent downregulation across all HCC cell lines. Similarly, all HCC cell lines treated with BioRNA/let-7-5p agents also demonstrated lower ABCC5 protein level with small differences between individual isoforms. In contrast, little to no effect on the protein levels of transporters ABCC1-4 was observed following treatment with individual BioRNA/let-7-5p isoforms. These results illustrate the differences of let-7-5p family isoforms in the regulation of target gene expression in HCC cells, providing insight into how miRNA level, target complementarity, and regulatory strength may affect the anticancer potency of individual miRNA isoforms. Additionally, these results demonstrating downregulation of ABCC5 following BioRNA/let-7-5p treatment will inform the direction of future study exploring rational combination with chemotherapies in HCC.

819

A Treatment to Eliminate Respiratory Viral Infections Associated with Asthma Exacerbations

Ivana Daniels[1], Jessica Saunders[2], Laura Smith[1], Taiya Edwards[1], Ryan Relich[1], Benjamin Gaston[1], Michael D. Davis[1]

Indiana University School of Medicine[1] Joe DiMaggio Children's Hospital[2]

Background: Low airway pH is implicated in many airways diseases. Furthermore, low airway surface pH impairs antimicrobial host defense and worsens airway inflammation. Many respiratory viruses require low endosomal pH to enter airway epithelial cells, activate viral surface proteins, and to replicate. Respiratory syncytial virus (RSV) and human metapneumovirus (hMPV), both members of the *Paramyxovirdae* family, are leading causes of acute asthma exacerbations. Inhaled Optate, an alkaline buffer, safely raises airway surface pH in humans and raises intracellular and endosomal pH in primary human airway epithelial cells (HAECs). We have recently demonstrated that Optate inhibits SARS-CoV-2 infection in primary HAECs. Here, we hypothesized that Optate treatment would decrease viral infection and replication in RSV and hMPV in primary HAECs.

Methods: We grew primary HAECs from healthy subjects, infected them with RSV or hMPV tagged with green fluorescent protein (RSV-GFP1 or MPV-GFP1, ViraTree), and used 120 mM Optate (concentrations used in humans *in vivo*) to determine whether Optate would prevent viral infection and replication. GFP-RSV or GFP-MPV (multiplicity of infection = 1) and Optate or PBS control were co-administered to HAECs. Supernatant from the infected cells was collected after a 4-hour incubation period and then every 24 hours for 3 days. Viral infection and replication were determined with fluorescence quantification, immunoblot assays, enzyme-linked immunosorbent assay (ELISA), and fluorescent particle counts via plaque assays.

Results: RSV and hMPV infection was significantly lower in cells treated with Optate compared to control, demonstrated by a significant decrease in fluorescence intensity (**Figure**). Additionally, RSV plaque-forming units significantly decreased in Optate-treated cells (p=0.0011). Finally, GFP protein levels significantly decreased when measured by western blot analysis and ELISA after Optate treatment (p=.0014 and p=.0023, respectively).

Conclusion: Optate inhibits RSV and hMPV infection in primary HAECs, similar to its inhibition of SARS-CoV-2. Our findings suggest that Optate may have potential as an inhaled therapeutic for patients with RSV or hMPV. Furthermore, these findings suggest that Optate may be suitable for a proof-of-concept clinical trial to evaluate airway pH modulation as a treatment for RSV or hMPV infections and their related asthma exacerbations.
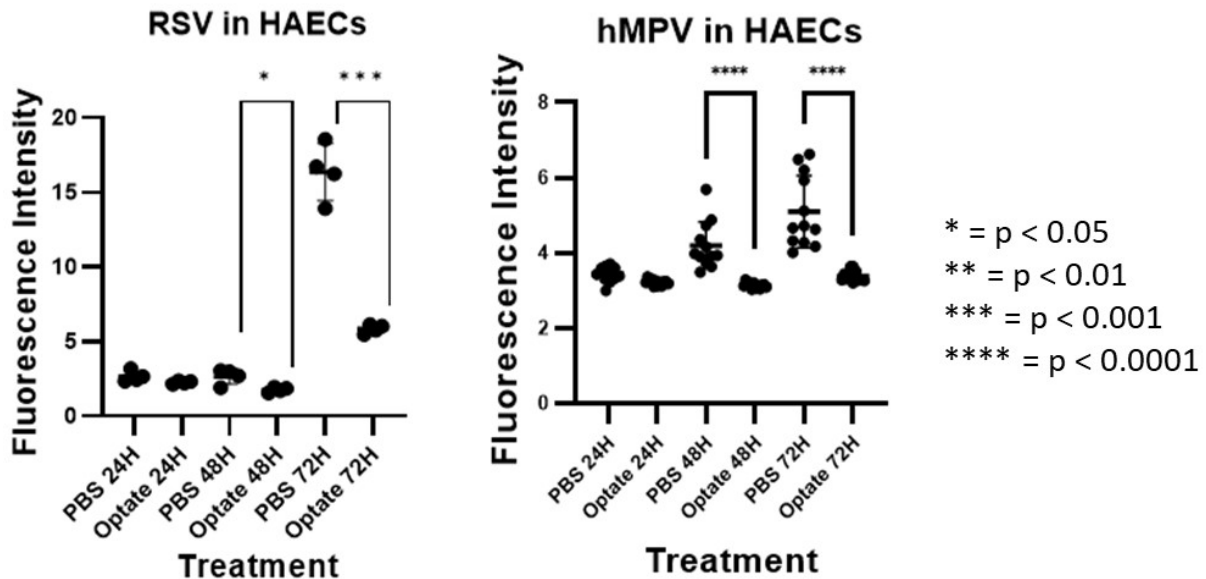
Optate decreases respiratory syncytial virus (RSV) and human metapneumovirus (hMPV) infection in human airway epithelial cells. ImageJ software was used to quantify fluorescence intensity, which is significantly decreased in the Optate-treated groups at 48-h and 72-h in RSV and hMPV infection models (*p<0.05, * **p < 0.001,* ***p < 0.0001).

820

Contribution of High Mobility Group Box 1 to Nicotine-Induced Podocyte Injury and Glomerular Sclerosis

Sayantap Datta[1], Goverdhan Puchchakayala[1], Mohammad Atiqur Rahman[1], Sai S. Koka[2], Krishna M. Boini[1]

University of Houston[1] Texas A & M University[2]

Cigarette smoking, a well-established risk factor for many diseases, plays a pivotal role in the incidence and progression of renal dysfunction. Smoking associated renal damage bears distinct physiological correlations in conditions such as diabetic nephropathy and obesity-induced glomerulopathy. However, the cellular and molecular basis of such an association remains poorly understood. High mobility group box 1 (HMGB1) is a highly conserved non-histone chromatin associated protein that largely contributes to the pathogenesis of chronic inflammatory and autoimmune diseases such as sepsis, atherosclerosis, and chronic kidney diseases. Hence, the present study tested whether high mobility group box 1 (HMGB1) contributes to nicotine-induced podocyte injury and glomerular sclerosis. In *in vitro*, biochemical analysis showed that nicotine treatment significantly increased the HMGB1 release compared to vehicle treated podocytes. However, prior treatment with glycyrrhizin, an HMGB1 binder abolished the nicotine-induced HMGB1 release in podocytes. Furthermore, western blot or immunofluorescent analysis showed that nicotine treatment significantly decreased the expression of nephrin and podocin compared to control cells. However, prior treatment with glycyrrhizin attenuated the nicotine-induced nephrin and podocin reduction. In addition, nicotine treatment significantly increased the toll like receptor 4 (TLR4), desmin expression and cell permeability compared to vehicle treated podocytes. However, prior treatment with glycyrrhizin attenuated the nicotine induced TLR4, desmin expression and cell permeability. In *in vivo* studies, Western blot and biochemical analysis showed that nicotine treatment significantly increased the HMGB1, TLR4, urinary protein, urinary albumin, glomerular damage index in nicotine treated mice compared to control mice. However, such nicotine-induced increase of HMGB1, TLR4, urinary protein, urinary albumin and glomerular damage index was significantly attenuated in glycyrrhizin treated mice. Based on these results, it is concluded that HMGB1 is one of the important mediators of nicotine-induced podocyte injury and glomerular sclerosis.

821

Associations Between Proinflammatory Cytokines, Laboratory-evoked Pain, and Opioid Response Profiles in Healthy Human Subjects

William Davis[1], Ami Mange[2], Nicole Brown[1], Yi Xie[3], Emma Patillo[3], Jennifer Ellis[3], Kelly Dunn[3]

Johns Hopkins School of Medicine[1] Yale School of Medicine[2] Johns Hopkins University[3]

Proinflammatory cytokines are recognized as key mediators in the initiation as well as persistence of pain via a variety of proposed mechanisms, such as direct activation of nociceptors, and peripheral and central sensitization of pain. However, little is known regarding how the role cytokines play in the acute pain response in the setting of opioid medications.
This study examines associations between cytokine levels and laboratory-evoked pain, as well as subjective response to the prototypic opioid hydromorphone (versus placebo) in healthy human subjects.

This was a double-blind, randomized, placebo-controlled within-subject comparison of the prototypical opioid hydromorphone vs placebo in healthy and opioid naïve men (N=50) and women (N=50). Participants completed quantitative sensory testing (QST) laboratory-based pain testing prior to admission to a residential research unit and blood samples were collected for cytokine analysis pre and post baseline QST. Participants then received hydromorphone (oral) and placebo using a within-subject design during study days 2-5. Blood samples were analyzed for the proinflammatory cytokines IFN-y, TNF-alpha, the interleukins IL-2, IL-4, IL-6, IL-8, IL-10, IL-12, IL-13, and the immunoglobulins IgA, IgG, and IgM. Cytokine levels at baseline and post-initial QST, as well as the magnitude of change between pre/post ratings were compared against response during QST and following subsequent hydromorphone dosing[AM1] .

Participants were 33.7 (SD=9.1) years old, 38% Caucasian/White, 46% Black/African American, 5% Asian, and 8% of Hispanic ethnicity. Of the 10 cytokines tested, only baseline levels of IL-6, showed any association with primary outcomes, in addition to the immunoglobulins IgA, IgG, and IgM. The levels of

these immunoglobulins at baseline were the most likely to be associated with various QST outcomes. However, neither the values post-QST nor the magnitude of change between baseline and post-QSR were meaningfully or reliably associated with QST response. Regarding the experience of hydromorphone, baseline IL-6 levels were significantly associated with having a more positive experience of hydromorphone as evidenced by greater ratings on positive reports (Drug Effects ($r(309)=.15$, $p<.01$), Good Effects ($r(309)=.15$, $p<.01$), High ($r(309)=.22$, $p<.01$), Like How I Feel ($r(309)=.18$, $p<.01$), and Talkative ($r(309)=.15$, $p<.01$). IL-6 levels were not associated meaningfully with negative reports (e.g., Bad Effects ($p=.71$), Nausea ($p=.19$)).

These data suggest that baseline levels of immunoglobulins IgA, IgG and IgM (but not the interleukin cytokines) may be differentially associated with response to laboratory-evoked pain (e.g., QST). However, the magnitude of change in cytokine response was not reliably related to the severity of pain evoked by QST. Data also provide initial evidence that higher baseline levels of IL-6 may confer a more positive experience relative to lower IL-6 levels. More focused research examining the contribution of IL-6 to individual variation in response to opioid medications is warranted.

822

Diverse Pathways in GPCR-mediated Activation of Ca^{2+} Mobilization in HEK293 Cells

Francesco F. De Pascali, Sushrut D. Shah, Jeffrey L. Benovic

Thomas Jefferson University

GPCRs are dynamic proteins that transduce extracellular stimuli into intracellular signaling pathways to ultimately induce a cellular response. Ca^{2+} mobilization is a well-known second messenger that can be induced by GPCR activation. The primary canonical pathway for GPCR-promoted Ca^{2+} mobilization involves Ga$_q$-mediated activation of phospholipase Cb (PLCb), while G$_{bg}$ subunits from activated G$_i$ can also induce Ca^{2+} mobilization through PLCb. Since previous studies support a role for G$_s$ in b$_2$-adrenergic receptor (b$_2$AR)-mediated activation of Ca^{2+} mobilization, here we evaluated whether different G$_s$-coupled receptors endogenously expressed in HEK293 cells utilized common pathways for mediating Ca^{2+} mobilization. For the b$_2$AR, we found an essential role for G$_q$ in mediating agonist (isoproterenol or formoterol) promoted activation of Ca^{2+} mobilization while disrupting G$_s$ using DGa$_s$ cells or G$_i$ using pertussis toxin (PTX) had no effect on this process. b-agonist promoted Ca^{2+} mobilization was also effectively blocked by the b$_2$AR-selective inverse agonist ICI 118,551 as well as the G$_q$-selective inhibitor YM-254892 (YM) and was not observed in DGa$_{q/11}$ cells. BRET analysis also revealed agonist-dependent association of b$_2$AR-Rluc with Nes-Venus-mG$_q$. We also evaluated Ca^{2+} mobilization through the endogenous prostaglandin E receptors EP2 and EP4 in HEK293 cells. EP2 has been reported to selectively couple to G$_s$ while EP4 couples to G$_s$ and G$_i$. When activated by their selective agonists, both EP2 and EP4 were able to induce Ca^{2+} mobilization in HEK293 cells. The EP2 response was pertussis toxin sensitive but YM insensitive, while EP4 was sensitive to both PTX and YM. Interestingly, both EP2 and EP4 were largely unable to induce Ca^{2+} mobilization in DGa$_s$ cells supporting a strong dependency of these receptors on G$_s$ signaling in HEK293 cells. Taken together, we identify differences in the signaling pathways that are utilized to mediate Ca^{2+} mobilization in HEK293 cells. The b$_2$AR primarily utilizes G$_q$, EP2 uses G$_s$ and G$_i$, and EP4 appears to utilize G$_s$, G$_i$ and G$_q$. Further characterization in other cellular models will be important to address the contribution of system bias to GPCR signaling.

823

Activation of neutrophil elastase-related serine proteases in myelomonocytic cells

Roxane Domain[1], Brice Korkmaz[2]

CEPR[1] Centre d'Etude des Pathologies Respiratoires, INSERM U1100[2]

Elastase, proteinase 3, cathepsin G and NSP4 (Neutrophil Serine Protease 4) are pro-inflammatory serine proteases found within the granules of promyelocytes during neutrophil differentiation in the bone marrow. The vast majority of NSPs are activated by cathepsin C and, to a much lesser degree, by NSPs-AAP-1 (NSP-Alternative Activating Protease-1) from their inactive precursor forms via proteolytic cleavage of their prodipeptides. In this work, we investigated the respective roles of cathepsin C and NSPs-AAP in the activation of NSPs in pro-monocytic cell lines (U937, THP-1) and in primary monocyte-derived macrophages. In U937 cells, we observed a neutrophil-like activation of NSPs involving cathepsin C and NSPs-AAP-1. In THP-1 cells, elastase and proteinase 3 were generated by cathepsin C and a unknown protease called NSPs-AAP-2, while cathepsin G was activated by cathepsin C. Furthermore, we showed that active forms of proteinase 3 and cathepsin G were not stable and proteolytically degraded in THP-1 cells, which explains the relatively low abundance of these NSPs in this cell line, compared to other myelomonocytic cells. In conclusion, our study shows that NSP activation in myelomonocytic cells is cell type-dependent and more importantly, that the human genome contains at least three proteases involved in NSP activation.

824

Structure-Based Design and Synthesis of Potent and Selective Serine/threonine Kinase Inhibitors from a Marine Natural Product Pharmacophore

Lin Du[1], Brice Wilson[1], Rohan Shah[1], Ning Li[1], Masoumeh Dalilian[1], Juliana M. Fiesco[1], Emily A. Smith[1], Antony Wamiru[1], Ekaterina I. Goncharova[2], Ping Zhang[1], Barry O'Keefe[1]

National Cancer Institute[1], Leidos Biomedical Research, Inc. [2]

The aplithianines A and B, bearing an unusual purine-thiazine-imidazole linked skeleton, represent a new class of marine-derived kinase inhibitors with potent inhibition of select serine/threonine kinases in the CLK and PKG families. Structure-based design strategies were applied to improve the potency of aplithianines targeting the rare oncogenic protein kinase A fusion protein J-PKAcα. A virtual library of over 2000 aplithianine analogs was screened by molecular docking using the J-PKAcα: aplithianine A co-crystal structure (PBD ID# 8FE2). The analog design was further evolved through bioisosteric replacement targeting several "Hotspots" within the aplithianine A binding pocket including the conservative "DFG" region. A series of potent apltithianine analogs with improved docking scores were synthesized and evaluated in an in-house biochemical assay against the J-PKAcα catalytic activity. The potency of the synthetic analogs was significantly improved from low-micromolar range (e.g. IC_{50} ~1 μM, aplithianine) to single-digit nanomolar range. Several synthetic analogs also showed cellular cytotoxicity (IC_{50}s 1-10 μM) against the COLO 741 human colon carcinoma cell line that has been reported to be sensitive to known PKA inhibitors. Further optimization of the "drug-like" properties of aplithianines is currently ongoing to improve their cellular activity.

825

Targeting Adenylyl Cyclase 1 for Development of Non-Opioid Pain Therapeutics

Tiffany Dwyer, Camryn Fulton, Shrinidhi Annadka, Brenton Smith, Val Watts, Daniel Flaherty

Purdue University

Treatment for chronic pain is limited, with opioids being the most efficacious analgesics for many types of chronic pain. Opioids activate the μ-opioid receptor (MOR), which in part, mediates analgesic activity via inhibition of adenylyl cyclase 1 (AC1), an enzyme that catalyzes conversion of ATP to cAMP, a second messenger. Additionally, MOR activation causes β-arrestin-mediated MOR internalization and subsequent tolerance. We hypothesize that targeting AC1 directly could avoid MOR-related side effects. AC1 has been implicated as a novel non-opioid target for treatment of chronic pain. AC1 is highly expressed in the brain and its activity is increased following inflammatory stimuli. Further, AC1 knockout (KO) mice had significantly reduced responses to inflammatory stimuli compared to wild-type (WT) mice. Knockout of AC8, a closely related isoform, had no effect compared to WT, whereas AC1/AC8 double KO caused memory deficits. Thus, selectively targeting AC1 represents an opportunity to develop non-opioid pain therapeutics with minimal side effects.

Our group previously identified a pyrimidinone-pyrazolyl-benzamide scaffold that selectively inhibits AC1 signaling in HEK Δ3/6 KO cells expressing AC1. The benzamide series suffered from poor solubility, however, medicinal chemistry efforts developed a pyrimidinone-pyrazolyl-benzylamine (PBL) scaffold with markedly improved aqueous solubility. Through further SAR of the PBL series, inhibition of AC8 was eliminated to reach nearly complete AC1 versus AC8 selectivity. Our lead analogs maintain full AC1 inhibition, with improved potencies of ~100 nM. Additionally, our lead analogs maintain selectivity versus other AC isoforms (AC2 and AC5), and display minimal cytotoxicity. For preclinical development, lead analogs have been investigated for metabolic stability and blood-brain barrier (BBB) penetration. *In vivo* plasma pharmacokinetics (PK) experiments in rats revealed moderate clearance. The *in vivo* BBB PK experiments in rats demonstrated that lead analogs accumulate to their IC_{50} concentrations in the brain up to 1 hour, and also maintain *in vivo* anti-allodynic activity.

Additional *in vitro* studies have explored the impact of our lead molecules on opioid receptor signaling in unique cellular models. The first model used CHO cells expressing the MOR and β-arrestin2 (βarr2), with or without AC1 (CHO-MOR-βarr2 or CHO-MOR-βarr2-AC1). Our second model used SH-SY5Y neuroblastoma cells, virally expressing AC1 and the MOR. In both models, AC1 expression was validated by selectively stimulating AC1 activity with A23817. This activity was then inhibited by an AC1-selective inhibitor, ST034307. MOR expression was validated by treating with the MOR agonist DAMGO, which dose-dependently inhibited cAMP accumulation. The CHO-MOR-βarr2-AC1 model was specifically used to assess the effects of the PBL analogs on MOR-mediated βarr2 recruitment. Both cellular models were then used to assess the effect of lead analogs on MOR-mediated cAMP inhibition, MOR-regulated Gβγ signaling, MOR desensitization, and MOR-induced heterologous sensitization. These experiments serve as validation that the PBL analogs do not modulate MOR-dependent signaling, but display similar efficacy to the MOR on AC1 inhibition and can prevent sensitization. This work provides *in vitro* translational cellular models from HEK293 and CHO cells to a model of neuronal function.

826

PACAP(6-38) Deletants as Peptide-based PACAP Antagonists

Wenqin Xu[1], Abigail Keith[1], Wenjuan Ye[2], Xin Hu[2], Giuseppe Deganutti[3], Mark Henderson[2], Patrick Sexton[4], Lee Eiden[5] *(poster presented by Lee Eiden)*
NIMH, NIH[1] NCATS, NIH[2] Coventry University[3] Monash Institute of Pharmaceutical Sciences[4] NIMH-IRP[5]

The receptor for pituitary adenylate cyclase-activating polypeptide (PACAP) is a Gs-coupled GPCR, designated PAC1. Antagonists of this receptor are being pursued for their potential to ameliorate atherosclerogenesis, depression, post-traumatic stress disorder, and migraine; discovery of agonists is also of interest for countering the neurodegenerative consequences of stroke and ischemia. However, obtaining small-molecule ligands (SMOLs) for this receptor has been challenging. Peptide-based antagonists include an N-terminally truncated version of PACAP38 (P38) itself, PACAP6-38 (P6-38). The

activity of P6-38 as an antagonist is consistent with models of PACAP binding to PAC1 in which the N-terminus of PACAP is required for receptor activation leading to signaling through the Gs protein, while the C-terminus is involved in initial binding (affinity-trapping) to PAC1. P6-38 has been shown repeatedly to block the action of P38 as well as the naturally occurring ligand PACAP1-27 (P27) both in vivo and in cells expressing endogenous PAC1. Several SMOLs reported to be PAC1 antagonists in the literature were tested for antagonist activity in HEK293 cells expressing the human PAC1 receptor and a cAMP biosensor (CBS)-based cAMP detection system; however not only these but also P6 -38 were without inhibitory effect in this assay system. Accordingly, we re-tested the inhibitory activity of P6-38 against both P27 and P38 in cells expressing CBS but with native expression of PAC1: the rat NS-1 pheochromocytoma cell line, and the human SH-SY5Y neuroblastoma cell line. Both CBS-based luminescent read-out, and generation of cAMP provoked by exposure to EC50 concentrations of P27 or P38 (0.2 nM) were blocked by 1 mM P6-38 which also blocked downstream signaling effects (neuritogenesis) of P27 and P38.

Recently, cryo-EM structures of a number of family B (secretin family) GPCR-ligand structures have been obtained, allowing detailed molecular dynamics analysis of ligand-receptor binding, and prediction of residues contributing most strongly to ligand engagement. Molecular dynamics simulations predicted initial receptor engagement with residues 6-30, but not 31-38, of P38. Accordingly, we synthesized a series of deletants of PACAP6-38 and tested their relative inhibitory potency in SH-SY5Y and NS-1 cells. PACAP6-30 (IC50 ~33 nM) was nearly as potent as PACAP6-38 (IC50 ~21 nM) as an inhibitor of cyclic AMP elevation by 0.2 nM P38 (the approximate EC50 for both the CBS-based and the direct cAMP assay, both carried out in the presence of phosphodiesterase inhibition by IBMX). PACAP6-27 was considerably less potent (IC_{50} >10 mM). Thus, the affinity-trap model for PAC1-ligand interaction successfully predicts the behavior of peptide-based inhibitors of P27 and P38 engagement with an endogenously expressed PAC1 receptor. We are currently engaged in peptide modification of P6-30 in order to increase the potency of this PAC1 antagonist.

827

Intestinal Dysbiosis Alters Seizure Burden and Antiseizure Medicine Activity Profile in the Theiler's Virus Model of Acute Encephalitis

Inga Erickson[1], Dannielle K. Zierath[1], Stephanie Davidson[1], Seongheon Rho[1], Kristen Peagler[1], Kenneth E. Thummel[1], Aaron Ericsson[2], Melissa Barker-Haliski[1]

University of Washington[1] University of Missouri[2]

Rationale: Brain infection with Theiler's murine encephalomyelitis virus (TMEV) in C57BL/6J mice models infection-induced acute seizures and epileptogenesis. Diet manipulation can modify the presentation of acute seizures in TMEV-infected mice (Zierath et al, BioRxiV 2023); however, no study has yet assessed whether antibiotic-induced intestinal dysbiosis influences the activity of antiseizure medicines (ASM) in the TMEV model. Whether the gut microbiome influences the phenotype of symptomatic seizures after TMEV infection is also unclear. We thus sought to define the extent to which antibiotic administration influences acute seizure presentation, the activity of ASMs, and the pharmacokinetic profile of ASMs in this mouse seizure model.

Methods: Male C57BL/6J mice (4-5 weeks-old) received a broad-spectrum antibiotic cocktail (ABX) containing ampicillin, metronidazole, neomycin sulfate, and vancomycin (n=55) or vehicle (n=60) by oral gavage once daily beginning at arrival (Day -2) to Day 7 post-TMEV infection. Mice were infected with either intracerebral TMEV or PBS on Day 0. Mice received carbamazepine (CBZ; 20 mg/kg, i.p.) or vehicle (0.5% MC) twice daily Days 3-7 p.i. and were assessed for handling-induced seizures 30 min after CBZ treatment. Plasma samples were collected on Day 7 p.i. at 15 and 60 min post-CBZ treatment to quantify the extent to which ABX-induced gut dysbiosis influences ASM pharmacokinetics.

Results: TMEV infection induced acute symptomatic seizures, regardless of pretreatment and ASM history as 18/25 (72%) ABX-CBZ mice, 7/20 (35%) ABX-VEH mice, 7/20 (35%) SAL-CBZ mice, and 15/20 (75%) SAL-VEH mice presented with seizures during the 7-day monitoring period. Average seizure burden was: 12.5 in ABX-CBZ, 4.7 in ABX-VEH, 5.7 in SAL-CBZ, and 16.1 in SAL-VEH mice. There was a significant pretreatment x ASM interaction ($F_{(1, 81)} = 16.0$, $p=0.0001$), with post-hoc tests revealing marked differences in seizure burden in SAL- versus ABX-pretreated mice ($p=0.004$). Further, the latency to Stage 5 seizure was substantially increased by CBZ during days 3-7 post-infection; an effect absent in ABX-treated mice similarly administered CBZ. In TMEV-infected mice, spleens were 0.32% of body weight in ABX-CBZ mice, 0.34% in ABX-VEH mice, 0.36% in SAL-CBZ mice, and 0.38% in SAL-VEH mice. In sham-infected mice, spleens were 0.45% of body weight in ABX-CBZ mice, 0.65% in SAL-CBZ mice, and 0.36% in SAL-VEH mice. Plasma CBZ concentrations in TMEV-infected mice receiving ABX were 9.8±2.0 mg/mL 15 min post-dosing and 4.0±0.5 at 60 min post-dose, consistent with published CBZ plasma concentrations in mice (Bialer et al, 2004) suggesting no pharmacokinetic differences because of ABX history.

Conclusions: Gut dysbiosis markedly alters the presentation of symptomatic seizures and acute disease burden in the TMEV mouse model, reflecting a novel therapeutic target for seizure control. The gut-brain axis is an understudied target in epilepsy that may benefit from greater investigation.

828

C-Path's Translational Therapeutics Accelerator: A Unique Solution to Successfully Bridge the Valley of Death in Academic Drug Discovery and Development

Maaike Everts, Mark Drew, Michelle Morgan, Kyla Oetting

Critical Path Institute

It is estimated that University affiliated research groups contributed to ca. 13% of FDA-approved new medical entities (NMEs) over the past 30 years. Despite this, academic-originated basic science often fails to convert into meaningful therapies for patients. Reasons include: funding shortfalls, translational failure, knowledge gaps concerning how to progress drug candidates or lack of repeatability of results. This failure to advance basic scientific discoveries into real-world patient impact has been termed the 'valley of death'. Critical Path Institute (C-Path) established the Translational Therapeutics Accelerator (TRxA), to provide both funding and access to research experts and regulatory scientists, to help academic groups successfully advance novel therapeutics in areas of high unmet medical need.

C-Path is an independent nonprofit, public-private partnership with the FDA, created under the auspices of the FDA's Critical Path Initiative program in 2005. TRxA is a disease agnostic, global drug discovery and development program, which supports early-stage programs in academia from early lead development to IND-enabling studies. TRxA offers resources and hands-on guidance, to develop comprehensive data packages for drug candidates, a key to garnering interest from biotechnology and pharmaceutical companies to invest in clinical trials.

We will present the TRxA funding opportunity, outlining the potential for academic researchers to move their discovery programs to key inflection points. Entry criteria for funding levels and stage-gated indicators of success will be presented.

TRxA is currently funded through a generous grant from the Frederick Gardner Cottrell Foundation
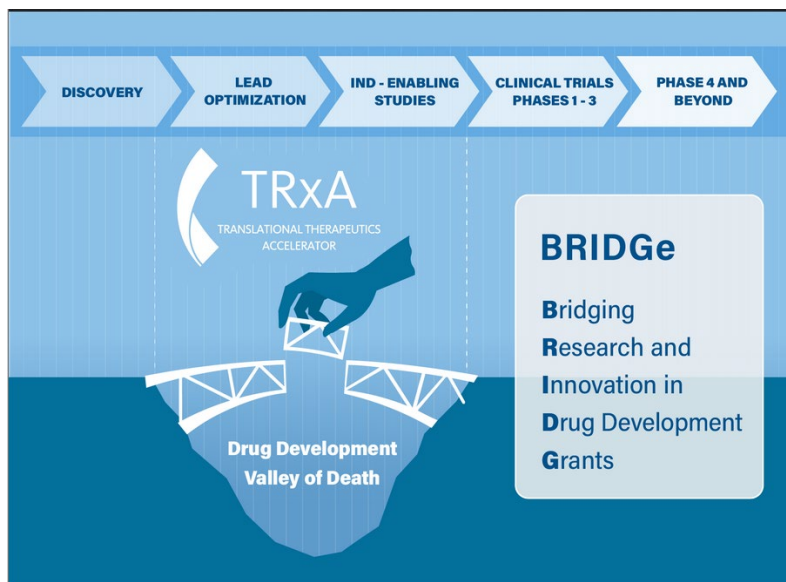
829

The Neuropeptide Receptor GPR83 Regulates Anxiety-Like Behavior

Amanda Fakira, Danya Aldaghma

Cooper Medical School of Rowan University

Anxiety disorders are prevalent in our society, one critical stressor of growing impact is social isolation. While our environment has seemingly become more connected due to technological advances, young adults are becoming more isolated socially. Loneliness and social isolation during the critical developmental period of adolescence is likely to have long-lasting impacts on brain chemistry and connectivity. In fact, there are recent reports indicating that isolation in adolescents had significant effects on the overall health, feelings of anxiety, as well as nicotine and alcohol intake. GPR83, whose endogenous ligand is a neuropeptide called PEN, was first identified as a protein regulated by the glucocorticoid dexamethasone, indicating that this receptor may play role in stress-responses. GPR83 expression is reduced mice treated with the glucocorticoids, corticosterone and dexamethasone. Knockdown of GPR83 in the BLA increases anxiety-related behaviors. Recently, we discovered novel small molecule ligands for GPR83, including Cpd 1(agonist) and Cpd 25 (antagonist), unveiling new avenues to investigate the biological role of this receptor. We are investigating whether treatment with Cpd 1 or Cpd 25 impacts anxiety-related behaviors in mice that were housed in isolation during adolescence.

830

Pharmacological potentiation of M4 muscarinic acetylcholine receptors suppresses excessive grooming in SAPAP3 knockout mice

Daniel Foster[1], Curran Johnston[1], Daniel Joyner[1], Yumin Choi[1]

University of South Carolina School of Medicine[1]

Repetitive behaviors are observed in numerous psychiatric and neurodevelopmental disorders, including obsessive-compulsive disorder (OCD) and autism spectrum disorder. The striatum is a brain region that has been demonstrated to play a critical role in regulating numerous different behaviors, including action selection and habitual behavior, and it is hypothesized that the striatum is a key hub for regulating repetitive behaviors. Acetylcholine signaling in the striatum can robustly modulate striatal physiology via numerous mechanisms, including regulation of striatal dopamine release and regulation of synaptic plasticity. Here, we examined grooming in SAPAP3 knockout mice that display an excessive grooming phenotype. Examining grooming in these mice is a measure of repetitive, self-directed, and patterned behavior and has the potential to inform studies that will further our understanding of how specific brain circuits regulate these behaviors. We found that administration of a positive allosteric modulator (PAM) with high selectivity for the M4 subtype of muscarinic acetylcholine receptor was able to normalize grooming in SAPAP3 knockout mice with little to no effect on grooming in WT littermates. Furthermore, this reduction in grooming was observed at doses (1mg/kg or less) that did not affect other active behaviors such as darting and rearing. In addition, we found that evoked dopamine signaling was enhanced in the dorsomedial striatum, but not the dorsolateral striatum, of SAPAP3 knockout mice using fast-scan cyclic voltammetry approaches. These studies suggest that M4 PAMs, a highly validated drug target for mediating antipsychotic-like effects, may also represent a novel therapeutic strategy for treating repetitive behaviors. Further studies using fiber photometry are being performed to determine the relationship between dopamine signaling and these repetitive behaviors and determine the mechanism whereby M4 PAMs suppress excessive grooming in SAPAP3 knockout mice.

831

Optimizing positive allosteric modulators to selectively target the high sensitivity (α4)2(β2)3 nicotinic acetylcholine receptor

Pradip Gadekar[1], Josue Gaona[2], Sahil Seth[1], Harvens Beauzile[1], Wilder Felix[1], M. Imad Damaj[3], Christie Fowler[4], Ganesh Thakur[1], Ayman Hamouda[2]

Northeastern University[1] The University of Texas at Tyler[2] Virginia Commonwealth University[3] University of California-Irvine[4]

Addiction to tobacco and nicotine products remains a leading cause of disease and death worldwide, and an increasing number of never-smokers are being exposed to nicotine via e-cigarettes. With only a few moderately efficacious smoking-cessation therapeutics available, achieving long-term abstinence from nicotine addiction is an unattainable goal for millions. The role of brain nicotinic acetylcholine receptors (nAChRs) in nicotine's behavioral effects leading to tobacco addiction is well recognized. However, the neurobiological basis underlying the role of specific nAChRs in nicotine's behavioral effects remains poorly understood. Our recently published findings have emphasized the role of the high-sensitivity isoform of the α4β2 nAChRs (the HS (α4)2(β2)3 nAChR) in nicotine-associated behavior. Therefore, our current efforts are focused on the development of novel positive allosteric modulators (PAMs) that selectively target the HS (α4)2(β2)3 nAChR for in vivo applications to probe the function of this major nAChR subtype as well as for potential therapeutic applications as smoke-cessation aid. Unlike classical nAChR agonists, which bind at the evolutionary conserved ACh binding site, PAMs bind to sites that are less conserved and potentially unique to the HS (α4)2(β2)3 nAChR making the subtype selectively more attenable. In addition, PAMs act only in the presence of the endogenous neurotransmitter, minimizing tonic activation, desensitization, receptor upregulation, and alteration in the pattern of cholinergic synaptic transmission seen with nAChR agonists. Using three nAChR PAM pharmacophores and computational ligand docking predictions, we synthesized a series of derivatives and examined their nAChR PAM activities (ability to enhance ACh-induced current responses) in vitro. Candidates with potent and efficacious in vitro HS (α4)2(β2)3 nAChR PAM activities are currently being evaluated for their ability to reduce nicotine self-intake and withdrawal symptoms in mice.

832

CDK Inhibition Impairs RNA Splicing: A Novel Therapeutic Approach for Merkel Cell Carcinoma

Khalid Garman[1], Tara Gelb[1], Dimitrios Anastasakis[1], Sarah Davies[1], Ahsan Polash[1], Matthew Hall[2], Markus Hafner[1], Isaac Brownell[1]

National Institute of Arthritis and Musculoskeletal and Skin Diseases[1] National Center for Advancing Translational Sciences[2]

Merkel cell carcinoma (MCC) is a rare, aggressive neuroendocrine skin cancer with a high case fatality rate. Currently, immune checkpoint inhibitors (ICI) are the first line of treatment for metastatic MCC, but 50% of patients do not achieve durable responses. To identify novel treatments for MCC, we screened 4,000 compounds for their ability to reduce MCC viability. Using the Area Under the Dose-Response Curve, we identified CDK inhibitors as efficacious against multiple MCC cell lines. *In vitro* studies demonstrated that CDK inhibition induced MCC cell death accompanied by cell size reduction, cell cycle arrest, DNA damage, and apoptosis. Further mechanistic studies using RNA-seq and phosphoproteomics in MCC cells surprisingly revealed that immediate effects of CDK inhibition included mRNA splicing defects resulting in accumulation of retained intron transcripts. *In vivo*, CDK inhibition significantly slowed tumor growth in a pre-clinical xenograft mouse model of MCC. Overall, our studies identified CDK inhibition as a promising novel treatment approach for MCC and support a clinical trial of CDK inhibitors in patients whose MCC has progressed despite ICI therapy.

833

Novel compounds that target epoxyeicosanoids protect rat kidney epithelial cells in organ transplant solution during cold storage

Samaneh Goorani[1], John Falck[2], Bruce Hammock[3], Eugen Proschak[4], Daniel Merk[5], Nirmala Parajuli[6], John Imig[7]

Univ of Arkansas[1] Department of Biochemistry, UT Southwestern Medical Center, Dallas, TX, USA[2] Department of Entomology, University of California Davis, Davis, CA, USA[3] Institute of Pharmaceutical Chemistry, Goethe University of Frankfurt, Frankfurt, Germany[4] Department of Pharmaceutical and Medicinal Chemistry, Ludwig Maximilian University of Munich, Munich[5] Univ of Arkansas for Medical Sciences[6] Departments of Pharmaceutical Sciences, Pharmacology & Toxicology, University of Arkansas for Medicine[7]

Background: Organ preservation solutions have been applied to diminish hypoxic injury during cold storage and subsequent re-warming (CS-RW), and this improve graft survival during kidney transplantation. Despite significant progress in the development of organ preservation solution and hypoxic injury mitigation, poor graft survival is still common. We studied 9 compounds that targets eicosanoid and nuclear receptor signaling on the adverse effects of CS-RW on normal rat renal epithelial cells (NRK-52E) and tested the hypothesis that these compounds have cytoprotective effects during CS-RW.

Methods: Kidney epithelial NRK-52E cells were incubated in University of Wisconsin (UW) solution at 4°C for 18h contained vehicle (0.1% DMSO, vehicle-CS-RW) or the test compounds (1, 3, and 10µM) in triplicates (n=6-9/group). Following18h cold exposure (CS), cells were washed off treatments and UW sooution and grown in cell culture medium at 37^0C for 6h (RW). Two epoxyeicosatrienoic (EET) acid mimetics, three multi-target drugs, one soluble epoxide hydrolase inhibitor (sEHi), one sEH phosphatase inhibitor (sEH-Pi), and two hydroxyeicosatetraenoic acid (20-HETE) antagonists were tested at 1, 3, and

10mM. Cell counting kit-8 (CCK-8) and CellTiter-Glo® 2.0 Cell Viability (CellTiter-Glo assay) assays were conducted to determine cell viability, and the number of the viable cells is expressed as % of cells of that were incubated in normal cell growth conditions without cold storage (control).

Results: Cell viability in control and vehicle-CS-RW was similar when analyzed with CCK-8 (89± 1 & 87 ± 1 %) or CellTiter-Glo(91± 2 & 91 ± 1 %) assays. Four compounds demonstrated cytoprotective effects comparable to SB202190, p38 MAPK inhibitor that is known to protect renal epithelial cells and kidneys during CS-RW. SB202190 maintained cell viability at 107 ± 3 and 113± 2% of control, in CCK-8 and CellTiter-Glo assays; respectively. Irrespective of the cell viability assay type, the EET mimetics demonstrated the strongest NRK-52E cytoprotective effects, followed by a sEH-Pi, and a dual sEHi / COX2 inhibitor. At 10µMconcentration, EET-A maintain maximum viable cell numbers at 100 ± 2 % (CCK-8) & 109 ± 1% (CellTiter-Glo assay) of control and SWE, a sEH-Pi maintain cell viability at 108 ± 2% (CellTiter-Glo assay) at 10µM concentration. Also, EET-C, an EET mimetic demonstrated strong cytoprotective effect and maintain cell viability at 96 ± 3 % (CCK-8; 3µM) & 104 ± 1% (CellTiter-Glo assay; 1µM) of control; respectively. Multi-target drug PTUPB that simultaneously acts as sEHi and cyclooxygenase-2 (COX-2) inhibitor, protected NRK-52E cells from CS-RW with lesser cytoprotective action. PTUPB maintain maximum cell viability at 97 ± 3 % (CCK-8; 3 µM) & 100 ± 1% (CellTiter-Glo assay; 1µM). Interestingly, ompounds that inhibited 20-HETE or included nuclear receptor agonism did not improve cell viability.

Conclusion: Our findings demonstrate renal cytoprotective effects during cold storage in transplant solution of a series of compounds that acts via epoxyeicosanoid signaling. EET mimetics, sEH-Pi, and dual sEHi / COX-2 inhibitor demonstrate potential to better preserve kidneys in cold storage and improve graft survival.

834

Neuroimmune Circuitry of Midbrain Dopamine Neurons

Adithya Gopinath[1], Emily Miller[1], Elijah Freedman[1], Aidan R. Smith[1], Leah T. Phan[1], Nikhil Urs[1], Olga Guryanova[1], Daniel Wesson[1], Michael Okun[1], Habibeh Khoshbouei[2]

University of Florida[1] McKnight Brain Institute of the University of Florida[2]

Objective: Dopamine neuronal regulation of peripheral immunity has gained increased attention in neurodegenerative and neuropsychiatric diseases. Our prior studies and the literature suggest that activation or inhibition of midbrain dopamine neurons modulates the immune responses, mediated by catecholaminergic inputs to peripheral immune organs.

Knowledge Gap: The pathway(s) from midbrain to periphery by which dopaminergic neurons signal to peripheral immune organs is less understood.

Hypothesis: Based on the literature and our prior studies, we predicted that the dorsal vagal complex (DVC) mediates a ventral midbrain-to-periphery circuit for immune modulation.

Design and Methods: We employed multiple complementary approaches to map the neural circuitry between midbrain and DVC. DATcre animals received intracranial injections of Cre-dependent anterograde AAV expressing eGFP or mRuby-tagged Synaptophysin into the ventral midbrain. Brains were collected one month after injection and examined for eGFP or mRuby fluorescence in the DVC. Next, to determine whether DVC neurons can respond to dopaminergic inputs, we examined expression of DRD1 and DRD2 in the DVC, using DRD1cre and DRD2cre mice crossed to Ai9-TdTomato mice,

resulting in red fluorescent cell bodies that express these receptors. Striatum and PFC projections were examined as positive control regions throughout.

Results: Our findings so far suggest that DAT+ midbrain dopamine neurons send projections to the DVC, as indicated by eGFP+ processes, and make synapses in the DVC, as indicated by mRuby-Synaptophysin puncta in the DVC. These processes originate in Cre-expressing midbrain neurons. In addition, we found DRD1+ neurons in the nucleus of the solitary tract (NTS) and DRD2+ neurons in the area postrema (AP), which are nuclei within the DVC. These findings indicate that not only do midbrain dopamine neurons send projections to and synapse onto the DVC, but also that the DVC expresses dopamine receptors necessary to respond to midbrain dopaminergic inputs.

Ongoing Studies: We will assess how optogenetic activation of midbrain dopamine terminals in the DVC modulates DVC neuron activity. In addition, using anterograde AAVs, we will map midbrain-to-DVC projections and the subsequent projections to peripheral immune organs such as liver, bone marrow, spleen, and thymus to identify immune compartments that may be modulated by dopamine neuronal activity.

Conclusions: These studies represent a transformative step investigating the mechanistic relationships between midbrain dopamine neuronal activity and peripheral immune responses, with broad implications for neurological and neuropsychiatric conditions where dopamine signaling has gone awry.

835

Monitoring G-Protein Coupled Receptors using a Bioluminescent, Homogenous, and High Throughput Formatted Assay for cAMP, cGMP, and IP$_3$

Said Goueli[1], Kevin Hsiao[2], Dareen Mikheil[2], Nate Murray[2], Tim Ugo[2], Hui Wang[2], Matt Larsen[2]

Univ of Wisconsin and Promega Corp[1] Promega[2]

Second messengers play a major role in mediating the effect of modulators of G Protein Coupled Receptors (GPCR) in a wide range of activities in cell signaling and human health. There are more than 800 GPCRs representing one of the major cell surface receptors families and encoding 3-4% of the human genome. The three most targeted G proteins for tracking GPCR activation are Ga_s, Ga_i, and Ga_q, resulting in activation of adenylate cyclase (Ga_s), inhibition of adenylate cyclase (Ga_i) and activation of phospholipase b (Ga_q), respectively. As researchers continue to study and target these pathways, it will be critical to develop assays that accurately determine the levels of second messenger molecules using one platform. Here we present sensitive and specific bioluminescent detection systems to monitor the levels of cAMP, cGMP, and IP$_3$.

Taking advantage of splitting an engineered luciferase from deep sea shrimp (Nanoluc) which has small molecular size (19 kD) and 100-fold more luminescence than firefly luciferase, we were able to use protein complementation platform to develop assays for the second messengers cAMP, cGMP, and IP$_3$. The enzyme is split into small BiT (Sm BiT,11 amino acids, 1.3kD) and large BiT (Lg BiT, 1.7 kDa), and by linking Sm BiT to the second messenger of interest via a linker (Sensor) and Lg BiT linked to antibodies selective for the target (cAMP, cGMP, and IP3), the interaction of the small molecule with the antibody, brings the Sm BiT to the Lg BiT leading to complementation of Nanoluc and generating luminescence upon addition of the substrate. We demonstrate the utility of these systems in both enzymatic assays and cell-based assays. We have tested these assays using cells that express the appropriate GPCR for generating or inhibiting cAMP production and those that result in IP$_3$ generation. We have successfully demonstrated the detection of the second messengers using stably transfected receptors as well as endogenous receptors. We also tested these assays for determining the potency of selective phosphodiesterase inhibitors for cGMP-PDE and cAMP-PDE and these assays yielded IC$_{50}$ values that are very similar to those reported in the literature.

These assays are easy to perform, homogeneous, highly sensitive, minimal, or no false hits, and compatible with high throughput formats. It is anticipated that these assays will be of significant value to aid in further understanding the role of second messenger signaling in physiology and support further drug discovery efforts towards the treatment of human disease.

836

The H$_2$S-releasing donor N-acetylcysteine may attenuate myocardial ischemia reperfusion induced acute lung injury via upregulating pulmonary Neuregulin-1

Yanjing He[1], Jiajia Chen[2], Chen He[1], Zhiming Shen[1], Yin Cai[3], Zhengyuan Xia[4]

Shenzhen Baoan Shiyan People's Hospital[1] Affiliated Hospital of Guangdong Medical University[2] The Hong Kong Polytechnic Univ[3] The First Affiliated Hospital of Jinan University[4]

Myocardial infarction is a leading cause of mortality globally, and prompt reperfusion of blood flow to previously ischemic myocardium can cause myocardial ischemia/reperfusion(I/R) injury. Myocardial I/R can also induce acute lung injury(ALI). The epidermal growth factor neuregulin-1(NRG-1) combines with ErbB receptors and regulates various human diseases. Previous studies showed that activation of NRG-1/ErbB signaling pathway had cardioprotective effects in myocardial I/R injury, but the activation of NRG-1/ErbB signaling pathway may increase epithelial permeability and exacerbate ALI. However, the role of NRG-1 in myocardial I/R induced ALI is unknown. Our previous study found that the donor of gasotransmitter hydrogen sulfide (H$_2$S) could upregulate NRG-1 gene expression in the lung. Antioxidant N-acetylcysteine(NAC) can also be the donor of H$_2$S. Thus, this study is aimed to explore the interplay of NRG-1 and the H$_2$S-releasing donor in the regulation of myocardial I/R induced ALI and its possible mechanisms. Here, the mouse model of myocardial I/R induced ALI was established by ligation of left anterior descending artery for 30 minutes following 2 hours reperfusion. H9c2 cardiomyocytes or MLE-12 epithelial cells hypoxia/reoxygenation(H/R) was established by exposing cells to glucose deprivation and hypoxia for 10 hours following 6 hours reoxygenation. We found that mRNA level of cystathionine-γ-lyase(CTH), the catalyzing enzyme of H$_2$S, was downregulated in both myocardial infarction tissue and lung after induction of myocardial I/R injury compared with control. By contrast, NRG-1 mRNA level did not significantly differ in heart tissue between the myocardial I/R group and the control group, while NRG-1 mRNA was significantly upregulated in the lung tissue after myocardial I/R injury that was coincident with post-ischemic lung tissue damage as compared with the control group. In vitro, in cultured H9c2 or MLE-12 cells subjected to H/R, NRG-1 mRNA level was downregulated in H9c2 cells but upregulated in MLE-12 cells after H/R, which was concomitant with significant downregulation of post-hypoxic CTH mRNA level in MLE-12 cells. Pretreatment with NAC at 1mM to H9c2 cells increased cell viability and decreased lactate dehydrogenase (LDH) release under H/R condition. In MLE-12 cells, NAC treatment similarly significantly increased post-hypoxic cell viability, but in the meantime, it also significantly increased both the NRG-1 and CTH mRNA levels under H/R condition. Findings of the current study is suggestive that both H$_2$S and NRG-1 are involved in myocardial I/R induced ALI and that the H$_2$S-releasing donor N-acetylcysteine may attenuate myocardial ischemia reperfusion induced acute lung injury via upregulating pulmonary Neuregulin-1.

837

THE VENTURE PHILANTHROPY MODEL OF DRUG DEVELOPMENT - WORKING WITH NON-PROFIT FOUNDATIONS AND GOVERNMENTS FROM CONCEPT TO DRUG APPROVAL

Eric Hoffman[1]

Binghamton Univ - State University of New York[1]

Regulatory authorities increasingly wish to hear and consider the voice of patient advocates and advocacy groups (foundations) in the development and marketing of new medicines. EMA encourages disease-specific Community Advisory Boards (CABs) to convene meetings with drug Sponsors during drug development EMA also includes trained patient advocates as members of EMA Scientific Advice Working Parties (SAWP) reviewing new medicines under development. Most efforts to date have focused on patient advocates engaged as advisors at arm's-length or external to the Sponsor (e.g. interactions with regulatory bodies that then interact with the Sponsor). In the vamorolone (Agamree) drug development program for Duchenne muscular dystrophy, patient advocates and advocacy groups (non-profit foundations) were directly involved in the design and day-to-day management of the drug development program from concept to drug approval. The multi-pronged approach to greater inclusion of the patient voice included foundation and government peer review and funding of many individual aspects of the vamorolone program. Much of this funding was under a 'venture philanthropy' model, where foundations receive 400% return on their investment based on later drug sales. Also, patient advocates advised on trial design, clinical trial site selection, and inspection readiness, again directly with the Sponsor. Indeed, the primary outcome successfully used in the vamorolone clinical trials, time to stand from the floor velocity, was chosen in large part due to patient advocates opinion that this was best related to their children's quality of life. While this motor outcome had not previously been used as a primary outcome in drug development programs previously, there was no pushback from competent authorities on clinical meaningfulness, in part due to the voice of the parent advocates. Critical government programs included European Commission Horizons 2020, NIH NINDS SBIR, and NIH NCATS TRND.

References:
https://mdaquest.org/agamree-vamorolone-now-fda-approved-offers-hope-for-children-living-with-duchenne-muscular-dystrophy/
https://www.duchenneuk.org/vamorolone-approved-in-the-us/
Guglieri M, Clemens PR, Perlman SJ, Smith EC, Horrocks I, Finkel RS, Mah JK, Deconinck N, Goemans N, Haberlova J, Straub V, Mengle-Gaw LJ, Schwartz BD, Harper AD, Shieh PB, De Waele L, Castro D, Yang ML, Ryan MM, McDonald CM, Tulinius M, Webster R, McMillan HJ, Kuntz NL, Rao VK, Baranello G, Spinty S, Childs AM, Sbrocchi AM, Selby KA, Monduy M, Nevo Y, Vilchez-Padilla JJ, Nascimento-Osorio A, Niks EH, de Groot IJM, Katsalouli M, James MK, van den Anker J, Damsker JM, Ahmet A, Ward LM, Jaros M, Shale P, Dang UJ, Hoffman EP. Efficacy and Safety of Vamorolone vs Placebo and Prednisone Among Boys With Duchenne Muscular Dystrophy: A Randomized Clinical Trial. JAMA Neurol. 2022 Oct 1;79(10):1005-1014.

838

EEG studies reveal estradiol-dependent differences in GluN2A-containing NMDAR function

Kimberly M. Holter[1], Mary Hunter Hite[1], Mckenna Klausner[1], Bethany Pierce[1], Robert W. Gould[1]

Wake Forest University School of Medicine[1]

Estrogen decline during menopause is a risk factor for the onset of schizophrenia as over 75% of patients diagnosed between 45-50 years of age are female. Compared to premenopausal women, postmenopausal women display more severe positive symptoms and worsened treatment response. However, the underlying mechanisms contributing to this increased risk are not understood. *N*-methyl-D-aspartate receptor (NMDAR) hypofunction is hypothesized to be a major contributor to schizophrenia pathology. Administration of NMDAR antagonists (i.e. MK-801) have thus been used in preclinical models to induce hyperlocomotion, social withdrawal, and cognitive impairment modelling positive, negative, and cognitive symptoms, respectively. However, efforts to identify subpopulation-specific therapeutic approaches have been met with a high failure rate in part due to limited translational screening tools sensitive to individual differences. Assessing brain waveforms using electroencephalography (EEG) represents a translational approach to identify targetable biomarkers and detect changes in neuronal activity. Abnormalities in EEG waveforms have been identified in patients with schizophrenia, including aberrant elevations in resting-state gamma power, corresponding to psychosis and cognitive impairment. Importantly, gamma power reflects cortical glutamate and GABA signaling and, thus, is sensitive NMDAR antagonists which also induce aberrant increases. These increases are hypothesized to be attributed to inhibition of NMDARs on cortical parvalbumin (PV)-containing interneurons, which leads to disinhibition of pyramidal neurons and hyperexcitability. NMDARs are heterotetrameric, comprised of two obligatory GluN1 subunits and two GluN2 or GluN3 subunits, with GluN2 splice variants including GluN2A-D. Interestingly, GluN2A, not GluN2B, antagonists increased gamma power in male rats. Further, post-mortem studies reported reduced GluN2A mRNA expression in PV-containing interneurons in patients with schizophrenia compared to healthy tissue. This may suggest GluN2A hypofunction contributes to aberrant elevations in gamma power. However, few studies have examined how hormones including 17β-estradiol (E2) influence NMDAR antagonist-induced changes in gamma power or if these changes are subunit-specific. We tested the hypothesis that E2 depletion reduces NMDAR function in an GluN2A-dependent manner. MK-801 (0.03-0.18 mg/kg, sc) was administered to 3-month-old female rats implanted with wireless EEG transmitters who remained ovary-intact (O-I) or were ovariectomized (Ovx) and implanted with an empty capsule (Ovx) or a capsule containing E2, a method of chronic delivery (Ovx+E). Data suggest, while there were no significant baseline differences, Ovx rats were more sensitive to MK-801-induced changes in gamma power compared to O-I and Ovx+E rats. Further, PEAQX (10-30 mg/kg, SC) and CP-101,606 (3-30 mg/kg, SC), a GluN2A-preferring and GluN2B-selective antagonist, respectively, were tested. Ovx rats were more sensitive to PEAQX-induced changes in gamma power; CP-101,606 produced no effect in either group. Ongoing studies are assessing differences in GluN2A, and GluN2B expression in cortical synaptoneurosomes. Ultimately, studies aim to establish a relationship between E2 and NMDAR function using gamma power as a translational biomarker to inform subpopulation-specific therapeutic approaches

839

G-protein coupled receptors expressed in human uterine tissues: Novel targets for labour management

Kylie K. Hornaday[1], Daniela Urrego[1], Stephen L. Wood[1], Donna M. Slater[1]

University of Calgary[1]

Introduction: Preterm birth is the leading cause of neonatal mortality and morbidity, yet pharmacological options for management of labour do not effectively prevent preterm birth and are associated with adverse side effects. For successful labour, the upper segment of the uterus must contract, and the lower segment must relax to allow passage of the fetus. G-protein coupled receptors (GPCR) are a promising area for target discovery, particularly those that couple via Gαq or Gαs subunits, which are implicated in smooth muscle contraction or relaxation, respectively. However, GPCR expression in the human uterus is largely unknown.

Hypothesis: We hypothesize that the transition from quiescent pregnancy to active, contractile labour is mediated by changes in the expression of pro-quiescent (Gαs) and pro-contractile (Gαq) GPCRs.
Aim: To profile GPCR expression in human myometrium (uterine smooth muscle) to identify novel GPCRs within the pregnant human uterus as potential drug targets for the clinical management of labour.

Methods: Myometrial (n=6) tissue biopsied at term Cesarean section was analyzed for the expression of 370 GPCRs using real time reverse transcriptase PCR. Additional myometrium (biopsied from both the upper and lower segments of the uterus) in n=4-6/group (term not-in-labour TNL, term labour TL, preterm not-in-labour PTNL, and preterm labour PTL) were analyzed via RNA sequencing to determine changes with labour, gestation, and spatial origin.

Results: In total, 330 and 307 GPCRs were identified in the upper and lower myometrium, respectively. Of which, 4 and 40 GPCRs, respectively, were significantly differentially expressed with labour (preterm or term). Of interest, purinergic receptor P2Y (P2RY2, Gαq-coupled) expression was 1.9±0.5-log2fold higher with term labour (p-adj=0.02) and pyramidinergic receptor P2Y, (P2RY6, Gαq-coupled) expression was 3.0±0.7-log2fold higher with preterm labour (p-adj=0.007) in the lower myometrium. Term labour was also associated with 1.5±0.5-log2fold lower expression of arginine vasopressin receptor 2 (AVPR2, Gαs-coupled) in the lower myometrium (p-adj=0.04). Spatial differences (upper vs lower) in GPCR expression were observed in term uteri (27 differentially expressed GPCRs), and to a much lesser extent in preterm uteri (4 differentially expressed GPCRs), suggesting that spatial regionalization is characteristic of term uteri, but not preterm.

Conclusion: These results suggest that the maintenance of quiescence and onset of labour may be regulated by multiple GPCRs, particularly in the lower segment myometrium. In addition, spatial regionalization of select GPCRs within the pregnant uterus may be utilized to promote contraction and/or quiescence. The potential role of purinergic receptors as ligand-gated ion channels in the human uterus presents a novel direction for insight into the mechanism of labour and uterine contraction. Future work will aim to functionally screen these GPCRs to identify novel targets for treating preterm labour.

840

Effects of total flavone of Litchi Semen on the hepatocellular carcinoma cell proliferation and apoptosis

Jingzhu Huang

Objective: To investigate the effects and molecular mechanism of total flavone of Litchi Semen (TFL) on hepatocellular carcinoma cell proliferation and apoptosis.Method: Methyl thiazolyl tetrazolium colorimetric (MTT) assay was used to detect the effect of different doses TFL and cisplatin on the proliferation of HepG2 and Huh7 cells. MTT can detect the best dose and time to suppress hepatoma cells HepG2 and Huh7 proliferation, thus selecting the optimal dose of TFL 320 ug/mL for the follow-up experiment. The apoptosis rate of HepG2 cells and Huh7 cells were determined by flow cytometry. qRT-PCR was used to detect the gene expression of PTEN, PI3K and AKT after the intervention by TFL. Western blot was used to detect the expression of key proteins in the PTEN-PI3K/AKT signaling pathway after the intervention by TFL. Result: MTT assay showed that TFL could significantly reduce the cell viability of HepG2 cells and Huh7 cells in a concentration-and time-dependent manner. The half maximal inhibitory concentration (IC50) was found to be 324.2 ug/mL in HepG2 cells and 343.8 ug/mL in Huh7 cells at 48 h. The results of apoptosis by flow cytometry showed significant differences intervention by TFL 320ug/mL in HepG2 cells and Huh7 cells. Compared with TFL 0 ug/mL, TFL 320ug/mL increased mRNA and protein expressions of PTEN, decreased mRNA and protein expressions of PI3K and AKT (P<0.05).Conclusion: TFL can inhibit proliferation and promote apoptosis in HepG2 cells and Huh7 cells. The mechanism for that is possibly through mitogen-activated protein PTEN-PI3K/AKT signaling pathway.

841

GPR55 Antagonist KLS-13019 Prevents and Reverses Chemotherapy-Induced Peripheral Neuropathy (CIPN) in Rats

Michael Ippolito, Hajra Sohail, Ian Barckhausen, Eleanor Labriola, Sara Jane Ward

Temple University

Neuropathic pain is a form of chronic pain that develops as a consequence of damage to the nervous system. Treatment of neuropathic pain is often incompletely effective, and most available therapeutics have only moderate efficacy and present side effects that limit their use. Opioids are commonly prescribed for the management of neuropathic pain despite equivocal results in clinical studies and significant abuse potential. Thus, neuropathic pain represents an area of critical unmet medical and novel classes of therapeutics with improved efficacy and safety profiles are urgently needed. Novel antagonist of GPR55, KLS-13019, was screened in rat models of neuropathic pain and morphine discrimination. Peripheral neuropathy was induced in rats with once daily 1mg/kg paclitaxel injections for 4 days. Rats were then administered KLS-13019 or comparator drugs on day 7 in an acute dosing paradigm or days 7-10 in a chronic dosing paradigm and allodynia was assessed by a Von Frey test. Allodynia was reversed in a dose dependent manner in the rats treated with KLS-13019, with the highest dose reverting the response to pre-paclitaxel injection baseline levels with both I.P. and P.O. administration after acute dosing. In the chronic dosing paradigm, 4 consecutive doses of KLS-13019 completely reversed allodynia for the duration of the phenotype. Additionally, co-administration of KLS-13019 with paclitaxel prevented the allodynic phenotype from developing in the animals. Finally, in an effort to characterize the in vivo pharmacology of KLS-13019 compared to opioid-class drugs, rats were trained to discriminate between morphine and saline via alternative and mutually exclusive lever presses as the "correct response" to treatment. After training, rats dosed with KLS-13109 did not respond as though they had received morphine. Additionally, cell and biochemical assays have suggested that this anti-allodynic effect is related to inhibition of GPR55 mediated calcium signaling and may be independent of ERK phosphorylation or arrestin interaction. Molecular modeling and structure activity relationship studies provide rationale for GPR55 selectivity for KLS-13019 over structural analogue CBD. Together, these data suggest that KLS-13019 represents a new class of drug that would be potentially useful for the treatment of neuropathic pain.

842

2-Substituted (N)-Methanocarba A_3 Adenosine Receptor Agonists: In silico, in vitro and in vivo Characterization

Kenneth Jacobson[1], Dilip K. Tosh[2], Chunxia Cronin[3], Matteo Pavan[4], Eline Pottie[5], Tina C. Wan[6], Eric Chen[4], Sarah A. Lewicki[4], Ryan G. Campbell[4], Zhan-Guo Gao[4], John A. Auchampach[6], Christophe P. Stove[5], Bruce T. Liang[7]

NIDDK/NIH[1] NIDDK, National Inst. of Health[2] University of Connecticut Health Center[3] NIDDK, National Institutes of Health[4] Ghent University[5] Medical College of Wisconsin[6] Univ of Connecticut[7]

A_3 adenosine receptor (AR) agonists are being developed for the treatment of autoimmune inflammatory diseases, chronic pain and cancer. A_3AR agonists are not limited by cardiovascular side effects observed with other adenosine (A_1 and A_{2A}) agonists that were in clinical trials. 2-Arylethynyl (North)-methanocarba adenosines have been explored as highly selective A_3AR agonists, which is largely a function of the pseudoribose (bicyclic fused cyclopropane and cyclopentane) ring that pre-establishes a preferred (N)

conformation for receptor recognition. Here, we compare analogues in the 5'-methylamide series having bulky C2-substitution, which either contain or lack an ethynyl spacer between adenine and a cyclic group. 2-Aryl compounds **11**, **13**, **14**, **19**, **22**, **23**, **27**, **29**, **31** and **34**, lacking an ethynyl spacer, displayed potent K_i values of 2–30 nM at the human (h) A_3AR, while other derivatives had greatly reduced affinity. The mouse (m) A_3AR affinity was highly variable, with 2-arylethynyl groups greatly favoring high affinity (**7**, **8**> **3c**, **3d** > **3b**) compared to 2-aryl analogues. However, 4′-truncated derivatives lacking a 2-ethynyl spacer had greatly reduced hA_3AR affinity, even for those analogues containing affinity-enhancing N^6-dopamine-derived substituents. This suggests that the 5'-methylamide group is especially important for anchoring these analogues in a deep hydrophilic subpocket in the receptor. hA_3AR homology modeling indicated that 2-aryl and 2-arylethynyl groups have different conformations and receptor environments. The directly connected 2-aryl groups interact with ECL2 of the hA_3AR, as opposed to the 2-arylethynyl groups, which interact with TM2. Functional assays of selected compounds in G protein-dependent and independent signaling were performed using engineered HEK293T cell lines. In hA_3AR miniG$\alpha_i$recruitment assay, **31** (MRS8062) was (slightly) more potent compared to a β-arrestin2 recruitment assay, and its maximal efficacy (E_{max}) was much higher (165%) than reference nonselective agonist NECA. Thus, in the 2-aryl series, A_3AR affinity and selectivity were variable and generally reduced compared to the 2-arylethynyl series, with a greater dependence on the specific aryl group present. Selected compounds were protective in an vivo ischemic model of peripheral artery disease (PAD), in which other A_3AR agonists demonstrated efficacy. Compounds **3a**–**3c** in the rigidified 2-arylethynyl series significantly decreased the % cell death in this model of skeletal muscle ischemia reperfusion injury/claudication, as previously shown only for moderately A_3AR-selective ribosides or (N)-methanocarba derivatives (all lacking the 2-arylethynyl group). Thus, we have expanded A_3AR agonist SAR for (N)-methanocarba adenosines and their application to skeletal muscle ischemia.

843

The Parabrachial Nucleus Modulates Anxiety in Alcohol Withdrawal and Abstinence Following Repeated Stress

Anel Jaramillo[1], Laith S. Kayat[2], Danny G. Winder[2]

University of Kentucky[1] Vanderbilt University[2]

Chronic intermittent ethanol vapor exposure (CIE) and two-bottle alcohol choice (2BC) paradigms produce neuronal adaptations in the bed nucleus of the stria terminalis (BNST), a region critical for affective behavior. The parabrachial nucleus (PBN), a sensory alarm, sends calcitonin gene related protein (CGRP) and pituitary adenylate cyclase activating peptide (PACAP) projections to the BNST that remain relatively unexplored in abstinence.

Calca-CRE (gene name for CGRP) male mice (n=5-10/sex/virus group) received bilateral injections of hM4D(Gi) DREADDs or control virus in the PBN. Anxiety was measured in early-withdrawal from CIE (4-6 hr) with the elevated plus maze (EPM) paired with the hM4D(Gi) ligand, CNO (3 mg/kg, IP). PACAP-CRE female mice (n=4-9/sex/genotype/stress group) received bilateral injections of hM4D(Gi) DREADDs in the PBN and were exposed to 2BC. Anxiety was measured in prolonged-withdrawal (2 wks) from 2BC with the novelty suppressed feeding task (NSFT) followed by repeated restraint stress (RRS) paired with CNO (3 mg/kg, IP). Post-RRS anxiety was measured with NSFT.

PBN(CGRP) inhibition increased EPM time immobile in CIE-withdrawal (2-way ANOVA vapor p=0.05; treatment p=0.01). PBN(PACAP) inhibition induced a trend for decreased latency to feed in NSFT with no changes on RRS behavior in 2BC prolonged withdrawal. A history of RRS paired with PBN(PACAP) inhibition blunted RSS-induced increase in NSFT latency (2-way ANOVA stress p=0.004, genotype p=0.0481).

These data demonstrate PBN(CGRP) and PBN(PACAP) neurons modulate anxiety-like behavior in alcohol-abstinence. Given the prominent role of the BNST in abstinence-induced anxiety current studies investigate changes in PBN◊BNST circuit activity. Given pharmaceutical treatments for migraines targeting CGRP and PACAP inhibition are bioavailable, these studies inform a potential role for treatments in alcohol-abstinence.

844

Fatty Acid Metabolizing Cytochrome P450 4F11 as a Novel Drug Target for Lung Cancer Treatment

Huiting Jia[1], Bjoern Brixius[1], Simone Brixius-Anderko[1]

University of Pittsburgh, School of Pharmacy[1]

Lung cancer is the leading cause of cancer deaths worldwide. Lung cancer patients often develop drug resistance during therapy, hence, identifying new therapeutic targets is important for alternative treatment approaches. The potent lipid mediator 20-hydroxyeicosatetraenoic acid (20-HETE) regulates the blood pressure in humans. However, 20-HETE also promotes cell proliferation and migration in cancer. It is generated by the cytochrome P450 (P450, CYP) family 4A/F through a selective ω-hydroxylation of arachidonic acid. The unselective inhibition of 20-HETE-producing CYP4 enzymes attenuates the lung cancer tumor growth in xenograft mouse models, yet the clinical exploitation of CYP4 enzymes as drug targets has not been realized due to a lack of functional and structural studies. The isoform CYP4F11 is the only w-hydroxylase that is significantly overexpressed in lung tumor tissue. However, the exact role of CYP4F11 in lung cancer has not been established yet. We hypothesize that CYP4F11-mediated 20-HETE production promotes lung cancer cell proliferation and migration and that CYP4F11 is a novel drug target for lung cancer therapy.

To investigate the role of CYP4F11 in lung cancer, the impact of CYP4F11 on cell proliferation and migration was first investigated by knocking down and overexpressing CYP4F11 in three lung cancer cell lines with different CYP4F11 expression levels. We found that the knockdown of CYP4F11 significantly inhibits lung cancer cell proliferation and migration while a CYP4F11 overexpression promotes both when compared to control cells. We confirmed that the 20-HETE levels were significantly decreased in knockdown cells compared to control cells. The addition of exogenous 20-HETE rescued the cell proliferation back to control cell levels.

To further evaluate the role of CYP4F11 as a therapeutic target, we first measured the catalytic efficiency of recombinant CYP4F11 and found that CYP4F11 only poorly metabolizes arachidonic acid. We then evaluated the inhibitory effect of the CYP4 pan inhibitor HET0016 on CYP4F11. HET0016 binds tightly to CYP4F11 and inhibits 20-HETE production with high inhibitory efficiency. Unfortunately, the efficacy of HET0016 is low when applied to lung cancer cell lines and exhibits serious off-target effects. However, HET0016 might provide a scaffold for future structure-based drug design. Ongoing studies are focused on other CYP4F11 substrates that have an implication on lung cancer growth such as the endocannabinoid anandamide and the eicosanoid 15-HETE which both are metabolized by CYP4F11. Thus, the high expression of CYP4F11 in lung cancer might not only affect 20-HETE production but also other lipid mediators with an impact on cell proliferation and migration.

Our studies show that CYP4F11 is a potential new drug target for lung cancer therapeutics. Future studies aim to elucidate metabolic pathways affected by CYP4F11 expression and the metabolism of additional lipid mediators with an implication on lung cancer proliferation and migration.

845

**Psilocybin-induced anxiolytic effects supported by transient elevation of corticosterone**

Nathan Jones, John Razidlo, Zarmeen Zahid, Cody Wenthur

University of Wisconsin - Madison

Investigation into the clinical use of the serotonin (5HT-2A) receptor agonist psilocybin in conjunction with psychotherapy has shown promising therapeutic results in the treatment of psychiatric disorders. Correlations between drug-induced cortisol elevation and treatment outcomes have been reported for human studies during psilocybin-assisted psychotherapy; however, the mechanistic relationship between psychedelic-associated alterations in plasma corticosterone (CORT) responses and anxiolytic efficacy remains unclear. A time course for psilocybin to induce anxiolysis in the absence of any intervention was conducted with C57/Bl6 mice and LC-MS/MS. Serum samples tested at doses of 0.3, 1, and 3 mg/kg found peak concentrations at 15 min post-injection. In the open field test 15 minutes post-injection, mice that received 3mg/kg psilocybin demonstrated decreased center time, while the 0.3 mg/kg exhibited a dose-dependent increase. However, at 4 h post-injection, the reverse was found, in that 0.3mg/kg psilocybin decreased center time. This dose-dependent interaction correlates with psilocybin-induced increases in CORT levels that peak at 15 min and return to baseline by 4 h.

In addition, the non-hallucinogenic compound lisuride and NDMAR antagonist ketamine were used and demonstrated a transient increase in corticosterone concentrations at 15 min and returned to baseline by 4 h. When tested in the novelty-suppressed feeding test, all three compounds reduced the latency to feed 4 h post-injection. Although following exposure to chronic oral CORT and when administered the glucocorticoid antagonist, mifepristone, both psilocybin and ketamine lost this anxiolytic effect. Chronic exposure to CORT and mifepristone suppressed the psilocybin-induced stress response and increased CORT. At a dose of 3 mg/kg, IP psilocybin was found to have post-acute anxiolytic-like effects that were not altered by pretreatment with the non-hallucinogenic 5-HT2AR antagonist, ketanserin. These results suggest that psilocybin-induced stress response and increased plasma CORT levels are supportive of the observed anxiolytic effects. This study demonstrates that psilocybin-induced corticosterone release is a critical factor driving reductions in anxiety-like behavior in mice in the hours following drug clearance. That ongoing, unresolved glucocorticoid elevations can invert the long-term outcome of psilocybin administration on anxiety-like behavior up to seven days later. These findings point to HPA axis activation and changes in glucocorticoid concentration profiles over time as critical translational factors for mechanistic consideration when investigating classical serotonergic psychedelic-assisted therapy for the treatment of psychiatric disorders.

Psilocybin + Vehicle

Psilocybin + Chronic CORT
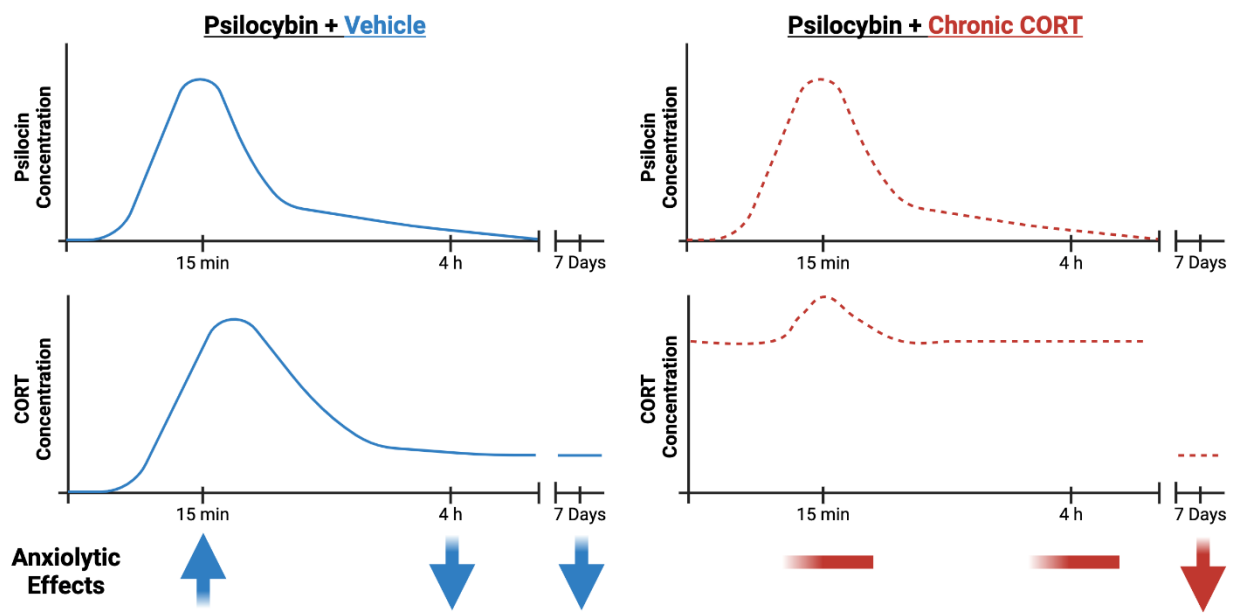
Comparative Analysis of Psilocin and Corticosterone (CORT) Concentrations and Anxiolytic Effects Following Psilocybin Administration with Vehicle and Chronic Corticosterone (CORT) Treatment

846

Simultaneous Inhibition of Soluble Epoxide Hydrolase and Fatty Acid Amide Hydrolase Prevents Nitroglycerin-induced Hypersensitivity in Female Rats

Ram Kandasamy[1], Tiffany Chacon[1], Christopher Chin[1], Stevan Pecic[2]

California State University, East Bay[1] California State Univ Fullerton[2]

Migraine is the most common neurological disorder in the world, and is characterized by severe headaches, nausea, and light sensitivity. Current migraine treatments, including opioids and triptans, produce dangerous and uncomfortable side effects. Moreover, modern anti-migraine drugs lack novel mechanisms of action, often resulting in side effects similar to traditional approaches. Our aim is to revolutionize migraine pain management by finding new medications with novel mechanisms that can provide relief from migraine without causing any negative side effects. Fatty acid amide hydrolase (FAAH) and soluble epoxide hydrolase (sEH) are two pain-related enzymes. The potential benefits of dual-enzyme inhibitors include fewer drug-to-drug interactions and improved drug synergism compared to the administration of just one enzyme inhibitor. Importantly, these dual inhibitors may require lower doses than the traditional anti-migraine agent, sumatriptan. We hypothesized that simultaneous inhibition of FAAH and sEH using a dual sEH/FAAH inhibitor will alleviate migraine-related pain in rats. We previously identified a potent dual inhibitor SW-17 with IC_{50} values of 9.8 nM and 2.5 nM in human FAAH and human sEH enzymes, respectively. Interestingly, SW-17 was significantly less active in mouse sEH, but was very potent in rat sEH with IC50 value of 3.9 nM. In this study, we synthesized 19 follow-up analogs of SW-17 to test the importance of the sulfonamide group. After evaluation of their potencies at inhibiting human, mouse, and rat enzymes, it appears that SW-17 is the most potent dual inhibitor; therefore, SW-17 was scaled up and evaluated *in vivo*. In migraineurs, an injection of nitroglycerin typically triggers a migraine attack, which makes it a useful tool to generate headache-like pain in animals. An injection of nitroglycerin produces hypersensitivity in periorbital and hindpaw regions. Thus, we investigated the effects of various doses of dual inhibitors of sEH and FAAH in a rat model of nitroglycerin-induced pain to assess its efficacy. To induce migraine pain, we injected 10 mg/kg nitroglycerin, a vasodilator that induces migraine-like pain. Thirty minutes prior to the injection of nitroglycerin, we pre-treated rats with a dose of SW-17,

the sEH/FAAH dual inhibitor, in varying doses (0.1, 0.3, and 1 mg/kg) or sumatriptan. Mechanical thresholds in the hindpaw were assessed 30, 60, and 120 minutes after nitroglycerin injection. A nitroglycerin injection lowered sensory thresholds in female rats indicating migraine-like pain. A pre-treatment of SW-17 and sumatriptan prevented nitroglycerin-induced decreases in mechanical hypersensitivity. Finally, a wheel running test indicated that SW-17 does not decrease voluntary activity in rats indicating that this drug may not produce motoric side effects. Future studies will determine the full efficacy of FAAH and sEH inhibition in alleviating migraine-like pain in rats.

847

Developmental Impacts of Adolescent Intermittent Nicotine Vapor Exposure on the Murine Hippocampus

Jack Keady, Jill Turner

University of Kentucky

Electronic cigarette (e-cig) use is rapidly rising, especially among adolescents and younger adults. Despite their development as a smoking cessation aid, young adult (18-24 yo) e-cig users are generally also "never smokers" (less than or equal to 100-lifetime cigarettes consumed), suggesting that many new nicotine users are initiating use with e-cigs. This trend is troubling, as nicotine dependence during adolescence is associated with numerous health-related outcomes later in life, including a higher risk for psychiatric disorders. Adolescence represents a period of dynamic brain development, particularly in the prefrontal cortex and limbic regions. One limbic region of particular interest is the hippocampus, which directly contributes to both cognitive and affective nicotine withdrawal symptoms, and its maturation during adolescence is significantly impacted by nicotine exposure. However, mechanistic understanding of this process and how to leverage this knowledge for treatment is unknown. In order to investigate the developmental impacts of chronic nicotine exposure, we first used the La Jolla Research, Inc. nicotine vapor chambers to expose adult (9-week) C57BL6 mice to intermittent nicotine via inhalation. Mice had food and water available ad libitum and were maintained on a 12-hour light-dark cycle (lights on at 7:00 AM). We exposed mice during the dark phase and varied puff duration, number of puffs a cycle, and time between cycles to produce concentrations of plasma cotinine comparable to heavy human smokers and the canonical nAChR upregulation seen in both human smokers and rodents exposed to chronic nicotine. This novel method provides a non-invasive nicotine exposure model, produces nicotine inhalation topography that more closely matches human users, and only exposes mice to nicotine during their active phase. Using this newly developed exposure model, we treated adult (9-week) and adolescent (5-week) C57BL6 mice to two weeks of nicotine exposure, followed by 2 weeks of abstinence. On the 14th day of abstinence, mice were sacrificed, and hippocampal samples were taken for RNA-sequencing. Preliminary cell-type-specific RNA-sequencing data from adult exposed mice suggests that during acute nicotine withdrawal, immune signaling pathways are disrupted. However, at the prolonged withdrawal time point of two weeks, the adolescent nicotine-exposed mice have unique changes in their neuronal transcriptome not present in the adult-exposed mice. Further validation of the developmental impacts of nicotine on the hippocampal neuronal transcriptome is ongoing, and possible proteomic changes will be investigated in validated genes of interest.

848

High Fructose - High-Fat Diet Accelerates Non-Alcoholic Fatty Liver Disease Possibly Mitigating Hepatic Nuclear Lipocalin Prostaglandin D$_2$ Synthase

Rhema Khairnar, Sunil Kumar

St. John's University

Nonalcoholic fatty liver disease (NAFLD) is the most prevalent chronic liver disease worldwide over the last decade with no FDA-approved treatment available yet. NAFLD is a spectrum of disorders ranging from non-alcoholic fatty liver disease (NAFLD) to non-alcoholic steatohepatitis (NASH), with or without fibrosis/cirrhosis. The prevalence and rising threat of end-stage liver disease in obese and diabetic populations has garnered serious attention in the field. To prevent the worsening of this progression, it is important to discover novel therapeutic targets. Our *in-vivo* study showed severe fatty liver disease in lipocalin prostaglandin D$_2$ synthase (L-PGDS) knockout mice kept on high-fat diet. Briefly, L-PGDS functions as a prostaglandin synthase where it catalyzes the isomerization of PGH$_2$ to PGD$_2$. PGD$_2$ regulates its physiological function via two individual G-protein coupled receptors named DP1 and DP2. This exciting finding prompted us to investigate the role of L-PGDS in fatty liver disease via dietary manipulation where male and female C57BL/6 mice were fed either fructose or high-fat diet alone or a combination of both for 22 weeks. Our histological and biochemical results clearly showed significant hepatosteatosis in fructose as well as high-fat combination diet groups in both male and female mice. Most exciting, the mice fed a high-fat diet showed significantly decreased nuclear L-PGDS protein expression while sterol-regulatory element binding protein-1 (SREBP1), gene involved in fatty acid biosynthesis, expression significantly increased suggesting a strong interplay of L-PGDS and NAFLD. Similarly, fructose-fed group also showed similar results with reduced L-PGDS expression. Therefore, to understand the detailed mechanism, we aimed to investigate the differential regulation of L-PGDS in presence of fructose and palmitic acid using HepG2 cells. HepG2 cell line is an appropriate *in-vitro* model to study gluconeogenic, hepatokine, and lipogenic gene-expression pattern similar to the one observed in *in-vivo* settings. Briefly based on our preliminary results, HepG2 cells will be cultured with different concentrations of fructose (5.5, 10, 25, 50 and 100mM) with or without palmitic acid 250uM concentration for 24, 48, 72 and 96 hrs. Change in hepatic lipid accumulation will be the experimental outcome which will determined including Oil Red O staining, cell lysate and supernatant triglyceride measurement. Further, fructose and palmitic acid treated cell lysates will be subjected to determine subcellular changes in L-PGDS along with lipogenesis and lipolysis related proteins and mRNA expressions. Obtained results will be recapitulated in our established L-PGDS silenced HepG2 cells. Once we fully understand the regulation of L-PGDS in fatty liver disease, further studies will be carried out using appropriate mice model in the future. In summary, understanding the regulation of L-PGDS under the influence of dietary manipulation will possibly bring a potential future therapeutic target of fatty liver disease.

849

Utilizing Ancestral Sequence Reconstruction to Generate a Novel Recombinant Humanized L-Asparaginase with Enhanced Chemotherapeutic Properties

Kristopher Knight[1], Harrison C. Brown[2], Kinnede R. White[1], H. Trent Spencer[1], Christopher B. Doering[1], Sunil S. Raikar[1]

Aflac Cancer and Blood Disorders Center, Department of Pediatrics, School of Medicine, Emory[1]
Expression Therapeutics[2]

L-asparaginase (L-ASNase) has been a critical component of acute lymphoblastic leukemia (ALL) chemotherapy regimens for several decades, however, recent preclinical data has shown that L-ASNase may also be beneficial in several adult solid malignancies such as pancreatic cancer, colorectal cancer and metastatic breast cancer. Current clinical L-ASNases are bacterial in origin and are thus highly immunogenic, with reactions ranging from silent inactivation to severe anaphylaxis. Additionally, adults can have significant liver and pancreatic toxicity with L-ASNase, with studies showing this is at least partly related to the glutaminase co-activity seen in bacterial L-ASNases. Thus, development of a less immunogenic L-ASNase with reduced glutaminase activity is essential to overcome the current limitations of L-ASNase and expand its use beyond ALL.

Human L-ASNase has evolved to have inferior catalytic properties which restricts its candidacy as a therapeutic enzyme. However, the utility of L-ASNase as a chemotherapeutic was first established in guinea pig (GP) L-ASNase, discovered first by J.G. Kidd in 1953 and then confirmed by J.D. Broome in 1963. GP L-ASNase has significantly superior enzyme kinetics compared to human L-ASNase and shares ~70% sequence identity with human L-ASNase compared to ~30% by bacterial L-ASNases and is thus predicted to be less immunogenic. Additionally, GP L-ASNase has no known glutaminase co-activity. Thus, GP L-ASNase is the ideal ortholog to serve as a template for optimization to create a more humanized less toxic L-ASNase variant. Ancestral Sequence Reconstruction (ASR) is an innovative protein drug discovery and optimization platform that can be leveraged to improve the pharmaceutical properties of L-ASNase. Analysis of the predicted molecular evolution of L-ASNase maps the functional divergence of extant orthologs by means of evolutionary intermediaries, enabling the identification of critical residues responsible for superior activity.

ASR was performed utilizing 54 extant L- ASNase sequences, aligned using MUSCLE and an evolutionary tree inferred using MrBayes. 53 ancestral L-ASNase sequences were identified and ten ancestral variants spanning the ancient primate and GP lineage resurrected. E. coli codon optimized complementary DNA sequences were subcloned into an expression vector and transformed into E. coli BL21 (DE3) cells for protein expression. An-ASNase candidates were isolated through Ni2+ affinity chromatography, followed by purification with size exclusion chromatography. L-ASNase activity was assessed using a modified Nessler's reagent assay in a continuous spectroscopic enzyme-coupled assay. At an enzyme concentration of 0.1 mg/mL and an asparagine substrate concentration of 1 μM, An-88, An-104, and An-107 exhibited outstanding L-ASNase activity, comparable to clinically relevant E. coli and Erwinia L-ASNases. An-88 has 81% similarity, while both An-104 and An-107 ASNases shared an 88% identity with human L-ASNase. Preliminary cytotoxicity assessments of An-104 and An-107 on a T-ALL cell line, CCRF-CEM, demonstrated comparable anti-leukemia cytotoxicity to existing bacterial L-ASNases, with An-107 demonstrating the highest cytotoxicity.

Thus, we have shown that ASR is a viable platform to bioengineer a less toxic humanized L-ASNase drug candidate. Lead candidate toxicity profile will be defined, and chemotherapeutic potential will be measured against hematologic and solid tumors.

850

TARGETED DRUG DELIVERY OF LEUKOMIMETIC NANOPARTICLES TO ALLEVIATE PERIPHERAL NEUROPATHY IN CHARCOT-MARIE-TOOTH 1X

Harshita Kondeti[1], Maleen Cabe[1], Lauren Soehlke[1], Kelly Langert[1], Charles Abrams[2]

Loyola University Chicago[1] University of Illinois Chicago[2]

Charcot Marie Tooth disease is an inherited peripheral neuropathy for which there are few effective therapeutic options, many of which cause undesirable side effects. The blood-nerve barrier (BNB) restricts access of the circulation to nerves and limits the advancement of novel therapies. To address

this challenge, the Langert Laboratory is investigating targeted delivery strategies in the connexin 32 knockout (Cx32KO) mouse model of Charcot Marie Tooth 1x.

The lab has adapted the use of nanoparticles (NPs) coated with monocyte-derived plasma membrane vesicles, deemed leukomimetic NPs. We hypothesize that these leukomimetic NPs, which we demonstrate are enriched with the chemokine receptor CCR2, will be recruited to nerves, given that CCL2 is upregulated in Cx32 deficient nerves over the course of their lifespan. Using *in vitro* chemotaxis assays, we demonstrate that plasma membrane vesicles isolated from mouse (WEHI) monocytes are enriched with CCR2 and other plasma membrane proteins and migrate towards CCL2-containing media. We quantify the vesicles passing through a transwell insert to assess chemotaxis. We established *in vivo* methods to generate single-cell suspensions from sciatic nerves harvested from Cx32KO mice and subsequently analyze immune infiltrates using flow cytometry.

Preliminary data suggest that nerves from Cx32KO mice contain more cells than nerves from wildtype age-matched controls. Immunohistochemistry results show elevated CD68 and ICAM-1 in nerves of 6-month Cx32KO mice compared with wildtype age-matched controls. A time course indicating the pattern of immune cell infiltration into the affected sciatic nerves is being determined currently through immunohistochemistry and flow cytometry studies. From this time course, we will identify some windows of opportunity for treatment, in which the BNB is less restrictive and immune infiltration rates are high. Once determined, we will utilize these windows to administer treatments, such as Cx32 gene therapy, to alleviate neuropathy and demyelination phenotypes within the Cx32 KO mouse models.

851

Utilizing Orthogonal Mass Spectrometry Approaches to Understand Metallodrug Pharmacokinetic Parameters for *in vitro* Lead Compound Optimization

Samuel Krug

University of Maryland, Baltimore

Historically, pharmacokinetic evaluation of metallodrugs has been solely relied on ICP-MS. Gallium Nitrate, marketed as Ganite, has shown renal toxicity issues due to free gallium accumulating in the kidney. Due to physiochemical similarities between gallium and iron, our team has shown that gallium salophen is able to mimic heme and bind in the heme pocket of HasR from *Pseudomonas aeruginosa,* decreasing heme dependent signaling and virulence. While ICP-MS can give us information about to exposure of the gallium, this analysis is limited to metal core and does not give information on how long the entire drug molecule stays intact or if there are active metabolites driving the pharmacodynamic response. We sought to evaluate and rank 15 analogs of gallium based metallodrug, GaSal, through the gamut of microsomal clearance, whole blood stability, and CaCO2 permeability assays to evaluate how successfully these drugs can be characterized with traditional DMPK screening approaches. LC-MS/MS of metallodrugs is challenging due to limitations in solubility, however, part of the strategic scaffold design for the GaSal analogs is to include solubilizing groups equatorially off of the core so that there is no interference in the binding pocket. By utilizing LC-MS/MS in conjunction with ICP-MS, it is possible to perform a mass balance on the total amount of gallium in the sample with the concentration of the intact metallodrug. This further allows us to show that dosing with GaSal will not result in immediate release of gallium from the scaffold, resulting in the same toxicity issues as seen with gallium nitrate. Whole blood partition experiments were performed by incubating whole blood from six individual human selectivity lots with 500 ng/mL of metallodrug. B/P partition ratio ranged from 0.325-0.445 for the GaSal analogs that could be detected by LC-MS/MS and were in agreement with the ICP-MS analysis. Gallium Nitrite, serving as the control, gave a B/P ratio of 0.114 ± 0.026, indicating that the distribution of GaSal is

different than free gallium. Moreover, this demonstrates GaSal analogs can be stable in whole blood at physiological temperature for at least several hours.

Only utilizing ICP-MS is prohibitive from understanding clearance of the intact metallodrug. To further understand if our metallodrugs are impacted by metabolic activity, microsomal incubation occurred over the course of 30 minutes and showed GaSal compounds were either undetectable after immediately starting the incubation or there was no change in concentration during the time course. Additional experiments are needed to understand if drugs undetectable by LC-MS/MS is due to gallium being released from the compound or metabolite formation in biorelevant media.

Future studies will involve *in vivo* dosing of candidates detectable by LC-MS/MS to see if pharmacokinetic parameters, such as intrinsic clearance and blood/plasma coefficient, are translatable from *in vitro* performance.

852

$P2Y_{14}$ Receptor Antagonists: Heteroaromatic Piperidine Bioisosteres in 4-Phenyl-2-Naphthoic Acid and Aryl-Triazolyl-Biphenyl Series

Siva Hariprasad Kurma[1], Zhiwei Wen[1], Asmita Pramanik[1], Matteo Pavan[1], Sarah A. Lewicki[1], Paola Oliva[1], Katharina S. Erlitz[1], Anna Junker[2], Young-Hwan Jung[1], Joseph Kousouros[3], Zhan-Guo Gao[1], Jonathan F. Fay[3], Kenneth Jacobson[1]

[1]*National Institute of Diabetes and Digestive and Kidney Diseases, National Institutes of Health, USA*
[2]*European Institute for Molecular Imaging (EIMI), Waldeyerstr. 15, D-48149, Münster, Germany*
[3]*Dept. of Biochemistry and Molecular Biology, University of Maryland School of Medicine, USA*

G_i-coupled $P2Y_{14}$ receptor ($P2Y_{14}R$) antagonists are efficacious in reducing chronic pain (Daniela Salvemini et al.) and inflammation in mouse models. Many analogues of the prototypical naphthalene-based $P2Y_{14}R$ antagonist PPTN have been reported. We now extend the antagonist SAR by replacement of the piperidine moiety with small heteroaromatics. C-linked 1,2,3-triazol-4-yl **10** (MRS4916) and pyrazol-3-yl **11** (MRS4917) piperidine substitutions in the naphthalene series gave potent IC_{50} values at human $P2Y_{14}R$ of 3.69 and 2.88 nM, respectively, in a fluorescent antagonist binding assay. Furthermore, using StarDrop (Optibrium) pharmacokinetic calculations, antagonist **11** and other small heterocyclic analogues were predicted to cross the blood brain barrier. However, appending 1,2,3-triazol-1-yl in the 3-(1*H*-1,2,3-triazol-1-yl)benzoic acid series, i.e. two 1,2,3-triazoles (**16**), reduced affinity 1900-fold compared to its corresponding piperidine reference compound **4**. Charged phosphate and extended alkyl-amino groups were strategically placed at various positions, to probe the ligand's binding site vicinity. However, the phosphate groups did not enhance affinity. A molecular model based on homology to a nucleotide-bound G_i-coupled $P2Y_{12}R$ structure (PDB ID: 4PXZ) and critical cationic residue R253 predicted recognition elements and an energetically stable antagonist pose (using molecular dynamics simulation). The synthetic work to discover new heterocyclic bioisosteres also served to inform the molecular modeling leading to an updated model that explained the observed affinities. This pose differs in some details from our previously reported model, but the relative orientation of the piperidine group and its heterocyclic replacements facing the extracellular medium is consistent. Thus, we have expanded the SAR of potent $P2Y_{14}R$ antagonists, which have potential for disease treatment, and used new mutagenesis data to update our molecular modeling hypothesis.

853

Developing 2-Aminothiophene Derivatives as Positive Allosteric Modulators of Glucagon-Like Peptide 1 Receptor

Zhijun Li,Jeffrey A. Campbell, Phu Do, Zhiyu Li, Faisal Malik

Saint Joseph's University

The Glucagon-like peptide 1 receptor (GLP-1R) belongs to the Class B G-protein coupled receptors (GPCRs) and is a well-established target for treating type 2 diabetes. Recent clinical-trial data suggest that GLP-1R agonistic drugs not only significantly reduce body weight in individuals with obesity, but may also offer protection against serious heart disease and drug/alcohol addiction related issues. Consequently, GLP-1R has become one of the most intriguing and extensively studied Class B GPCRs. Although GLP-1R agonist-based therapies, including various GLP-1 analog drugs, are highly successful and available in the market, most are peptidic in nature and require intravenous (*iv*) mode of administration. Thus, it remains a challenge to develop nonpeptidic agonist drugs targeting GLP-1R. A promising approach, involves the development of small molecule positive allosteric modulators (PAMs) of GLP-1R, which have a greater potential for more convenient oral (*po*) administration. Building upon our prior work that identified two 2-aminothiophene-based small-molecule PAMs of GLP-1R, we conducted a series of structural SAR optimizations, as well as *in vitro* and *in vivo* studies. This effort led to the identification of 2-aminothiophene derivative, **I-187** (MW 299), which exhibited an approximately 2-fold increase in insulin secretion at 5 µM when combined with the GLP-1 peptide at 10 nM. I*n vivo* studies using CD1 mice revealed a 50% reduction in glucose levels after 60 minutes at a dose of 10 mg/kg b.w. More notably, co-treatment with sitagliptin, an inhibitor of the GLP-1 degrading enzyme dipeptidyl peptidase IV, demonstrated that **I-187** synergistically lowered blood glucose levels by approximately 75% after 60 minutes, confirming its effectiveness as a PAM of GLP-1R. These promising results, coupled with the favorable drug-like properties of the compound, suggest that **I-187** is a compelling lead compound for future drug development. Furthermore, this approach can potentially be applied to the development of allosteric modulation of other GPCRs.

854

A New Class of Drug-like Negative Allosteric Modulators of Mu-Opioid Receptor

Mengchu Li, Douglas McMillian, Brennan Watch, Jess Duque, Andrew Alt, Jason Rech, John Traynor

University of Michigan

There is a significant unmet need for alternative and improved treatments for opioid use disorder (OUD) and opioid overdose. In 2019 alone, approximately 1.6 million people suffered from OUD, and 10.1 million people misused opioids. All three treatments approved by FDA for OUD are orthosteric mu-opioid receptor (MOR) ligands. The full agonist methadone and partial agonist buprenorphine are effective in reducing craving and managing opioid drug taking, but themselves are abused and methadone can cause severe respiratory depression. The MOR antagonist naltrexone has very poor patient compliance due to dysphoria and requires prior detoxification. Therefore, we sought to discover and develop better medications with different mechanism of action. Negative modulators of MOR (MOR-NAMs) target MOR outside of the orthosteric binding pocket in a non-surmountable fashion. This non-competitive approach may overcome the adverse effects of current medications and reduce relapse rate.

Through virtual screening using a b-arrestin recruitment assay at MOR, we identified a hit compound, MCTI-489, a pyrazolypyridine. We designed and synthesized a set of derivatives of MCTI-489 that ranged in potency to inhibit MOR-stimulation from 3 mM-1 mM. We extended the scaffold from pyrazolypyridines to benzothiazoles, most of which possess low micromolar potency, including MCTI-519, with a NAM

potency of 1 mM. In vitro functional experiments showed that MCTI-519 was effective in reducing the efficacy or potency of various MOR agonists including morphine, fentanyl, methadone as well as the standard MOR peptide DAMGO. MCTI-519 was also confirmed to act non-competitively using ligand-binding assays. MCTI-519 entered the brain following i.p administration and this resulted in partial inhibition of morphine-induced antinociception in mice. Taken together, the findings suggest MCTI-519 is a bioactive MOR-NAM that could serve as a lead compound for the development of medications for OUD. Supported by R37 DA039997; R41 DA56254 and the Michigan Center for Therapeutic Innovation.

855

Elucidating the Disposition and Metabolism of Benzalkonium Chloride compounds in C57BL/6 mice

Vanessa Lopez, Marie Brzoska, Ryan P. Seguin, Sydney Arnzen, Libin Xu

University of Washington

Benzalkonium chlorides (BACs) are quaternary ammonium antimicrobials widely applied in domestic, agricultural, clinical, and industrial settings (e.g., disinfectant sprays, food processing, pharmaceutical formulations, wood preservation, etc.). Despite the widespread usage of BACs for over 70 years, the FDA is now seeking additional safety data on their usage in healthcare and consumer antiseptic products, including information on pharmacokinetics, ADME, and BAC metabolites. Literature suggests BACs are absorbed following oral ingestion, and biomonitoring studies have found that BACs are detectable in up to 98% of human blood samples; However, there is little information available on the presence or levels of BAC metabolites. The study presented here describes the disposition of BACs, including metabolites, in C57BL/6 male and female mice following oral exposure to C12-BAC or C16-BAC at 120 µg /g/day for one week. UPLC-MS/MS analysis of tissue extracts (brain, heart, spleen, lung, liver, kidney, intestine), as well as fecal, urine, and blood samples from BAC-treated mice demonstrated the absorption and metabolism of BACs. Both parent compounds, C12- and C16-BAC, were detected in all the aforementioned tissues with levels from highest to lowest in the following order (big intestine (1.4-18 µM), ileum (0.6-5 µM), jejunum (3.2-13 µM), duodenum (1-8µM), spleen (15-72 nM), heart (10-370nM), liver (11-60 nM), lung (3-274 nM), brain (149-1550 pM)), whereas BAC metabolites were detected in all tissues except for brain or spleen. Our lab previously discovered that BAC metabolism is mediated by cytochrome P450 (CYP) enzymes, with ω- and ω-1 oxidized BACs (hydroxy, ketone, diol, and COOH) presenting as the major products of human BAC metabolism. Similar to the human metabolism, major metabolites quantified in mice were the ω- and (ω-1)-oxidized metabolites, as well as β-oxidized BAC-COOH products. Notably, metabolite to parent ratios within the aforementioned tissues highlight metabolizing capability in liver, intestine, lung and heart. Of all analytes quantified within the liver, up to 90% of them are metabolites. Furthermore, evidence of metabolizing capability in other tissues like lung (up to 70%), heart (50%), and intestine (80%) demonstrate novel understandings of BAC disposition and metabolism within an in-vivo model. Additionally, our work demonstrates evidence of preferential metabolism of C16-BAC over C12-BAC. Within big intestine, and fecal extracts at two separate time points (day 4 and day 7), there are higher metabolite to parent ratios in the C16-BAC treated mice (80%) compared to the C12-BAC treated mice (50%). Previous work in human microsomes has evaluated the metabolizing capability of the following tissues in the order of liver, kidney, intestine and lung. Future studies will assess the metabolic capacities of specific tissues by measuring rates of BAC metabolism in liver, lung, and kidney microsomes prepared from both male and female BAC-treated and untreated mice. Together, this work advances our understanding of BAC biodistribution and metabolism.

856

Reversal of Mechanical Hypersensitivity by 2R,6R-Hydroxynorketamine by Activation of Group 2 Metabotropic Glutamate Receptors

Irwin Lucki[1], Kaitlin Castell[2], Maria Campanile[2], Caroline A. Browne[2]

Uniformed University of the Health Sciences[1] Uniformed Services University[2]

(2R,6R)-hydroxynorketamine ((2R,6R)-HNK) is a non-hallucinogenic metabolite of ketamine and a potential analgesic agent. Its mechanism of action for producing analgesia is not known. The literature suggests that (2R,6R)-HNK can modulate glutamatergic neurotransmission and metabotropic glutamate receptors 2/3 (mGlu2/3Rs) are implicated in pain modulation. Activation of mGlu2/3Rs produces anti-nociception in several preclinical pain models. The aim of these studies was to test the hypothesis that mGlu2Rs mediate the analgesic effects of (2R,6R)-HNK on inflammatory pain in mice. ((2R,6R)-HNK) and the mGlu2/3R agonist LY379268 produced dose-dependent reversal of mechanical hypersensitivity produced by injection of λ-carrageenan (2.5% solution, 0.02 ml) injected subcutaneously into the plantar region of the left hind paw. The effects of both drugs were persistent lasting for at least 24 hours post-injection. Combining ((2R,6R)-HNK) with LY379268 produced additive effects. Pretreatment with the selective mGluR2 negative allosteric modulator VU6001966 prevented the analgesic effects of ((2R,6R)-HNK) and LY379268. The results indicate that ((2R,6R)-HNK) produces long-lasting analgesic effects using a mechanism involving the activation of mGluR2Rs.

857

In Vivo Production of Novel RNA Molecules and Computational Modeling of Their 3D Structures

Frank Mao[1], Meijuan Tu[1], Aiming Yu[2], Gavin Traber[2]

Univ of California, Davis[1] UC Davis School of Medicine[2]

Developing therapeutic RNAs and RNA-targeted small molecule drugs involves producing new RNA agents and understanding RNA structures. In this study, we aimed to employ our tRNA/pre-miRNA-based technology to produce two novel recombinant RNA (BioRNA) molecules and investigate their 3D structures through computational modeling. BioRNA expression plasmids were constructed through molecular cloning and verified via DNA sequencing. Following transformation and fermentation production, target BioRNAs were purified from total bacterial RNAs using an anion exchange FPLC method. High Purity (>99%) was confirmed through urea-PAGE and HPLC analyses, with high yields (9.91 and 4.56 mg per 250 mL culture) and minimal endotoxin levels (≤ 0.13 EU/μg RNA). Further, we employed Rosetta FARFAR2 and RNAComposer to predict the 3D structures of BioRNAs and assess potential differences as indicated by the root mean square deviation (RMSD). Our results showed that RNAComposer excelled Rosetta in modeling the known malachite green aptamer structure (RMSD = 2.558Å) while the latter demonstrated refinement with the increase of structure models (RMSD = 9.702Å to 6.895Å from 600 to 2000 models). On the other hand, Rosetta (RMSD=12.125Å) outperformed RNAComposer (RMSD= 22.944Å) in modeling the structure of human selenocysteine tRNA. Likewise, the 3D structures of novel BioRNAs predicted by Rosetta and RNACompoer were obviously different. As both programs recapitulated the empirical cloverleaf structure of the human leucine tRNA segment, the hsa-pre-miR-34a components within BioRNAs predicted by Rosetta were more stretched out while more curved by RNAComposer. Interestingly, the deviations between Rosetta and RNAComposer predictions increased with the size of RNAs (e.g., hsa-pre-miR-34a, RMSD=15.21Å; entire BioRNA, 21.231Å). These distinctions are likely attributed to the fact that RNAComposer uses larger fragments and allows efficient recognition of homologous elements or even the whole known structures, offering faster processing. By contrast, Rosetta relies on the Monte Carlo process, involving repeated random sampling to simulate near-native structures, which takes a rather much longer time. These predicted 3D structures of novel BioRNAs are amenable to experimental validation.

858

Inhibition of the Cysteine Protease Cathepsin K Attenuates Diabetic Neuropathic Pain

Vitoria Mattos Pereira, Cameron J. Campbell, Sreejayan Nair

University of Wyoming

Background and Aim. Diabetes mellitus is escalating at epidemic proportions worldwide, posing a huge clinical and economic burden on society. Diabetic peripheral neuropathy (DPN) is a painful and debilitating complication of diabetes that develops in 30-50% of diabetic patients. The drugs currently available to treat DNP lack specificity and only transiently relieve neuropathic pain. Recent studies demonstrated that the cysteine protease cathepsin K plays a critical role in the development of nociceptive pain, and genetic knockout of cathepsin K protects against chemical hypersensitivity in mice. The present study was undertaken to assess the efficacy of cathepsin K inhibition in alleviating DNP. ***Methods.*** Five-week-old C57BL/6J mice were rendered diabetic through a single intraperitoneal injection of streptozotocin (STZ, 150 mg/kg, dissolved in 50 mM citrate buffer), while the control animals received the buffer (n=10 per group). DNP was confirmed in diabetic mice using baseline measurements of peripheral nerve functions by determining mechanical response latency. Diabetic animals were challenged with a single intraperitoneal injection of Cathepsin K inhibitor II (0.01 mg/kg, EMD Millipore # 21937), and the measurements were repeated. Data were expressed as mean ± S.E.M and statistically evaluated using the paired Student t-test. ***Results***. STZ injections induced diabetes in the mice as evidenced by elevated blood glucose levels (459.22 ± 35.8 mg/dL). Diabetic mice exhibited mechanical hyposensitivity as indicated by a twofold increase in the von Frey filament threshold (4.75 ± 0.54 g) relative to controls (2.76 ± 0.55 g, $p \geq 0.05$, n=10). Treatment with cathepsin inhibitor II resulted in a complete reversal of the diabetes-induced mechanical hyposensitivity (2.42 ± 0.60 g, $p \geq 0.05$) (Fig. 1). Cathepsin K inhibitor did not alter the blood glucose levels in these animals. ***Conclusion.*** Inhibition of cathepsin K may represent a viable strategy to treat DNP.
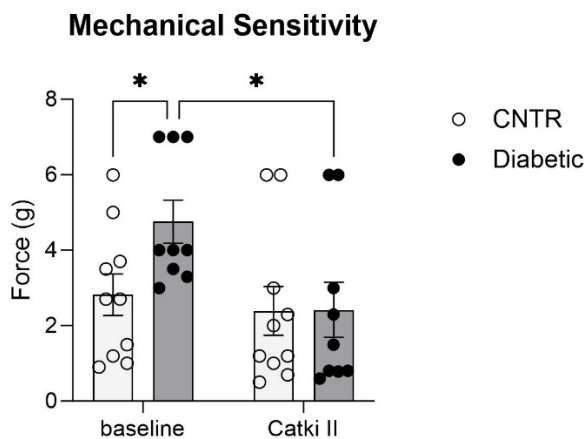
Figure 1: Treatment with cathepsin inhibitor II, one hour post-administration, reversed diabetes-induced mechanical hyposensitivity.

859

The Effect of Senolytic Therapy in a Mouse Model of Post-Traumatic Epilepsy

David J. McFall, Bevan Main, Mark Burns, Patrick Forcelli

Georgetown University

While there are dozens of anti-seizure medications available for patients with epilepsy, up to one third of patients experience seizures refractory to treatment. Identifying treatments that prevent epileptogenesis is an unmet need. Epileptogenesis involves DNA damage, apoptosis, and inflammation, features also relevant to the cellular senescence program. Senescent cells (SCs) arise in response to extreme stress or injury, leading to a decline in normal functioning and increased inflammation. Ongoing studies from our group show that both genetic and pharmacologic ablation of SCs normalizes spatial memory and reduces seizure burden in the status epilepticus mouse model. However, no studies have looked at the contribution of SCs in the development of post-traumatic epilepsy (PTE), where recurrent seizures develop following a traumatic brain injury. (TBI) This model is translationally compelling because the inciting epileptogenic event (a TBI) is often brought to clinical attention, making prophylactic anti-epileptogenic drugs a clinically viable strategy to prevent PTE. Here, we investigate the effects of dasatinib and quercetin (DQ) combination therapy on seizure burden and behavioral comorbidities in the PTE mouse model.

3-4mo old p16-TdTomato reporter mice on a C57Bl/6 background were given a controlled cortical impact (CCI) or sham surgery with the following parameters: 5.25m/s velocity, 2mm depth, 0.1sec dwell time, 3.5mm diameter impounder tip. Mice were then randomly assigned to receive either DQ or a vehicle injection IP once per week for the duration of the study. 2 months after injury, mice were tested in a battery of behavioral tests in order to assay object and spatial memory and anxiety, common behavioral phenotypes associated with PTE. After behavioral testing, at 3.5 months after injury, telemeters were implanted in the mice, and EEGs were recorded continuously for 2 weeks with synchronous video. Following EEG recording, mice were tested with a chemoconvulsant challenge (pentylenetetrazole-PTZ, a GABA-a antagonist) as a secondary measure of seizure-protective effects. Mice were then euthanized, and their brains were fixed for histology to confirm SC ablation and assess neurodegeneration. A similar number of animals were used from each sex. Analysis of behavior, EEGs, and histology were all performed blinded.

Mice given a CCI displayed a robust seizure phenotype, with a majority of animals exhibiting electrographic seizures. DQ-treated CCI mice have significantly fewer SCs compared to their vehicle-treated counterparts. SC ablation appears to reduce behavioral deficits in the open field test, elevated plus maze, and novel location test, although at the time of writing we lack the power to claim so conclusively. Finally, DQ-treated mice have a significantly longer latency to reach motor seizures and tonic-clonic seizures when challenged with PTZ.

This study assesses the use of senolytic therapy in a translationally-compelling context, PTE. While DQ does reduce SC burden in the PTE mouse model, more work is needed to understand the mechanisms of epileptogenesis in PTE and the role SCs play therein. Therefore, further work will explore the effect of DQ on rescuing CCI-mediated deficits in long-term potentiation and the effect of DQ on the transcriptome of CCI-injured mice.

860

Tetrahydroisoquinoline-Based Small Molecule Inhibitors of the Chemokine Receptor CXCR4

Eric J. Miller[1], Petra Gregorova[1], Carrie Q. Sun[1], Leon Jacobs[1], Zafer Sahin[1], Yesim Altas Tahirovic[1], Samantha L. Burton[1], Priscilla Davidson[1], Hyungyu Lee[1], Yanli Yang[1], Nicholas Vugman[1], Rebecca S. Arnold[1], John A. Petros[1], Haydn T. Kissick[1], Larry J. Wilson[1], Dennis C. Liotta[1]

Emory University[1]

CXCR4 is a physiologically important chemokine receptor that is expressed on hematopoietic stem cells (HSCs), endothelial progenitor cells (EPCs), and various immune cell subsets. These CXCR4-expressing cells traffic along concentration gradients of the sole endogenous chemokine ligand CXCL12, which disseminates from stromal niches in lymph nodes, lung, liver, and bone marrow. As a prime example, CXCL12 secretion from bone-associated stroma drives migration and retention of CXCR4-expressing cells, especially HSCs, in the bone marrow. Additionally the CXCR4/CXCL12 axis is pathophysiologically hijacked by various cancer types, over 50 of which are characterized by dramatic CXCR4 and/or CXCL12 upregulation. Roughly half of all RCC tumors, for example, are driven by deactivating mutations in tumor suppressor VHL, which negatively regulates CXCR4 and CXCL12 expression. This chemokine network misregulation (1) hyperactivates CXCR4 cancer cell survival signaling, (2) overstimulates intratumoral infiltration of CXCR4-expressing EPCs and immunosuppressive subsets (*e.g.*, reulatory T cells, TRegs, and myeloid-derived suppressor cells, MDSCs), and (3) pushes into overdrive the metastatic expansion of CXCR4-expressing cancer cells to distant CXCL12-secreting niches. As a consequence, there has been significant interest and progress over the last 25 years on the development of bicyclams, cyclic peptides, and small molecules that inhibit CXCR4-CXCL12 interactions. Although bicyclam plerixafor and cyclic peptide motixafortide have been approved by the FDA for HSC mobilization, both require administration via injection, and neither have unlocked the full therapeutic potential of CXCR4 antagonists in oncology. To address this gap, our team has been developing orally bioavailable, tetrahydroisoquinoline-based small molecule CXCR4 antagonists since the late 2000's. Through organic synthesis and pharmacological evaluation of nearly 500 compounds, a foundational understanding of associated structure-activity relationships has emerged. However, increased understanding is often paired with the realization of greater complexity, and that is certainly operative here. With our robust tool kit of small molecules and a growing panel of *in vitro* assays designed to measure different aspects of CXCR4 biology, a significant component of this collaborative research program will be dedicated to elucidating the nuances of complex CXCR4 function. In parallel, our best-in-class orally bioavailable CXCR4 antagonists will continue to be progressed through the pre-clinical pipeline and IND-enabling studies.

861

Leveraging a Novel GPCR ITIM Motif that Drives Gradient Signaling for Targeted Antibody Design and Peptide Inhibitor Development

Catherine C. Moore[1], Lili T. Belcastro[2], Ryan D. Paulukinas[3], Christina Adams[3], Catherine C. Moore[1]

West Center for Computational Chemistry and Drug Design, SJU, Philadelphia PA[1] Cancer Biology Program of the Wistar Institute, currently at Bristol Myers Squibb[2] Department of Pharmaceutical Sciences, Philadelphia College of Pharmacy[3]

CXCR4, a chemokine GPCR, is essential for migration of neuronal and hematopoietic cells during embryonic development, and for migration of breast cancer cells during metastasis whereby CXCR4 dysregulation promotes cell motility and invasion. Following uniform SDF stimulation, CXCR4 is rapidly phosphorylated on serine and threonine residues in the C-terminal tail, which initiates b-arrestin recruitment, receptor desensitization, and trafficking to endocytic sites. Here we show that stimulation with gradient SDF however, significantly delays this receptor phosphorylation and trafficking, leading to sustained signaling to a novel CXCR4-SHP2-ERK pathway. SHP2 is a tyrosine phosphatase implicated in

HER2+ and triple-negative breast cancers (TNBC), whereby it transduces mitogenic and migratory signals driving hyper-proliferation and invasion. SHP2 is recruited to tyrosine phosphorylated ITIM motifs (immunoreceptor tyrosine-based inhibitory consensus motifs), a hallmark of inhibitory immune receptors with little evidence for their presence in GPCRs. Here we identify a novel ITIM motif in the chemokine GPCR CXCR4, that drives gradient signaling to SHP2 and directional motility. Specifically, first we show that gradient SDF stimulation of the CXCR4 receptor 1) delays receptor phosphorylation and trafficking, and 2) sustains signaling to a novel CXCR4-SHP2-ERK pathway. Next, we identify an ITIM motif in the CXCR4 receptor that drives gradient SDF mediated 3) sustained signaling to SHP2, and 4) directional migration in TNBC cells. Additionally, we demonstrate that this novel ITIM motif can be 5) leveraged for targeted antibody design, and 6) peptide inhibitor development. Overall our data demonstrate that gradient SDF delays receptor Ser/Thr phosphorylation and internalization thereby sustaining signaling to SHP2-ERK and driving SHP2-dependent migration. Furthermore, a CXCR4 ITIM motif is critical for transducing this SDF gradient sensing to SHP2 binding and signaling, and directional motility. Coupled with our ITIM targeted antibody and peptide inhibitor development, these data have therapeutic implications for metastatic diseases driven by aberrant CXCR4 and SHP2 expression.

862

Regulation of Dopamine Receptor Subtypes by G Protein-Coupled Receptor Kinase Isoforms

Amy E. Moritz[1], Nora S. Madaras[1], Kirsten K. Snyder[1], Noelia M. Boldizsar[1], Raphael Haider[2], Julia Drube[2], Arun K. Ghosh[3], John JG. Tesmer[3], Carsten Hoffmann[2], David R. Sibley[1]

Molecular Neuropharmacology Section, NINDS/NIH[1] University of Jena[2] Purdue University[3]

Dopamine receptors (DARs) are G-protein coupled receptors (GPCRs) that regulate diverse physiological functions including cognition, mood, movement, and reward-related behaviors. They are classified as either D1-like (D1R and D5R) or D2-like (D2R, D3R, and D4R) based on structural homology and pharmacological properties. The D1-like DARs couple to Gs and Golf to increase cAMP levels, while the D2-like DARs couple to Gi/o to decrease cAMP levels. All DARs also recruit β-arrestin which activates distinct signaling cascades and can also initiate receptor desensitization and internalization. There are seven GRK isoforms (GRKs1-7), with GRK2, GRK3, GRK5, and GRK6 being widely expressed. Using systematic mutational analyses, our lab has previously mapped the GRK-mediated phosphorylation sites on both the D1R and D2R, with phosphorylation occurring exclusively on ICL3 for the D2R, and both ICL3 and the C-terminus for the D1R. GRK-mediated phosphorylation of the D1R was found to be required for subsequent β-arrestin recruitment. In contrast, while GRKs play a role in β-arrestin recruitment to the D2R, GRK-mediated D2R phosphorylation is dispensable for this process. We have now sought to determine which GRK isoform(s) are involved in regulating β-arrestin recruitment to these receptors using cell lines in which the expression of specific GRK isoforms were selectively eliminated via CRISPR, as well as by utilizing isoform-selective GRK inhibitors. β-arrestin recruitment to both the D1R and D2R was severely impaired in cells lacking all GRKs (total KO), whereas selective expression of GRK isoforms 2, 3, 5 and 6 in the total KO cells was able to rescue β-arrestin recruitment. The kinase activity of each GRK was required for this recue for the D1R. Interestingly, the GRK2/3 and GRK5/6 isoforms differed in their requirement of kinase activity for the rescue of β-arrestin recruitment to the D2R. Individual and double GRK KO cells revealed that the GRK5/6 subfamily is more important for β-arrestin recruitment to the D1R, while the GRK2/3 subfamily is more important for the D2R. Treatment with GRK2/3-selective inhibitors recapitulated these findings with the GRK KO cells in that they impaired β-arrestin recruitment to the D2R, but had limited effect on this process for the D1R. Intriguingly, in cells with endogenous levels of GRK expression, β-arrestin recruitment to both the D1R and D2R were unaffected by inhibitors of GRK5/6. However, these inhibitors could block the rescue of β-arrestin recruitment to the D2R observed with GRK5 or GRK6 overexpression but had little effect on the rescue of β-arrestin recruitment to the D1R or the Gs-coupled β2 adrenergic receptor. As GRK distribution varies by tissue and brain region, it is intriguing to postulate that DAR regulation, and GPCR regulation in general, by specific GRK isoforms can add layers of regulatory fine-tuning through differentially directing signaling or trafficking outcomes.

863

Extracellular Loop 2-Dependent Mechanism of Action for Orphan Receptor GPR52 Allosteric Agonists

Ryan M. Murphy, Haiying Chen, Jia Zhou, John A. Allen

University of Texas Medical Branch

GPR52, identified by GWAS as a schizophrenia risk gene, is a class-A orphan G protein-coupled receptor primarily expressed in D2 medium spiny neurons in the human striatum, where it activates the G_s/cAMP signaling pathway. Recent cryo-EM and x-ray crystallography studies have suggested that GPR52 is a self-activating receptor occurring through a unique conformation of its extracellular loop 2 (ECL2) domain that interacts with a canonical orthosteric ligand-binding pocket. Here we utilize receptor mutagenesis, functional cAMP assays, and computational docking models to determine the mechanisms for both GPR52 self-activation and agonism by novel ligands. In real-time cell-based studies using the GloSensor assay, GPR52 is highly constitutively active for increasing G_s/cAMP signaling. Expression of low levels of wildtype human GPR52 in HEK293 cells increases basal cAMP levels over 100-fold, with further elevation more than 300% over basal in response to saturating concentrations of GPR52 tool agonist FTBMT and an optimized lead agonist PW0787. Molecular docking studies of both ligands into the recently solved GPR52 crystal structure identified a conserved binding mode in an allosteric side-pocket, stabilizing interactions between the ECL2, TM1, TM3, TM7, and N-terminus domains. Mutation of key residues in the receptor structure have profound effects on both constitutive GPR52 cAMP activity and agonism in HEK293 cells. Alanine-span mutation of the "agonist-like" motif of the ECL2 (residues 182-190) decreases basal cAMP by more than 80% while also eliminating all agonist activity, indicating an allosteric mechanism of agonism that requires self-activation of the receptor by the ECL2 domain. A disulfide bond from TM3 C114 to ECL2 C193 locks the ECL2 "lid" motif onto the canonical class-A orthosteric site, and disruption of this unique cysteine bond by point mutation decreases basal cAMP by more than 90%. However, agonism by FTBMT and PW0787 rescues cAMP activity back to wildtype GPR52 basal levels in these mutant receptors, supporting a model of ECL2 self-activation that can be stabilized independently by either the receptor ECL2-TM3 disulfide bond or allosterically by the agonist ligands. Mutagenesis of coordinating residues in our ligand binding model significantly impede or eliminate agonist activity for both FTBMT and PW0787, independent of effects on GPR52 basal cAMP activity. This effect is most profound in disrupting hydrogen-bonding interactions between these agonists and the ECL2, in which we find that interaction with residues 188-191 is essential for the ECL2-stabilizing agonist mechanism of action. These docking and mutagenesis studies have been used to inform our continuing drug discovery program for iterative, structure-guided design of novel small molecule GPR52 allosteric agonists with potential therapeutic use for numerous psychiatric disorders, including schizophrenia and substance use disorders.

864

Discovery of Natural Product ITPK1 Inhibitors using a Luciferase-Based High-Throughput Screen

Martin Ng, Brice Wilson[1], Quan Khong[1], Nasim Dalilian[1], Lin Du[1], Tanja Grkovic[1], Barry O'Keefe[2]

NCI/NIH[1] NIH/NCI[2]

Inositol phosphates (IPs) are regulatory molecules important in many cellular functions. Inositol-1,3,4,5,6-pentaphosphate (Ins(1,3,4,5,6)P_5) and inositol hexaphosphate (IP$_6$) interact with biological processes that are highly dysregulated in cancers, including telomere maintenance, DNA repair, transcription regulation, necroptosis, apoptosis resistance, and chromatin structure regulation. Inositol 3,4,5,6-tetraphosphate (Ins(3,4,5,6)P_4) modulates calcium-activated chloride ion channels, which is important in mitigating cystic fibrosis symptoms. IP6 has also been shown to be a co-factor for HIV-1 capsid formation. Inositol-tetrakisphosphate 1-kinase (ITPK1) phosphorylates Ins(3,4,5,6)P_4 to produce Ins(1,3,4,5,6)P_5, the precursor of IP$_6$. Therefore, ITPK1 can regulate the cellular flex of IP$_6$ and is thus an attractive target for cancer therapies and other diseases. We used a luciferase-based high-throughput screen to assess pre-fractionated natural product extracts. Following assay-guided fractionation of active pre-fractionated extracts, we discovered small molecules from natural products that inhibit ITPK1. Rational drug design will be employed to enhance potency in biochemical, cellular, and animal model assays.

865

Characterization of NCGC1360 and NCGC1366 as Highly-Selective D$_2$ Dopamine Receptor Antagonists and Lead Candidates for the Treatment of Neuropsychiatric Disorders

Ashley N. Nilson[1], John N. Hanson[1], Tej Poudel[2], Andres E. Dulcey[2], Ramona M. Rodriguiz[3], Kuo Hao Lee[4], R. Benjamin Free[1], Raul R. Calvo[2], Lei Shi[4], William C. Wetsel[3], Juan J. Marugan[2], David R. Sibley[1]

Molecular Neuropharmacology Section, National Institute of Neurological Disorders and Stroke, NIH[1] Division of Pre-Clinical Innovation, National Center for Advancing Translational Sciences, NIH[2] Department of Psychiatry and Behavioral Sciences, Duke University Medical Center[3] Computational Chemistry and Molecular Biophysics Section, National Institute of Drug Abuse, NIH[4]

The D$_2$ dopamine receptor (D2R) is a G protein-coupled receptor (GPCR) and a validated drug target for the treatment of many neuropsychiatric disorders, including psychosis. All currently available antipsychotics are antagonists of the D2R; however, all of these drugs exhibit polypharmacology resulting in a plethora of off-target side effects including weight gain, dysphoria, and sedation, among others. A highly-selective D2R antagonist might overcome these pitfalls and increase patient compliance with taking antipsychotic medications. Previously, our lab conducted a high-throughput screen to identify D2R-selective antagonists with reduced activity at other GPCRs. This screen identified a promising hit compound that was chemically optimized into the lead drug candidates, NCGC1360 and NCGC1366. These drug leads have relatively high binding affinities at the D2R (~80 and ~50 nM, respectively), while displaying >100-fold selectivity over the D3R and >24-fold selectivity over the D4R. A β-arrestin recruitment assay revealed even higher D2R selectivity (>100-fold) of these compounds over the D3R and D4R. In a screen against an array of 46 GPCRs, channels, and transporters using radioligand binding assays, NCGC1360 and NCGC1366 only inhibited radioligand binding to the D2R. A functional screen of 168 GPCRs further determined that NCGC1360 and NCGC1366 were exceptionally selective with each compound completely antagonizing β-arrestin recruitment to the D2R with only minor effects at a few other receptors. Schild-type analyses using dopamine-stimulated β-arrestin recruitment revealed that both compounds are competitive antagonists. A comparative molecular docking study using the active structures of both the D2R and D3R showed that NCGC1366 occupies the orthosteric binding pocket of the D2R with extended contacts with residues in extracellular loop 2 (ECL2). The contacts in ECL2 are not conserved between the D2R and D3R, which may confer D2R selectivity. We thus swapped the ECL2 of the D2R and D3R and found that a D2R mutant with the D3R ECL2 exhibited diminished affinity for NCGC1360 and NCGC1366. Conversely, a D3R mutant with the D2R ECL2 exhibited increased affinity for NCGC1360 and NCGC1366, consistent with the molecular docking study. Pharmacokinetic studies of NCGC1360 in mice revealed a half-life of 1.8 hr in plasma and 1 hr in brain with excellent brain penetration. Finally, NCGC1360 was characterized in animal models that are predicative of antipsychotic efficacy and on-target side effects. NCGC1360 dose-dependently decreased

amphetamine-induced hyperlocomotion in mice and also rescued deficits in pre-pulse inhibition induced by amphetamine. Importantly, NCGC1360 did not induce catalepsy up to the highest dose tested (10 mg/kg), suggesting that it would not induce extrapyramidal side effects in patients. Taken together, these studies provide support for continuing the development of this scaffold with preclinical and IND-enabling studies.

866

Betulin, a Compound Isolated from *Crinum asiaticum* Bulbs Exerted Anti-Silicosis and Pulmonoprotective Effects Through the Inhibition of NF-κB activation in Rat model

Michael Ofori[1], Joshua Asante[2], Comfort Nyarko Snr[3]

Dr. Hilla Limann Technical Univ[1] Kwame Nkrumah University of Science and Technology[2] Kwame Hkrumah Univ of Sci and Tech[3]

Silicosis is an interstitial lung disease that causes shortness of breath, cough, fever, and blue skin and causes a heavy burden to patients both physically and mentally. Silicosis at the moment has no effective treatment, and patients depend on bronchodilators, antitussives, and mucolytic medicines for survival. After all other treatment alternatives have been exhausted, lung transplantation may be the sole choice. Silicosis is a serious global public health threat that requires immediate action to curb it. It prolongs hospital stay, increases the cost of medication, and increases the death toll recorded annually.
Betulin (BET) isolated from *Crinum asiaticum* bulbs (CAE) has exhibited a multitude of powerful pharmacological properties ranging from antitumor, anti-inflammatory, anti-parasitic, anti-microbial, and anti-viral activities. This work sought to investigate the anti-silicosis and pulmonoprotective effects of betulin and CAE as well as elucidating the possible mechanism in mitigating pulmonary silicosis in crystalline silica induced silicosis in rat model.
The results showed that CAE and BET reduced significantly ($\rho < 0.0001$) the levels of NF-κB, TNF-α, IL-1β, IL-6, hydroxyproline, collagen types I and III when compared with the negative control group. On broncho alveoli lavage fluid (BALF) biomarkers such as macrophages, lymphocytes, monocytes, and neutrophils, CAE and BET were able to reduce their levels significantly ($\rho < 0.0001$). The CAE and BET were investigated for their anti-oxidant activity and were shown to increase the levels of catalase (CAT) and superoxide dismutase (SOD) while lowering the level of malondialdehyde (MDA). There was also an improvement in lung function when lung tissues were examined histologically.
In conclusion, CAE and BET possessed anti-silicosis effect and occurred through the down regulation of NF-κB and some pro-inflammatory cytokines and also acted as protective mechanisms, facilitating the preservation of the lung's physiological integrity. The outcome of this study could for serve as leads in
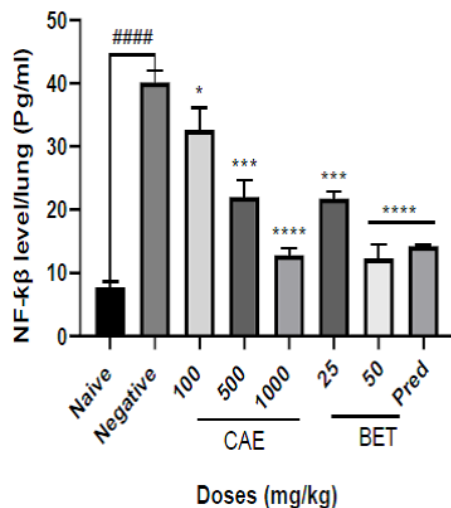
Fig 1. Effect of CAE and BET on NF-ƙβ level

867

Green Silver Nanoparticles Synthesized from *Moringa Oleifera* Stem Bark Elicits Effective Antidiabetic Effect in Alloxan-Induced (Type I) Diabetic Wistar Rats

Frank Ogundolie[1], Grace Adebayo-gege[1], Ruqayah A. Aliyu[2], Queen Ozegbe[1], Aasia J. Muhammed[1], Toyin D. Alabi[1]

Baze University, Abuja, Nigeria[1] Baze University Abuja, Nigeria[2]

The use of nanomaterials in antidiabetic research is on the rise because of their special qualities, like their small size, biocompatibility, and capacity to penetrate cell membranes for drug delivery. In this study, the efficacy of an aqueous extract of *Moringa Oleifera* (MoSB) in crude and nanosized form using silver nanoparticles was observed. MoSB and its nanoparticles (MoSB-AgNPs) were prepared according to standard procedures and their effect was assessed on relevant enzymes associated with diabetes. Male Wistar rats were randomly separated into 7 groups of five rats each. The induction of diabetes in rats was by a single intraperitoneal injection of alloxan (180 mg/kg body weight). Rats were grouped as follows: Group 1 (normal Control); Group 2: (diabetic control); Group 3 (diabetic + 15 mg/kg nanosized extract); Group 4 (non-diabetic + 15mg/kg nanosized extract); Group 5 (non-diabetic + 250mg/kg aqueous extract); group 6 (diabetic+250mg/kg aqueous extract); group 7(diabetic+ 5mg/kg Glibenclamide (standard drug). The experiment lasted for 21 days. The results revealed that the blood glucose levels were significantly lower (P< 0.05) in rats administered MoSB-AgNPs when compared with the diabetic control group. Furthermore, administration of MoSB extracts and MoSB-AgNPs attenuated oxidative stress by decreasing MDA levels, enhancing superoxide dismutase, catalase and reduced glutathione activities, reinstated the lipid profiles and liver marker enzymes to nearly normal levels and restored pancreatic histological integrity in diabetic rats. The results reveal that *M. Oleifera* and MoSB-AgNPs exert their antidiabetic effects through the modulation of glycemic and atherogenic indices as well as the mitigation of free-radical-mediated damages. The present findings revealed that plant-mediated silver nanoparticles significantly improved the alloxan-induced diabetic changes in various treated rats and might be used in the treatment/ management of diabetes.

868

Structure-Activity Relationship of 5-Arylethynyl Derivatives of (2-Aminothiophen-3-yl) (phenyl) methanones as A$_1$ Adenosine Receptor Positive Allosteric Modulators

Paola Oliva[1], Rama R. Suresh[1], Silvia Pasquini[2], Veronica Salmaso[1], Edward Will[1], Dilip Tosh[1], Zhan-Guo Gao[1], Naili Liu[1], Oksana Gavrilova[1], Fabrizio Vincenzi[2], Katia Varani[2], Kenneth Jacobson[1]

NIDDK/NIH[1], University of Ferrara[2]

Adenosine is a physiological extracellular modulator acting via four distinct G protein-coupled receptors. The G$_i$-coupled A$_1$ adenosine receptor (A$_1$AR) is a target for antinociceptive anti-seizure and anti-ischemic therapeutics, and the in vivo efficacy of various selective A$_1$AR agonists has been demonstrated. Efforts to target the A$_1$AR in clinical trials of selective orthosteric agonists have been limited by various cardiovascular side effects. Here we explore an alternative strategy by targeting the A$_1$AR with a positive allosteric modulator (PAM) of endogenous adenosine, which is elevated under stressed conditions. Our goal was to design and synthesize a new series of 2-amino-3-benzoyl thiophene derivatives (a known class of A$_1$ PAMs) able to bind the A$_1$AR allosteric site with both tissue-specific and receptor-specific modulation capabilities. The synthesis was patterned after previously reported A$_1$ PAMs, and the new analogues were obtained in good yields and high purity. The most potent synthesized compounds were identified in human A$_1$AR agonist radioligand saturation and competition assays. More specifically, the activity of 2-amino-3-benzoyl thiophene A$_1$AR PAMs can be increased considerably by appropriate substitutions at the 4- and 5-positions of the thiophene ring. Also, the presence of the 4-neopentyl substitution can further enhance activity. Lastly, we also included 5-arylethynyl substitution of the thiophene moiety to determine which phenyl substitution optimizes PAM activity. The most potent analogues contained 2-F, 3,4-F$_2$, and 2-CF$_3$ substitutions of the 5-terminal phenyl ring. These compounds achieved strong PAM enhancement effect, each increasing the Bmax shift by ~73%, compared to reference compound with ~77%. Lastly, molecular modeling analysis based on a cryo-EM structure (PDB ID: 7LD3) allowed us to predict molecular details of binding with identification of key interactions. A$_1$AR PAMs represent potential new drug molecules. It is our interest to further investigate the pharmacokinetic properties and in vivo efficacy of our compounds as possible candidates in the treatment of neuropathic pain, hypoxia, and ischemia-induced injury.

869

A Gα$_s$ and Gα$_i$ Chimera Alters cAMP Kinetics and Appears to Inhibit GRK Function

Ogochukwu F. Orabueze[1], Bradley Andresen[1], Dominique Brown[1], Garima Sharma[1], Murat Bastepe[2]

Western University of Health Sciences[1] Massachusetts General Hospital and Harvard Medical School[2]

Canonically, GPCRs interact with the GDP-bound heterotrimer G protein (Gαβγ) in a cytosolic pocket in the receptor, and when signalling is terminated the Gαβγ return to the receptor. GRKs utilize the same pocket to interact with the active GPCR. We hypothesize that the returning inactive Gαβγ and GRKs compete for the same binding site if the receptor remains in the active conformation. To investigate this, a chimera containing a portion of Gα$_{i1}$ was inserted into the first half of the helical domain of Gα$_s$ (G$_s$-60-G$_{i1}$-138-G$_s$), named *sis*. To exclude background effects of endogenous Gα$_s$, Gnas$^{E2-/E2-}$ MEFs with endogenous β2-adrenergic receptors (β2-ARs) were transfected with Gα$_s$ or *sis* and a split luciferase cAMP probe. The difference between 1 μM isoproterenol (ISO)-mediated Gα$_s$ and *sis* cAMP accumulation and decay kinetics was investigated. The accumulation kinetics demonstrate that sis produces more cAMP (Gα$_s$ = 2.4-fold & *sis* = 3.1-fold, p = 0.005) but at a slower rate (Tau: Gα$_s$ = 3.4 & *sis* = 4.8 min, p = 0.003), and the decay kinetics were drastically different. The cAMP decay kinetics of *sis*-expressing cells fits zero order kinetics versus first order kinetics for Gα$_s$ cells (p = 0.0014), resulting in a much slower

decay (Tau: $G\alpha_s$ = 22.8 ± 12.6 & *sis* = 57.9 ± 24.7 min). To determine if the change in decay kinetics is due to prolonged receptor activation, 10 µM propranolol (PROP) was added 12 minutes after ISO stimulation. PROP induced *sis* cAMP decay kinetics to follow first-order kinetics (p = 0.0070), resulting in *sis* reaching baseline (Tau: 29.1 ± 13.3 min, p = 0.0117 vs *sis* w/o PROP). The PROP-induced changes indicate that the *sis* construct allows the β2-ARs to remain in an agonist-bound active state for a longer duration. Transfection of GRK2,4,5, and 6 failed to decrease ISO-mediated cAMP production in *sis* cells; therefore, 10 µM GRK inhibitor (CMPD101) was used to observe the role of GRKs in $G\alpha_s$-mediated cAMP production. Although underpowered, the data demonstrated that inhibition of GRKs changed half the $G\alpha_s$ samples cAMP decay kinetics to zero-order linear kinetics (p = 0.2821); however, more experiments are being conducted to match a power analysis. To determine if *sis* cycles rapidly, NanoLuc was inserted into $G\alpha_s$ and *sis* to examine Gαβγ association and dissociation with a split Venus Gβ and Gγ via BRET; these experiments are ongoing. The data supports the hypothesis that increasing the kinetics of G protein cycling interfere with GRK-mediated inhibition of canonical receptor signalling.
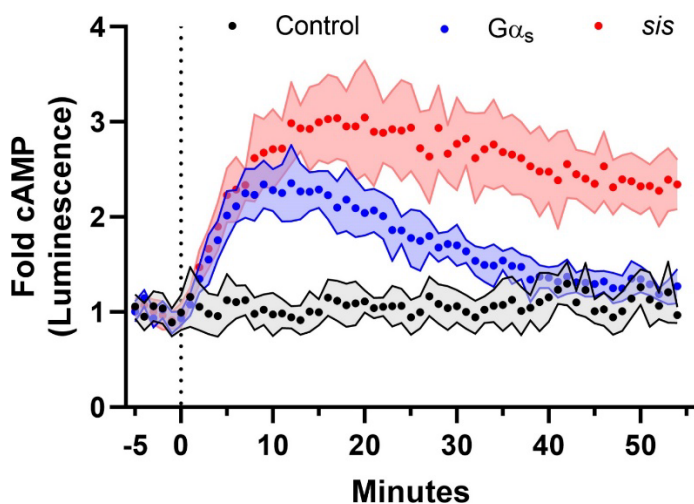
Fig 1. Fold change in ISO-mediated cAMP production. Gnas[E2-/E2-] MEFs, MEFs + $G\alpha_s$, and MEFs + sis was stimulated with 1 µM ISO after 4 minutes of basal reading cAMP was measured via Promega GlowSensor cAMP assay (n=8). Mean ± 95% CI (shown as the shaded range); generated using GraphPad Prism 10.

870

A GPT4-based Patient Simulation to Enhance the Integration of Pharmacology with Clinical Decision Making in a PharmD Program

Karim Pajazetovic[1], Dayanjan Wijesinghe[2], Ashim Malhotra[1]

California Northstate University[1] Virginia Commonwealth University[2]

Artificial intelligence (AI) is a powerful tool with the potential to engender disruptive and transformative educational changes in pharmacology teaching and learning. While legitimate concerns about AI focus on potential plagiarism, novel strategies that apply "out-of-the-box" thinking promise to revolutionize pedagogy, assessment, practice, implementation, and learner engagement. We implemented generative AI (GPT4)-based patient simulators for Team Based Learning application exercises in the immunology-pharmacology course sequence in our four-year Doctor of Pharmacy (PharmD) program. Our collaborative inter-university team of pharmacology and pharmacotherapy faculty, PharmD and graduate

students created 11 GPT4-based "artificial patient simulators" to interact with student teams and present an immunology case in a patient counseling setting. An online platform using Amazon Web Services with user authentication was created by the pharmacotherapy team at VCU which hosted the GPT4-student teams interaction interface. Faculty and a PharmD student created a splenectomy patient case using peer-reviewed StatPearls and developed a rubric for the GPT4 to grade students on their responses. While the case was the same in content, care was taken to impart a different patient "personality" to each ChatGPT4 "patient," essentially creating many different scenarios. The code for the generative AI was published in an open-access journal after first piloting it in Enterprise Google Cloud and eventually migrating it to Amazon Web Services. From an instructional design perspective, the indications for splenectomy, patient symptoms, and pathophysiology were integrated into the patient case and designed to be presented by the AI chat bot. Twelve student teams (N=59 students) were presented the patient case by the AI bot through stepwise interaction. The AI bot presented dynamically altered scenarios based on the questions asked by the student teams. The teams were required to create a pharmacotherapeutic care plan, with emphasis on counseling regarding specific infections common in splenectomy patients as the pharmacists' responsibility. We utilized a mixed methods approach to evaluate the impact on student learning and perceptions of learning. Data from student responses were automatically graded by the AI-bot using our rubric. Overall, our results showed that all student teams were scored by the AI-bot at least at a 75% competency level in assessing the patient simulation, identifying the immunology disease state, and patient counseling. Furthermore, all teams graded the activity above 90% in the following categories on the student perception instrument: 1) engagement, 2) optimal use of class time, 3) enhancing understanding and application of the material, and 4) confidence-building. Among the limitations identified by students were the time required for the class activity and the potential to use a similar ChatGPT interface to resolve the case. We plan to address this through the use of technology in future iterations by enabling browser lockdown and geofencing technology which stops students within the premise from accessing public facing generative AI models in that location and time,

871

NF-κB Inhibition Mitigates Colorectal Cancer Lung Metastasis

Hua Pan[1], Luke E. Springer[1], Antonina Akk[1], Rujula Polu[1], Jeremy Cho[1], Yuqian Xie[1], Samuel A. Wickline[1], Christine Pham[2]

Washington University School of Medicine[1] University of South Florida[2]

Globally, colorectal cancer (CRC) stands as the third-leading cause of cancer-related mortality, impacting over 1.85 million individuals and resulting in more than 850,000 deaths annually. Alarmingly, at the time of diagnosis, 20% of patients present with metastatic cancer, while 25% of those initially diagnosed with localized disease eventually develop metastases. Lung metastases afflict 15% of metastatic CRC (mCRC) patients, with the lung emerging as the second most common site of metastasis occurrence, following the liver. The constitutive activation of canonical NF-κB has been observed in at least 40% of CRC tissues, promoting tumor cell proliferation and chemo-resistance. Here, we hypothesized that NF-κB inhibition could mitigate CRC lung metastases. CT26-Luc cells, mouse colorectal tumor cells with $KRAS^{G12D}$ mutation and stably transfected with Luciferase, were intravenously injected into 5-week-old BALB/cJ mice at a dose of 1×10^5 cells per mouse. Seven days after tumor cell injection, the mice were randomly divided into two treatment groups: control and p5RHH-p65 siRNA nanoparticles at dose of p65 siRNA of 0.5mg/kg (Rx). The treatments were administrated three times a week for two weeks. On each treatment day, mice were injected with D-Luciferin, potassium salt at a dose of 150 mg/kg for IVIS imaging. The quantification of IVIS imaging results (Fig. A) suggested that the treatment significantly reduced the burden of lung metastasis as confirmed by H&E staining (Fig. B-C). The mice were euthanized 72 hours after the last treatment dose. Blood was collected via cardiac puncture, and safety of the treatment was validated by normal blood chemistries. Moreover, the treatment did not suppress innate and adaptive immune responses, as evidenced by the number and composition of splenocytes, as well as the T-cell responses to stimulations. Since tumoral CD8+ infiltration is correlated with favorable

CRC prognosis, we evaluated CD8+ T cell infiltration by immunofluorescence staining. The results showed that canonical NF-κB inhibition promoted CD8+ T cell infiltration (Fig. D (Ctrl)-E (Rx)). Moreover, cell proliferation, as indicated by Ki67 staining showed that the treatment inhibited tumoral proliferation (Fig. F(Ctrl)-G(Rx)). In conclusion, NF-κB inhibition by p65 selective siRNA nanoparticles could be further investigated for mitigating lung metastases in mCRC patients.
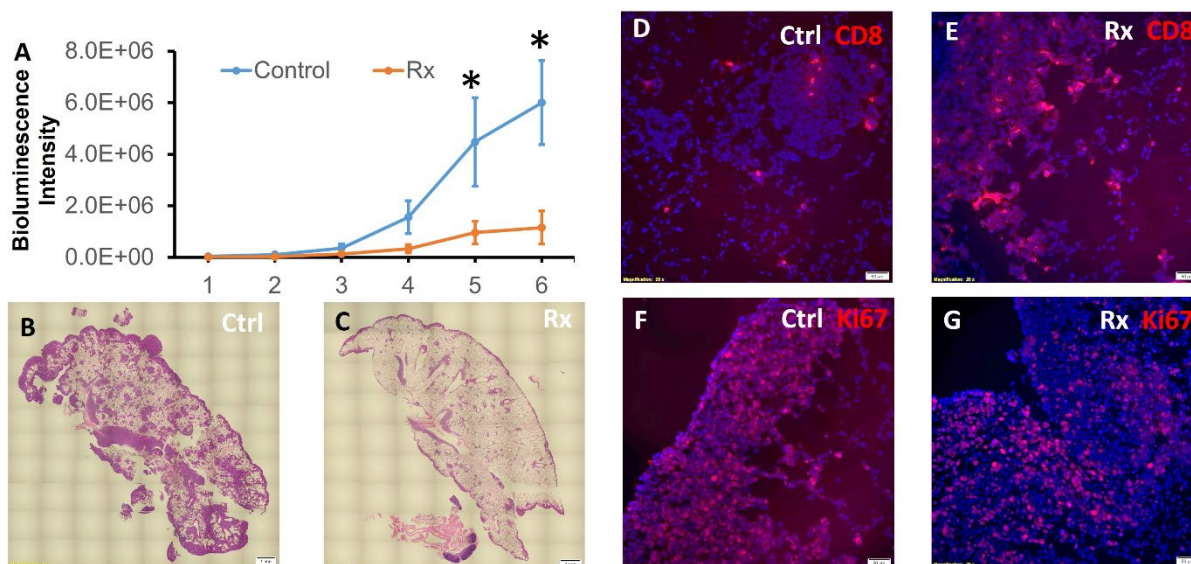
Figure. Canonical NF-κB inhibition in lung metastasis caused by colorectal tumor cells with KRAS^{G12D} mutation. The treatment significantly reduced lung metastasis (A. Lung metastasis burden over time, n= 5 and 6, control and Rx, respectively, *: $p<0.05$; B: control, and C: treated), increased the number of CD8 (Red) cells (D: control, and E: treated), and decreased the number of Ki67 positive (Red) cell (F: control, and G treated). (Scale bar: B-C: 1 mm; D-G: 50 µm).

872

Targeting Exon 7-Associated 7TM C-Terminal Variants of the Mu Opioid Receptor Gene for Mitigating Adverse Effects of Mu Opioids Without Altering Analgesia in Pain Management

Yingxian Pan[1], Shan Liu[1], Raymond Chien[1], Ayma Malik[2], Tiffany Zhang[3], Valerie P. Le Rouzic[3], Jin Xu[1], Grace Rossi[4], Arlene Martinez-Riverrra[5], Anjali M. Rajadhyaksha[5], Rolen Quadros[6], Gurumurthy Channabasavaiah[6]

Rutgers New Jersey Medical School[1] Rutgers, The State Univ of New Jersey[2] Memorial Sloan-Kettering Cancer Center[3] Long Island University[4] Weill Cornell Medicine[5] University of Nebraska[6]

The single-copy gene (*OPRM1*) encoding the mu opioid receptor (MOR) undergoes extensive alternative splicing, generating multiple splice variants. One set of *OPRM1* variants, exon 7-associated full-length 7 transmembrane (TM) C-terminal splice variants (E7 variants), contain a unique intracellular C-terminal tail with 30 amino acids encoded by E7 that are highly conserved from rodents, primates to humans. E7 variants are abundantly expressed in the central nervous system with distinct distributions among brain regions. Cumulative evidence has indicated that these E7 variants play a crucial role in mediating various adverse effects associated with clinically used mu opioids, such as tolerance, reward, and respiratory depression. For example, truncating E7-enocded C-terminal tails in mice (mE7M-B6) attenuated

morphine tolerance and reward, while not affecting analgesia. The current studies further establish the role of E7 variants in mediating mu opioid-induced tolerance, reward, and respiratory depression in naïve mice and mE7M-B6 by using antisense oligos (ASOs) and a newly developed rabbit monoclonal antibody (RabmAb) that target E7 sequences. Intracerebroventricular administration of either the ASO or RabmAb attenuated morphine tolerance measured by radiant-heat tail-flick assay and reward measured by conditioned place preference (CPP) in mice. Additionally, we generated a new mouse model (mMOR-1O-KI) in which only a single E7 variant, mMOR-1O, is expressed to investigate the *in vivo* functions of mMOR-1O. The results showed that mMOR-1O-KI mice had enhanced morphine tolerance and reward (CPP), complementing those the results from mE7M-B6 mice and further supporting the role of E7 variants in mediating these effects. Furthermore, fentanyl-induced tolerance, reward and respiratory depression measured by whole body plethysmography were significantly reduced in mE7M-B6 mice. Together, these studies indicate that targeting E7 variants presents a promising approach to mitigate tolerance, reward, and respiratory depression associated with clinically used mu opioids, while preserving their analgesic properties mediated by other *Oprm1* 7TM variants.

873

Nanoencapsulation of Curcumin-Piperine Complex for Targeting CYP17A1 in Castration-Resistant Prostate Cancer

Amit Pandey[1], Jibira Yakubu[1], Evangelos Natsaridis[2], Oya Tagit[2], Therina du Toit[1]

University of Bern[1] University of Applied Sciences and Arts, Northwestern Switzerland[2]

Androgens play a pivotal role in prostate cell survival and are implicated in both early-stage and advanced, castration-resistant prostate cancer (CRPC). During the past decade, new treatments have targeted the androgen signaling axis either by inhibiting the binding of androgens to androgen receptor (AR) and AR nuclear translocation or by inhibiting androgen production through the cytochrome P450 enzyme CYP17A1. Given its crucial role in androgen production, CYP17A1 has become a major target for cancer therapies. Current treatments targeting CYP17A1 in prostate cancer are not very specific. In CRPC patients on CYP17A1 inhibitors, the development of drug resistance and hypertensive crisis through the inhibition of CYP21A2 and or its substrate is a recognized challenge.

In this study, we employed a mini-evaporation technique to nanoencapsulate curcumin, exploring its impact on CYP17A1 activity in human adrenal NCI-H295R cells. CYP17A1 and CYP21A2 assays were carried out using radiolabelled substrates. We performed full steroid profiling with LC-MS/MS, as well as gene and protein expression studies by qPCR and western blots. Prostate cancer cell proliferation assays were carried out using LNCaP, VCaP, PC3, and DU145 carcinoma cell lines. Cell cycle analysis was done using flow cytometry.

Experiments performed in adrenal NCI-H295R cells showed that our curcumin-piperine nanoparticles efficiently suppress the CYP17A1-17α-hydroxylase activity that converts progesterone to 17-hydroxy-progesterone. Our nanoparticles also demonstrated inhibitory effects on the CYP17A1-17,20 lyase activity, which converts 17α-hydroxy-pregnenolone to dehydroepiandrosterone (DHEA). Compared to the effect of known CYP17A1 inhibitor abiraterone in NCI-H295R cells, our nanoparticles did not show any inhibitory effects on CYP21A2-hydroxylase activity, which metabolizes the production of deoxy corticosterone and 11-deoxycortisol. Curcumin and piperine combined in nano-capsules greatly increased the inhibitory effects on CYP17A1 activity. Furthermore, gene and protein expression analysis by qPCR and western blot investigations of the interaction of nanoparticle preparations on cells did not show any changes, and flow cytometry analysis did not reveal cell cycle effects.

We further confirmed the efficacy of our nanoformulation by testing its impact on the growth of androgen-sensitive (LNCaP, VCaP) and insensitive (PC3, DU145) prostate cancer cell lines. Notably, steroid profiling by LC-MS/MS revealed that nanoencapsulation improved curcumin's inhibitory effects on DHEA production via CYP17A1. Surprisingly, the curcumin-piperine nano-capsules enhanced these effects while not affecting CYP21A2, offering a promising option for prostate cancer treatment.

Our study reveals the promise of nanoencapsulated curcumin-piperine as an option for targeting CYP17A1, either alone or in combination with other drugs loaded on nanoparticles, for improved prostate cancer therapy. The synergistic benefits observed in our study open new avenues for addressing the difficulties associated with androgen deprivation therapy.
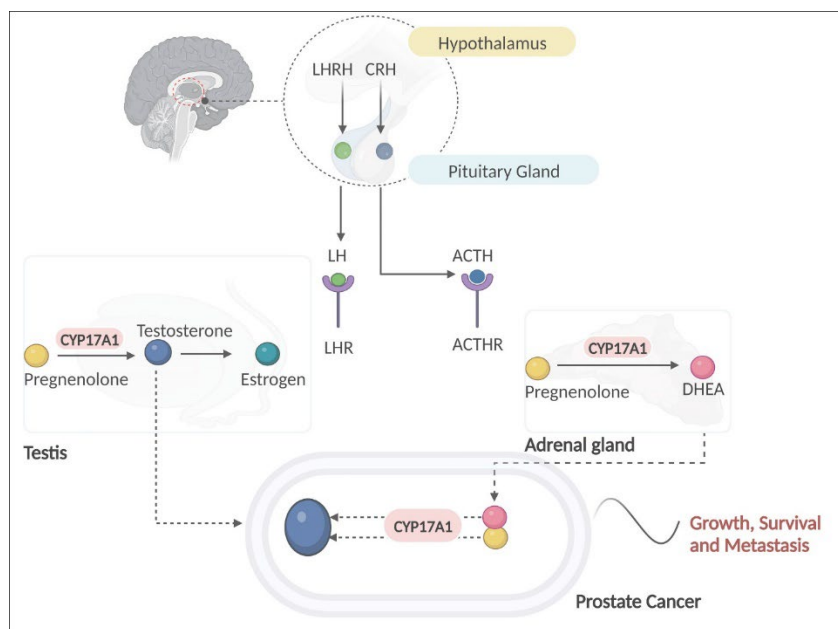
874

Low Dose Methylphenidate Modulates Risky Decision Making and Prefrontal Catecholamine Regulation in a Sex-Dependent Manner Following Repeated Mild Traumatic Brain Injury

Eleni Papadopoulos[1], Anna Abrimian[2], Christopher P. Knapp[1], Karen Joyce[1], Barry D. Waterhouse[1], Rachel L. Navarra[1]

Rowan-Virtua School of Translational Biomedical Engineering and Sciences[1] Rowan-Virtua School of Osteopathic Medicine[2]

Head trauma impairs higher-order decision making processes mediated within the prefrontal cortex (PFC) of the brain and often leads to increased risk-taking behavior. Mild forms of TBI (mTBI), often labeled concussion, account for over 75% of reported TBI cases. Although many individuals including athletes and military personnel experience repeated mild traumatic brain injuries (rmTBIs), the consequences of sustaining multiple traumatic events and whether effects are sex-dependent remain elusive. Additionally, there are no FDA-approved treatments for rmTBI. The catecholamine neurotransmitters, dopamine (DA) and norepinephrine (NE), modulate the PFC's actions and require precise regulation for optimal

processing. Imbalances in catecholamine function have been associated with TBI and are theorized to underlie TBI-induced increases in risky decision making. The psychostimulant, methylphenidate (MPH), elevates catecholamine levels by blocking DA and NE reuptake transporters (NET). Due to MPH's efficacy in reducing impulsive and risky behavior in patients with attention deficit hyperactivity disorder (ADHD), it has been considered as a potential therapy for alleviating similar neurocognitive symptoms following TBI. However, it is unknown how MPH can influence risk/reward decision making and levels of catecholamine regulatory proteins within specific PFC subregions following rmTBIs. Here we used a closed head-controlled cortical impact model to induce up to 3 mTBIs, the probabilistic discounting task of risky decision making, and western blotting to determine the effects of chronic low-dose MPH (0.5 and 2 mg/kg, i.p.) on risky behavior and catecholamine regulatory protein levels within specific PFC subregions following rmTBI in male and female rats. Our results show that rmTBI alone increases risky choice preference in saline-treated females, but not males. MPH prevented injury-induced risky choice behavior in females for up to 3 weeks post-rmTBI. Conversely, MPH promoted risky choice behavior in rmTBI males. Within the medial PFC, expression levels of packaging protein vesicular monoamine transporter (VMAT) were decreased in both male and female saline-treated rmTBI groups. MPH treatment normalized VMAT levels in injured females, but not injured males. Within the orbitofrontal cortex, VMAT and NET were decreased in the MPH-treated rmTBI males only. Our results suggest that females are more susceptible to rmTBI-induced behavioral disruption and rmTBI reduces transporter levels within regions of the PFC. In addition, MPH treatment produces restorative benefits in females, but exaggerates pathological outcomes in males. This study is the first to reveal a potential sex-specific psychostimulant therapeutic strategy for rmTBI-induced risky behavior and neuropathological outcomes.

875

Identification and characterization of extrahelical allosteric binding site for 1*H*-imidazo[4,5-c]quinolin-4-amine A$_3$ adenosine receptor positive allosteric modulator

Matteo Pavan[1], Courtney L. Fisher[2], Veronica Salmaso[3], Robert F. Keyes[2], Tina C. Wan[2], BALARAM Pradhan[1], Zhan-Guo Gao[1], Brian C. Smith[2], Kenneth Jacobson[1], John A. Auchampach[2]

NIDDK/NIH[1], Medical College of Wisconsin[2], University of Padua[3]

The A$_3$ adenosine receptor (A$_3$AR) is an appealing therapeutic target for treating various pathological conditions, such as cancer, chronic pain, ischemic and inflammatory diseases, as demonstrated by orthosteric agonists IB-MECA and Cl-IB-MECA reaching clinical phase 2/3 for cancer, liver diseases, and psoriasis. Side effects associated with orthosteric agonists could be overcome by using positive allosteric modulators (PAMs) that would allow for site- and time-specific receptor activation limited to the affected tissue having elevated adenosine. Although many A$_3$AR PAMs of the 2,4-disubstituted-1*H*-imidazo[4,5-c]quinolin-4-amine class have already been reported in the literature, the rational discovery of novel chemotypes and the optimization of already identified ones have been hampered so far by the absence of structural characterization of their allosteric binding site. In the present study, we employed an integrated structure-based molecular modeling pipeline, alongside mutagenesis and SAR expansion, to model the active-state A$_3$AR structure, identify the allosteric binding site for LUF6000 (the prototypical 2,4-disubstituted-1*H*-imidazo[4,5-c]quinolin-4-amine PAM), and characterize its binding mode. The identified allosteric binding site for LUF6000 and its analogs, predicted through molecular modeling and validated by mutagenesis, is an extrahelical lipid-facing pocket located at the interface between helix 8 and the cytosolic ends of TM1 and TM7. According to the model, the nearly planar 1*H*-imidazo[4,5-c]quinolinamine ring system lies parallel to the transmembrane segments, inserted into an aromatic cage formed by π-π stacking interactions with the side chains of Y284$^{7.55}$ in TM7 and Y293$^{8.54}$ in H8, and by π-

H bonding between Y284[7.55] and the exocyclic amine. The 2-cyclohexyl group is positioned 'upward' within a small hydrophobic sub-pocket created by residues in TM1 and TM7, while the 3,4-dichlorophenyl group extends into the lipid environment. An H-bond between the N-1 amine of the heterocycle and the carbonyl of G29[1.49] further stabilizes the interaction. MD simulations predicted two metastable intermediates, one resembling a pose determined by molecular docking and a second involving transient interactions with Y293[8.54]; in simulations, each of these intermediates converges into the final bound state. Structure activity relationships for the replacement of either of the identified exocyclic or endocyclic amines with heteroatoms lacking H-bond donating ability were consistent with the hypothetical pose. The present work showcases a mixed computational-pharmacological pipeline that could support the rational discovery and development of novel PAMs in the absence of an experimental A₃AR structure, provides a convincing SAR for the 2,4-disubstituted-1*H*-imidazo[4,5-c]quinolin-4-amines series, and represents the first example of a PAM targeting this allosteric pocket among class A GPCRs.

876

Multitarget-Directed Ligands with Soluble Epoxide Hydrolase and Fatty Acid Amide Hydrolase Inhibitory Activities for Treatment of Chronic Pain

Stevan Pecic[1], Ram Kandasamy[2], Jeannes Angelia[1]

California State University, Fullerton[1] California State University, East Bay[2]

The combined inhibition of soluble epoxide hydrolase (sEH) and fatty acid amide hydrolase (FAAH) represents a novel approach to non-opioid pain management, drawing from the known functions of these enzymes in pain and inflammatory pathways. Using multi-target directed ligands (MTDLs), a medicinal chemistry approach where a single drug modulates two or more biological targets simultaneously, our lab previously identified several benzothiazole-phenyl MTDLs with potent dual sEH and FAAH inhibition. Here, we report several in vivo evaluations of our previously identified dual sEH/FAAH inhibitor SP 4-5, the data received from National Institute of Mental Health's Psychoactive Drug Screening Program (PDSP) and a follow-up structure-activity relationship (SAR) study of quinolinyl-phenyl-based MTDLs that were synthesized using a microwave-assisted Suzuki coupling reaction. SP 4-5 was evaluated against persistent inflammatory pain. An intraplantar injection of Complete Freund's Adjuvant (CFA) was used to induce hindpaw inflammation. 1 and 3 mg/kg SP4-5 were administered 24 hours after inflammation. Neither dose alleviated mechanical or thermal hypersensitivity. However, when administered 2.5 hours after CFA, 3 mg/kg SP4-5 increased mechanical withdrawal thresholds indicating antinociception. In addition, PDSP screening showed that SP 4-5 does not bind to delta, mu and kappa opioid receptors. Our SAR study showed that quinoline moiety can successfully replace benzothiazole ring yielding potent compounds in human FAAH and human, rat, and mouse sEH inhibition assays. The most potent dual sEH/FAAH inhibitor identified in this study, JA112, showed inhibition potency in the low nanomolar range (1.7 nM -17.2 nM) for human FAAH, human sEH, rat sEH and mouse sEH enzymes. JA-112 was evaluated for its ability to reverse acute inflammatory induced by an intraplantar injection of dilute formalin. This revealed that JA-112 produces antinociception against formalin-induced inflammatory pain. Further, the differences observed between Phase 1 and Phase 2 of the Formalin Test indicate that JA-112 produces antinociception in a manner consistent with drugs that prevent pro-inflammatory states such as non-steroidal anti-inflammatory drugs (i.e., in non-opioid manner). Future experiments will investigate the effects of JA-112 against persistent inflammatory pain states and determine any adverse effects.

877

The Effects of Taurine on Alcohol-Associated Liver Disease are Dose-Dependent Associated with Alterations of Taurine-Conjugated Bile Acids and FXR-FGF15 Signaling

Jingdan Pei[1], Guihua Pan[1], panpan Huang[1], Rahul Pushparaj[1], Lihua Zhang[1], Wenke Feng[1]

Tulane University[1]

Background and Aims: Taurine is a sulfur-containing amino acid and is important for bile acid homeostasis. Previous studies showed that taurine attenuated alcohol-associated liver disease (ALD). However, the treatment regime and the underlying mechanism are unclear. We aimed to evaluate whether taurine supplementation may regulate intestinal Fxr-Fgf15 mediated signaling pathway and bile acid homeostasis in ALD in mice.

Methods: Male C57BL/6J mice were subjected to NIAAA alcohol exposure model (10-day chronic Lieber DeCarli diet containing 5% EtOH, and an EtOH binge at 5g/kg by gavage). Taurine was supplemented in the liquid diet at three doses (1, 3, 10 g/kg body weight) 10 days before alcohol induction. At the end of the experiments, serum, fecal samples, ileum, and liver tissues were collected, and intestinal and hepatic injury and fatty liver were evaluated. Intestinal microbiota was analyzed by 16S rRNA sequencing. Bile acids in the liver and plasma were analyzed.

Results: Alcohol-feeding (AF) significantly increased hepatic fat and serum ALT and AST levels. Liver and serum bile acids were significantly higher in AF mice compared to pair-fed (PF) mice. Supplementation of taurine at 1 g/kg reduced serum ALT and AST levels and liver lipid accumulation by alcohol feeding, along with the activation of intestinal Fxr-Fgf15 signaling. Metagenomic analysis showed that taurine supplementation significantly increased *Bilophila wadsworthia*, which uses taurine as its substrate and produces H_2S, which is anti-microbial molecule that mediates gut eubiosis. In contrast, supplementation of taurine at the doses of 3 g/kg and 10 g/kg produced toxic-like effects in the liver, indicated by elevated serum ALT and AST levels and liver fat accumulation. Interestingly, taurine supplementation did not increase liver taurine concentration under alcohol feeding. TβMCA/βMCA ratio was markedly increased suggesting a reduced Fxr activation. Moreover, liver levels of taurine-conjugated bile acids, including TCDCA, TDCA, TUDCA, and THDCA, were decreased in AF mice after taurine supplementation at higher concentrations. These tauro-bile acids have been shown with beneficial effects on multiple cellular mechanisms including promotion of monocyte differentiation via TGR5, inhibition of apoptosis and lowering liver lipid accumulation. Taurine-upregulated gene 1 (Tug1), a lncRNA that regulated Fxr expression through inhibition of miR192/194, was upregulated by 1 g/kg taurine supplementation but remained unchanged by 3 and 10 g/kg taurine supplementation.

Conclusions: Our results demonstrate that the effects of taurine supplementation on ALD are dose dependent. Low dose of taurine suppresses, while high dose of taurine exacerbated, alcohol-induce steatosis and liver injury. Low dose taurine supplementation enhances Fxr-Fgf15 signaling in the setting of alcohol exposure in mice, while the mechanisms underlying the detrimental effects of high dose taurine on ALD warrant further investigation.

878

Inhibitors of the Gram-negative cell envelope stress response as anti-infectives and antibiotics

Anh Pham[1], John Alumasa[2], Kenneth Keiler[1]

Pennsylvania State University[1], Miami University[2]

Urinary tract infections (UTIs), particularly recurring UTIs, pose a serious public health problem because they are common and associated with high healthcare costs. The primary causative agents of UTIs are Gram-negative bacteria, including uropathogenic *Escherichia coli, Klebsiella pneumoniae,* and *Pseudomonas aeruginosa*. Given the high recurrence rates and increased antimicrobial resistance among uropathogens, there is an urgent need for new therapeutic treatments for UTIs.

The σ^E cell envelope stress response pathway is a potential target for new anti-infectives and antibiotics because it is required for virulence or viability in Gram-negative pathogens. We used a high-throughput cell-based screen to identify small molecules capable of inhibiting the σ^E pathway. Structure-activity relationship studies on the primary hit compound showed responsive and drug-like properties, including MIC (1.7 µg/ml to >200 µg/ml), IC_{50} for *in vitro* transcription (2.6 – 80 µg/ml), cytotoxicity (7 – 21% at 20X MIC), serum binding (94 – 100%), microsome stability (0.4 – 5 ml/min/g liver), and CYP inhibition (IC_{50} 1.5 – 33 µM). The *in vitro* inhibitory effect of compounds on σ^E was determined by single-round transcription assays using the *rybB* gene under the control of a σ^E-dependent promoter and [^{32}P]-UTP to track newly synthesized transcripts. The IC_{50} of active compounds was determined by single-round and multi-round transcription assays. The on-target activity of active compounds was further assessed using an engineered *E. coli K12* reporter strain in which an *yfp* gene is under the control of a σ^E-dependent promoter. Microscale thermophoresis was used to quantify the effect of active compounds on the binding affinity of σ^E to *E. coli* RNA polymerase core enzyme. Bacterial growth inhibition and killing were determined by measuring the MIC and MBC against *E. coli ΔtolC* to establish efflux-independent target-based activity*,* followed by a panel of Gram-negative pathogen and clinical isolates, including drug-resistant strains*.*

Because σ^E is not found in eukaryotes and human RNA polymerase has no sequence or structural similarity to bacterial RNA polymerases, concerns regarding on-target toxicity are minimal. Eukaryotic cytotoxicity was assessed by MTS and LDH release assays in mouse 3T3 fibroblasts, human endothelial HuVEC cells, and human liver HepG2. *In vitro* ADME assays were performed to determine the water solubility, microsomal stability, serum stability, and plasma binding. *In vivo* murine infection model trials are planned to measure efficacy.

879

Comparative Analysis of Dopamine Neuron Activity in Pavlovian Versus Non-Contingent Methamphetamine Exposure

Leah Phan[1], Douglas Miller[1], Min Lin[1], Devon Borg[1], Alexander Newman[1], Dylan Guenther[1], Adithya Gopinath[1], Emily Miller[1], Habibeh Khoshbouei[2]

University of Florida[1] McKnight Brain Institute of the University of Florida[2]

There is a notable increase in methamphetamine abuse. Despite this increase, the distinct impacts of environmentally associated (Pavlovian) and non-contingent (uncoupled) methamphetamine exposure on the activity of midbrain dopamine neurons and the dynamics of neuronal networks are not well understood. Our data suggests that acute non-contingent exposure to methamphetamine increases firing rate of dopaminergic neurons and alters neuronal network dynamics, evidenced by increased synchrony, modularity, and assortativity (N=5, p<0.05). However, the effects of exposure to methamphetamine in an environmentally conditioned versus an unconditioned context on dopamine neurons remain unknown. Our data, and the literature, support the hypothesis that Pavlovian versus uncoupled methamphetamine exposure influences dopamine neuron activity and neuronal network connectivity in distinct ways and differential mechanisms. In the current study, male and female mice were administered methamphetamine (2mg/kg, intraperitoneally) or saline, either through a conditioned place preference paradigm or in their home-cage environment. Forty-eight hours after the last drug administration, we employed ex vivo patch-clamp electrophysiology to measure the baseline firing activity of dopamine neurons in the ventral tegmental area (VTA). Our data indicates that forty-eight hours after the last drug

administration non-contingent administration of methamphetamine increases the baseline firing activity of VTA dopamine neurons (n=6, p<0.05) and leads to sensitization upon exogenous methamphetamine application (n=6, p<0.05). This effect could potentially be attributed to the desensitization of inhibitory D2 receptors. Current studies are exploring whether environmentally conditioned drug exposure similarly or differently influences the baseline activity of dopamine neurons and examining potential sex-dependent responses in each drug exposure model. This research offers important insights into the neurobiological effects of various methamphetamine exposure models in the context of developing pharmacological treatments for patients.

880

The KRAS-G12C Inhibitor Sotorasib Induces Cancer Therapy Resistance by Activating Human Pregnane Xenobiotic Receptor

Satyanarayana R. Pondugula[1], Julia M. Salamat[1], Kodye L. Abbott[2], Elizabeth L. Ledbetter[1], Chuanling Xu[1]

Auburn University[1] Yale School of Medicine[2]

During administration of cancer therapy protocols containing multi-drug regimes, activation of human pregnane xenobiotic receptor (hPXR) has been shown to play a role in the development of resistance to anti-cancer drugs. Mechanistically, single or multiple agents within a multi-drug regime could act as an hPXR agonist, resulting in upregulation of hPXR transcriptionally regulated genes involved in drug metabolism and transport. This is a major cause of concern, as hPXR is the master regulator of the major drug-metabolizing enzymes and drug-efflux pumps, such as cytochrome P450 3A4 (CYP3A4) and multidrug resistance protein 1 (MDR1). CYP3A4 and MDR1, contribute to the metabolism and disposition of over 50% of clinical drugs. Therefore, multi-drug anti-cancer regimes are at extreme risk to drug-induced drug resistance, as drug induction of hPXR-regulated CYP3A4 and MDR1 leads to increased drug metabolism and transport. In turn, increased drug metabolism and efflux can greatly affect the therapeutic response of co-administered drugs, leading to chemoresistance. Sotorasib (SOT) is the first FDA approved KRAS-G12C inhibitor for the treatment of advanced non-small cell lung cancer with the KRAS-G12C mutation. At present, several clinical trials are evaluating the use of SOT in combination chemotherapy, with some chemotherapeutics that are substrates of hPXR target genes such as CYP3A4 and MDR1. It is currently unknown whether SOT can activate hPXR and upregulate hPXR target gene expression, leading to chemoresistance. We therefore sought to determine whether SOT, at its therapeutically relevant concentrations, could act as an hPXR agonist and upregulate CYP3A4 and MDR1, and induce resistance to anti-cancer drugs. SOT, at its therapeutically relevant concentrations, induced hPXR transactivation of CYP3A4 promoter activity in HEK293T human embryonic kidney, HepG2 human liver cancer, and LS180 & LS174 human colon cancer cells. SOT induced endogenous gene expression of CYP3A4 and MDR1 in human primary hepatocytes and LS180 & LS174T cells. SOT also induced MDR1 functional activity in LS180 & LS174T cells in Rhodamine 123 intracellular accumulation assays. The inductive effect of SOT on CYP3A4 promoter activity as well as endogenous CYP3A4 and MDR1 gene expression was inhibited by a specific hPXR antagonist, SPA70. Furthermore, SOT was also able to bind to the ligand-binding domain of hPXR in cell-free FRET assays. These findings suggest that SOT induces hPXR target genes by directly activating hPXR. While SOT activated hPXR, it failed to activate the mouse PXR and another related nuclear receptor, human constitutive androstane receptor in the reporter gene assays, suggesting that SOT activates PXR in a species-dependent manner and induces CYP3A4 and MDR1 in hCAR-independent manner. Notably, SOT decreased the sensitivity of LS180 & LS174T cells to both irinotecan and its active metabolite SN-38 in cell viability assays, suggesting that SOT can induce anti-cancer drug resistance by activating hPXR. Moreover, the SOT-induced resistance was reversed with use of hPXR antagonist, SPA70, suggesting that the SOT-induced resistance was hPXR-dependent. Taken together, our results suggest that SOT induces anti-cancer drug resistance by activating hPXR and inducing CYP3A4 and MDR1.

881

Lipid Trolling to Optimize A$_3$ Adenosine Receptor Positive Allosteric Modulators (PAMs)

Kenneth Jacobson[1], BALARAM Pradhan[1], Courtney L. Fisher[2], Matteo Pavan[1], Veronica Salmaso[3], Tina C. Wan[2], Robert F. Keyes[4], Noah Rollison[1], Rama R. Suresh[1], Zhan-Guo Gao[1], Brian C. Smith[4], John A. Auchampach[5]

NIDDK/NIH[1], Department of Pharmacology & Toxicology and the Cardiovascular Center, Medical College of Wisconsin[2], Department of Pharmaceutical and Pharmacological Sciences, University of Padua, Padua, Italy[3], Department of Biochemistry and the Program in Chemical Biology, Medical College of Wisconsin[4], Medical College of Wisconsin[5]

Adenosine acting through its four receptor subtypes has a generally anti-inflammatory action. The A$_3$ adenosine receptor (AR) is overexpressed in immune and cancer cells, adding to its potential as a possible therapeutic target for the treatment of inflammatory and ischemic conditions, cancer, and chronic pain. At present, orthosteric A$_3$AR agonists IB-MECA and Cl-IB-MECA are in Phase 2/3 clinical trials for psoriasis, liver diseases and cancer. The pharmacological advantage of positive allosteric modulators (PAMs) over orthosteric agonists is that they can be event- and site-specific in action. Previously reported A$_3$AR PAMs (2,4-disubstituted-1H-imidazo[4,5-c]quinolin-4-amines) increase the E$_{max}$ of A$_3$AR agonists, but not their potency, partly due to concurrent orthosteric binding site antagonism. Furthermore, their activity is minimal in rodent species due to species-dependent receptor recognition. We recently applied mutagenesis and homology modeling to locate a proposed lipid-exposed PAM binding site on the cytosolic side of the receptor. Subsequently, we modified the PAM scaffold to probe this binding hypothesis and to potentially increase allosteric binding. We included heteroatom substitutions of the imidazole moiety and modified C2 and exocyclic N^4 substitutions. PAMs with strategically appended (at the para position of an N^4-phenylamino group) linear alkyl-alkynyl chains having terminal amino/guanidino groups improved allosteric effects at both human and mouse A$_3$ARs. The effects on A$_3$AR PAM activity of varying the chain length, functionality and attachment position were evaluated. For example, **26** (MRS8247, 100 nM), having eight methylenes and alkyne-linked to the N^4-phenylamino group, and its homologues, increased both agonist (Cl-IB-MECA) E$_{max}$ and potency in [^{35}S]GTPgS binding. The designed compounds support our proposed extrahelical location of the PAM binding site. The putative mechanism is that terminally cationic chains penetrate the phospholipid layer to anchor the PAM electrostatically to phospholipid head groups or other cationic sites, suggestive of a concept we term 'lipid trolling'. Thus, we have qualitatively enhanced A$_3$AR PAMs pharmacologically through rational design based on a lipid-exposed binding site.

882

Membrane Raft Redox signalling pathway in Nicotine-Induced NLRP3 Inflammasome Activation and Podocyte Injury

Mohammad Atiqur Rahman[1], Sayantap Datta[1], Sai S. Koka[2], Krishna M. Boini[1]

University of Houston[1] Texas A & M University[2]

Recently we have shown that nicotine-induced Nlrp3 inflammasome activation contributes to podocyte injury and ultimate glomerular injury. However, the molecular mechanisms of how nicotine induces the

Nlrp3 inflammasome activation and podocyte damage is still unknown. The present study tested whether membrane raft (MR) redox signalling pathway plays a central role in nicotine-induced NLRP3 inflammasomes activation and contributes to podocyte injury. Using confocal microscopy, nicotine treatment was found to increase MRs clustering in the membrane of podocytes in a dose-dependent manner. Upon nicotine stimulation an aggregation of NADPH oxidase subunits, gp91(phox) and p47(phox) was observed in the MR clusters, forming a MR redox signalling platform. The formation of this signalling platform was blocked by prior treatment with MR disruptor MCD, NOX inhibitor DPI, and ASMase inhibitor amitriptyline. In addition, nicotine treatment significantly increased the ceramide expression, Asm activity, colocalization of Nlrp3 with Asc or Nlrp3 with caspase-1, IL-β production, caspase-1 activity and cell permeability compared to control cells. However, prior treatment with MCD, DPI and amitriptyline significantly attenuated the nicotine-induced ceramide expression, Asm activity, colocalization of Nlrp3 with Asc or Nlrp3 with caspase-1, IL-β production, and cell permeability. Furthermore, immunofluorescence analysis demonstrated that nicotine treatment significantly decreased the podocin and nephrin expression (podocyte damage), and prior treatments with DPI, MCD, WEHD (inflammasome inhibitor) amitriptyline attenuated this nicotine-induced podocin and nephrin reduction. In conclusion, our results demonstrate that nicotine induces ceramide production via ASMase and thereby stimulates membrane raft clustering in the membrane of podocytes to form redox signalling platforms by aggregation and activation of NADPH oxidase subunits, enhancing O_2^- production and leading to Nlrp3 inflammasome formation and activation in podocytes and ultimate podocyte injury.

883

EAATs for stroke: to modulate or not to modulate

Katelyn Reeb[1], Andreia Mortensen[1]

Drexel University College of Medicine[1]

Excitatory amino acid transporters (EAATs) are critical proteins in the CNS that regulate synaptic glutamate levels, crucially preventing excitotoxicity. The astrocytic transporter EAAT2 is responsible for the majority of glutamate clearance in the CNS. Aberrant EAAT2 activity and glutamatergic signaling occurs in many neuropsychiatric disorders. Our work focused on ischemic stroke, a condition that urgently needs new treatments. In ischemic stroke, excessive levels of released glutamate cause excitotoxicity, leading to secondary damage which ultimately results in cognitive deficits. We have developed novel allosteric modulators (AMs) of EAATs, including selective-EAAT2 positive allosteric modulators (PAMs), and non-specific and broad-acting analog AMs. We hypothesize the pharmacological activity of AMs is determined by differential interactions with critical amino acid residues located between the transporter's scaffold and transport domains. We have two main goals: to further understand the mechanism of these AMs, and to study their effects in an *in vitro* stroke model. Computational modeling predictions suggest some amino acid residues on EAAT2 that are critical to mediating the action of NA-014, an EAAT2-specific PAM. Dose-response assays evaluating the effect of NA-014 and other AMs offered further insights on which residues are important for their action, and what chemical moieties confer EAAT subtype selectivity and pharmacological action. Additionally, we evaluated potential translatability of EAATs PAMs in a model of ischemic stroke. We hypothesize that these compounds can restore glutamatergic homeostasis by augmenting glutamate clearance. We evaluated NA-014 in an *in vitro* model of ischemic stroke, oxygen glucose deprivation, in primary neuron-glia cultures, and found that it demonstrated neuroprotective properties. Collectively, these studies expand our mechanistic understanding of the EAAT AMs and demonstrate their clinical utility for ischemic stroke.

884

Blockade of Brain Angiotensin II AT1 Receptor Ameliorates Inflammation, YKL-40, and ROS Production from Astrocytes

Genesis Rodriguez[1], Mary Roman Perez[1], Fabiola Rodriguez Flores[1], Jessica Garcia[1], Yaritza Inostroza Nieves[1]

San Juan Bautista School of Medicine[1]

Alzheimer's Disease (AD) is the most common cause of dementia. AD patients had increased extracellular amyloid β plaques and intracellular hyperphosphorylated tau (p-tau) in neurons. YKL-40 is an inflammatory biomarker of AD. Recent studies have shown an association between the Renin-Angiotensin System (RAS) and AD. The involvement of RAS has been mediated through Angiotensin II (AngII), which is overexpressed in aging brains. However, the exact mechanism of how AngII contributes to AD is unknown. Thus, we hypothesize that AngII increases brain inflammation and YKL-40 production from astrocytes and increases ROS generation by its AT1 receptor (AT1R). In the human astroglia cell line, SVGp12, treatment with AngII increased YKL-40 production by 40% ($p<0.05$, n=4), and the AT1R antagonist, Losartan, blocked this effect. In addition, the effects of AngII on pro-inflammatory cytokines were studied. AngII upregulated the gene expression of IL-6 ($p<0.01$, n=4) and increased IL-6 concentrations by 68% ($p<0.05$, n=4), as measured by ELISA. Losartan blocked the changes in IL-6. Also, AngII induced the production of TNF-α, increasing its concentration by 76% ($p<0.05$, n=4), an increase that Losartan also blocked. We then quantified reactive oxygen species (ROS) production by using MUSE Oxidative Stress assay. In SVGp12 cells, ROS production was significantly increased by AngII ($p<0.05$, n=4), and treatment with Losartan blunted their production ($p<0.05$, n=4). These results suggest that AngII can activate astroglia cell pro-inflammatory responses and increase ROS production, which may contribute to the pathophysiology of CNS inflammation and AD. AT1R antagonists could be considered a possible therapeutic agent for AD due to its protective role against Ang II's effects.

885

Phosphorylation of Gαi shapes canonical Gα(i)βγ/GPCR signaling

Suchismita Roy, Saptarshi Sinha, Irina Kufareva, Pradipta Ghosh

University of California, San Diego

A long-standing question in the field of signal transduction is to understand the interplay between distinct signaling pathways that control cell behavior. For growth factors and heterotrimeric G proteins, the two major signaling hubs in eukaryotes, the mechanisms of independent signal transduction have been extensively characterized; however, if/how they may cross talk remains obscure. Here we use linear-ion-trap mass spectrometry in combination with cell-based biophysical, biochemical, and phenotypic assays to chart at least three distinct ways in which growth factors may impact canonical Gα(i)βγ signaling downstream of a GPCR (CXCR4) via phosphorylation of Gαi. Phosphomimicking mutations in a cluster of residues in the αE helix (Y154/Y155) result in the suppression of agonist-induced Gα(i) activation while promoting constitutive Gβγ signaling; others in the P-loop (Ser44, Ser47, Thr48) suppress Gi activation entirely thus completely segregating the growth factor and GPCR pathways. While most phosphoevents appear to impact, as expected, the core properties of Gα(i) (conformational stability, nucleotide binding, Gβγ association and release, etc.), one phosphomimicking mutation promoted mislocalization of Gαi from the plasma membrane: a novel and unexpected mechanism of GPCR signal suppression. A phosphomutation of C-terminal Y320 was sufficient to orchestrate such suppression by protein compartmentalization. Findings not only elucidate how growth factor and chemokine signals crosstalk through phosphomodulation of Gαi, but also how such crosstalk may generate signal diversity.

886

Activation of PTH1 receptor using chimeric peptide templated in situ click reaction of nanobody conjugates

Shubhra J. Saha[1], Ross Cheloha[2]

National Institutes of Health[1] NIH[2]

Bioactive compounds sometimes possess unfavorable properties for drug development due to on-target, off-tissue mediated side effects or poor pharmacological properties. Activation of drug targets expressed in tissues not involved in therapeutic responses can limit medical application. One solution is to use analogue(s) or fragments of bioactive drugs that become activated only at sites of interest. Herein we describe the development of fragments of a peptidic GPCR ligand that can react to form a bioactive product upon exposure to a dimerizing agent that stimulates *in situ* assembly. To enhance specificity, we developed methods for the directed delivery of such a dimerizing agent to cell types of choice.

We sought to apply this approach for activation of the parathyroid hormone receptor-1 (PTHR1), which regulates skeletal development and mineral ion homeostasis. The prototypical peptide agonist of PTHR1 (PTH_{1-34}) was separated into two constituent fragments (PTH_{1-11} and PTH_{12-34}), each of which possesses little to no biological activity alone. *In situ* synthesis of conjugates that resemble PTH_{1-34} was achieved through peptide template-induced dimerization and click (azide-alkyne) reactions between the fragment peptides PTH_{1-11} and PTH_{12-34}. Dimerization is facilitated through the binding of nanobodies (Nbs) to peptide tags as described below.

Nbs are single antigen recognition domains of heavy-chain only antibodies, which exhibit specificity and affinity for biological macromolecules comparable to conventional antibodies. Templated dimerization was achieved by fusing PTH fragments containing click chemistry handles to one of two Nbs that bind to short peptide epitopes. A heterodimeric peptide (HDP), comprised of the two distinct Nb-binding peptide epitopes, was used to bring fusions comprised of Nbs and PTH fragments with complementary click handles, into proximity. HDP-induced co-localization was designed to trigger the click reaction within the cellular medium at high dilution.

Gel electrophoresis analysis of the kinetics of the reaction between azide- and alkyne-functionalized Nbs showed that HDP-mediated dimerization accelerated reaction kinetics. In the context of a cell-based assays, PTH fragment-click handle-Nb conjugates were weakly active alone or when added in tandem. The addition of HDP to the tandem mixture resulted in strong activation (via *in situ* ligand assembly) of PTHR1. We further demonstrate that dimeric peptide-induced *in situ* assembly can be achieved with cell-type specificity and high efficiency via Nb-based delivery of dimerizing agent.

Altogether, this approach entails a new strategy for *in situ* synthesis of a bioactive agonist from its inactive fragment peptides. These results offer a path towards in situ assembly of bioactive molecules based on targeted delivery of dimerizing agents. These findings, coupled with the modular and programmable nature of our strategy, suggest the possibility of engineering similar approaches for the targeted synthesis of a diverse range of clinically relevant molecules in various *in vitro* and *in vivo* settings.

887

Preclinical model to assess the impact of myocardial maturity on drug responsiveness

Shatha Salameh, Luke Swift, Anika Haski, Nikki Posnack

Children's National Hospital

Background: The majority of cardiac medications administered to hospitalized children have not been formally studied in the pediatric population. Congenital heart disease (CHD) patients often require pharmacological interventions to improve contractile function after corrective surgery. Milrinone is among the most commonly prescribed inotropic agents administered to 98% of CHD patients. Studies suggest that the efficacy of milrinone may be age-dependent, as the developing heart undergoes changes in ionic currents, intracellular Ca^{2+} handling, and contractile function. To date, pediatric cardiac pharmacology research has been limited by the scarcity of human models; however, preclinical animal models can support our understanding of cardiac development, drug responsiveness, and age-appropriate therapies in order to optimize patient outcomes.

Objective: To examine the impact of postnatal age on baseline cardiac physiology and milrinone efficacy using a preclinical guinea pig model (neonatal–adult).

Methods: In vivo electrocardiograms (ECG) were collected from conscious (ecgTUNNEL system) and unconscious animals to analyze heart rate, beat rate variability, atrial (P-wave) and atrioventricular conduction (PR interval), depolarization (QRS) and repolarization time (QT). Isolated, intact heart preparations were maintained using a constant-pressure Langendorff-perfusion system. Ex vivo electrocardiograms were recorded and an electrophysiology stimulation protocol was performed. Optical action potentials and calcium transients were recorded using fluorescent dyes (Rhod-2AM, RH-237), during sinus rhythm and in response to external pacing. Cardiac metrics were compared between age groups at baseline, and after acute (15-min) exposure to milrinone.

Results: Age-dependent differences in ECG intervals were observed between neonatal and adult hearts at baseline. Neonatal heart rate (258±18.1 BPM) was faster than adults (175±11.6 BPM, $p<0.05$), and neonatal repolarization time (158±13.7 ms) was faster than adults (201±18 ms, $p<0.05$). Tachycardia was observed in all animals after 100 nM milrinone treatment, as noted by a 34% increase in neonatal and 35% increase in adult heart rate. At baseline, neonatal calcium transient duration time (CaD30:76.8± 8.1 ms, CaD70: 110.3±7.9 ms) was significantly shorter than adult calcium transient duration time (CaD30: 94.3± ms, CaD70: 127.5±9.4 ms; $p<0.01$). Neonatal hearts displayed only a modest shortening in the calcium transient duration time (4.6% CaD30, 9.3% CaD70) after milrinone exposure – while this effect was more exaggerated in adult hearts (11.8% CaD30, 12.4% CaD70).

Discussion: Cardiomyocytes undergo dynamic changes during postnatal development, which can influence cardiac physiology and drug responsiveness. Using a preclinical model, we observed that neonatal hearts have an abbreviated response to milrinone as compared to adult hearts. This finding is important, as pediatric patients may experience variable responses to milrinone treatment based on myocardial maturity.

888

MARY1 Promotes Recovery from Acute Kidney Injury through Induction of Mitochondrial Biogenesis

Paul Victor Santiago Raj, Jaroslav Janda, Rick G. Schnellmann

The University of Arizona

Background:
Acute kidney injury (AKI) is defined as a sudden and rapid loss of kidney function which is accompanied by elevated serum creatinine and mitochondrial dysfunction. Ischemia reperfusion (I/R) injury, sepsis, hypovolemia and drug induced nephrotoxicity are common initiators of AKI. AKI is an important public health concern with no FDA-approved treatments. We have shown that a number of pharmacological agents stimulate mitochondrial biogenesis (MB) and accelerate renal recovery in a mouse model of AKI. We have synthesized a new small molecule, MARY1, and examined MB and renal recovery of MARY1 following I/R induced AKI in mice.

Methods:
Male 8–10-week-old C57B/6NCrl mice were administered 0.3mg/kg of MARY1 or normal saline 24h following I/R and then every 24h over a 144h period (n=6/group). Kidneys were harvested and snapped frozen in liquid nitrogen. Renal cortex samples were used to analyze gene expression (qRT-PCR) and protein expression (immunoblot) post AKI. One way ANOVA followed by TUKEY multiple comparison test was used to determine statistical significance between treatment groups. A p-value of $p \leq 0.05$ was used to identify statistical changes.

Results:
Serum creatinine and Kidney Injury Molecule-1 (KIM-1) was measured and found to be maximally increased at 24h post I/R. Over 144h, MARY1 treatment exhibited greater decrease in serum creatinine and KIM1 compared to vehicle control. MARY1 restored PGC1α, master regulator of MB, mitochondrial dynamics proteins (MFN1, MFN2) mitochondrial copy number, mitochondrial complex proteins and total ATP at 144h. Transmission electron microscopy also revealed a decrease in the mitochondrial damage score following administration of MARY1 for 144h. Interestingly, administration of MARY1 also restored markers of key mitochondrial proteins involved in fatty acid oxidation.

Conclusion:
MARY1 restored mitochondrial homeostasis and accelerated renal recovery following I/R induced AKI in mice. Additional studies are needed to elucidate the cellular mechanism and the mechanism of renal recovery/function.

889

Sphingosine-1-phosphate receptor 1 (S1PR1) modulators acutely reverse paclitaxel-induced neuropathic pain signs in mice without downregulating S1PR1 in the CNS

Dana Selley[1], Abby M. Pondelick[2], Torin Honaker[2], Ruihua Chen[3], Matthew Harding[4], Mark A. Demitrack[3], Laura J. Sim-Selley[2], Imad Damaj[2]

Virginia Commonwealth Univ School of Medicine[1] Virginia Commonwealth University[2] Trevena, Inc.[3] Neuropharmacology Consulting[4]

Chemotherapy-induced neuropathic pain is a common side-effect that can limit the course of chemotherapeutic treatment and is difficult to alleviate. Preclinical evidence suggests that modulation of S1PR1 is a promising approach for neuropathic pain treatment. S1P is a bioactive lysolipid that is an endogenous ligand for S1P-receptors (S1PR) 1-5. The immunomodulatory prodrug, fingolimod, which activates S1PR 1, 3-5, attenuates pain signs in several neuropathy models, mainly through action at S1PR1. However, the mechanism of S1PR1-mediated antinociception is unclear because conflicting evidence indicates either S1PR1 agonism or functional antagonism. Here we compared fingolimod to a novel S1PR1-selective agonist (TRV045; Trevena Inc.), which unlike fingolimod does not produce lymphopenia and therefore may not cause receptor downregulation, in the paclitaxel (PAC)-induced neuropathic pain model. The ability of acutely administered TRV045 or fingolimod to reverse PAC-induced neuropathic hypersensitivity was determined in male C57Bl/6J mice. Mice received either vehicle or PAC (8 mg/kg, i.p.) every other day for one week and then a single injection of vehicle, 0.1-10

mg/kg TRV045 or 1 mg/kg fingolimod (p.o.) one week after the final PAC injection. Mechanical and cold sensitivity was assessed over a 6-hour post-injection period using the von Frey and acetone tests, respectively. TRV045 dose- and time-dependently reversed PAC-induced mechanical and cold hypersensitivity, with 10 mg/kg TRV045 producing complete reversal similar to 1 mg/kg fingolimod. Tolerance did not develop to this effect of TRV045 after repeated administration for 7 days. Concentration-effect curves for G-protein activation using [^{35}S]GTPgammaS binding was then determined in spinal cord, amygdala, periaqueductal gray (PAG), and cingulate cortex of naïve C57Bl/6J mice to compare TRV045 to the active form of fingolimod (fingolimod-P) and other S1PR agonists including the S1PR1-selective ligand ponesimod (also reported to alleviate neuropathic pain in rodents). In all regions tested, TRV045 was significantly less potent than fingolimod-P or ponesimod, but TRV045 and all other ligands tested acted as full or near full agonists. The effect of acute injection of 10 mg/kg TRV045 or 1 mg/kg fingolimod on S1PR1 protein levels was then determined in spinal cord, amygdala, and PAG of vehicle- or PAC-pretreated knock-in mice expressing GFP-fused S1PR1. GFP-S1PR1 protein in immunoblots was unchanged by any of the drug treatments, suggesting that S1PR1 downregulation was not produced by acutely administered TRV045 or fingolimod at doses that fully reversed PAC-induced hypersensitivity. These results suggest that S1PR1 downregulation in CNS regions associated with pain perception and modulation is not required to alleviate PAC-induced neuropathic pain signs. Ongoing work will assess the effects of repeated administration of these S1PR1 ligands on GFP-S1PR1 levels and S1PR1-mediated G-protein activation in the CNS.TRV045 is an investigational ligand that is not FDA-approved for human use.

890

Biased Allosteric Modulation of β₂-adrenergic Receptor Signaling and Bronchodilation by different β-agonists

Sushrut D. Shah, Francesco F. De Pascali, Deepak A. Deshpande

Thomas Jefferson University

Objective & Hypothesis: β-agonist serves as the frontline treatment of obstructive airway diseases like asthma and COPD to induce very essential functions - airway smooth muscle (ASM) relaxation and bronchodilation. However, due to β-arrestin mediated β₂-adrenergic receptor (β₂AR) signaling leads to receptor desensitization and loss of β-agonist efficacy. Therefore, new research for developing anti-asthma therapeutics is aimed at discovering biased ligands that augment beneficial Gs-mediated canonical signaling. We recently discovered allosteric modulators (AMs) of the β₂AR that augment Gs signaling and function in ASM cells using a prototypic β-agonist, isoproterenol (ISO). However, different endogenous and clinically used β-agonists induce different β₂AR conformational changes and thus potentially restricting the allosteric site on the β₂AR. The goal of the study is to establish the efficacy of these AMs on different B-agonists induced signaling and function. We **hypothesize** that AMs differentially modulate β₂AR signaling and bronchodilation induced by clinically distinct β-agonists.

Methods: HEK-293 cells transfected with human β₂AR and human ASM (HASM) cells were stimulated with different β-agonists at varying concentrations in the presence of vehicle/AMs, and cAMP levels were assessed using ELISA. β-arrestin recruitment was assessed by BRET assay in β₂AR transfected HEK-293 cells. Additionally, bronchodilation, a functional effect, was examined using murine Precision Cut Lung Slices (PCLS). Airway lumen area was measured before and 10 minutes after treatment with β-agonists in the presence of vehicle or AMs.

Results: Positive AM (PAM; cmpd 37) augmented ISO-induced cAMP generation. Interestingly, cmpd 37 had varying effects on different β-agonists-induced cAMP generation. Cmpd 37 augmented epinephrine-, formoterol-, and salmeterol-, but not albuterol- induced increase in cAMP levels. Further, in HASM cells –

a cell model expressing endogenous β_2AR, cmpd 37 failed to augment salmeterol-mediated cAMP generation. Conversely, negative AMs (NAMs – cmpds 36 and 42), had variable effect on cAMP generation induced by different β-agonists. In HEK-293 cells, NAMs cmpd 36 and 42 inhibited ISO-, albuterol-, epinephrine-, and formoterol-, but not salmeterol- induced cAMP generation. In murine PCLS, cmpd 37 augmented ISO-, epinephrine-, formoterol-, salmeterol-, and albuterol- induced bronchodilation, albeit to a varying degree. NAMs cmpd 36 and 42 inhibited ISO-, epinephrine-, and formoterol-induced relaxation of murine airways. Further, cmpd 42, and not cmpd 36, inhibited albuterol- and salmeterol-induced relaxation of murine airways.

Conclusion: Our findings suggest that the newly discovered AMs of the β_2AR modulate β_2AR-Gs signaling and bronchodilation by multiple b-agonists and could serve as a new therapeutic option for obstructive lung diseases by enhancing the bronchodilator effect of b-agonists. Further, these findings demonstrate the differential effect of biased AMs on different endogenous and clinically used β-agonists, possibly due to unique degree of the allosteric site accessibility induced by each of the agonists, positing the complexity of biased signaling. On-going computational studies are aimed at examining the mechanistic basis for differential effects of the AMs on different β-agonists.

891

Novel RGS2-Gaq Interaction Inhibitors Show Anti-Cancer Activity

Jocelyn Smith[1], Tarek Mahfouz[2], Dave Roman[3], Joshua Wilkinson[3]

Ohio Northern University[1], Raabe College of Pharmacy[2] Univ of Iowa[3]

The protein regulator of G-protein signaling 2 (RGS2) is from a family of approximately 30 proteins that bind to the alpha subunits of G proteins (Ga) and are implicated in many human diseases. RGS2 is overexpressed in the majority of solid breast cancers and metastatic prostate cancers. RGS2 is a potent and selective inhibitor of the Guanine nucleotide-binding protein subunit alpha (Gaq), whose knockdown promotes cancer metastasis. We hypothesized that inhibiting RGS2-Gaq interactions would have anti-metastatic effects. Here and using a structure-based approach, we sought to develop selective RGS2 inhibitors targeting the RGS2-Gaq interaction face to block RGS2-Gaq binding. The structure of the RGS2-Gaq complex was used to develop a pharmacophore model which was subsequently used to search chemical databases to identify potential inhibitors. Retrieved hits were further screened by docking to identify leads with high selectivity and potency towards RGS2. The search resulted in 10 compounds (AJ-1 through AJ-10) that successfully blocked RGS2-Gaq binding in cell-based assays. All 10 compounds inhibited the growth of different cancer cell lines with AJ-10 causing over 80% growth inhibition of the glioblastoma SNB-75 cell line at a concentration of 10 uM. In addition, AJ-3 is shown to preferentially bind RGS2, not Gaq, and it inhibits the migration ability of the invasive prostate cancer cell line LNCaP in wound healing assays. These results show that RGS2 inhibitors have anticancer properties. These inhibitors have the potential to be the first-in-class chemotherapeutic agents targeting metastasis by inhibiting RGS2-Gaq binding.

892

Discovery of agonists for orphan GPR52 using a ligand-based pharmacophore model and virtual screening

Hudson R. Smith, Ryan M. Murphy, Michelle A. Hagenimana, John A. Allen

The University of Texas Medical Branch

GPR52 is an orphan G protein-coupled receptor (GPCR) that is a promising target for neuropsychiatric disorders including schizophrenia and substance abuse disorders. GPR52 is a constitutively active receptor that couples to $G_{s/olf}$ G proteins to stimulate adenylyl cyclase and increase intracellular cAMP. As with most understudied GPCRs, there is a paucity of structural diversity among known GPR52 ligands. To expand the chemical space of GPR52 ligands, we utilized a proprietary ligand based-pharmacophore model and virtual screening method to identify new potential compounds for GPR52. Greater than 500k synthesis-ready compounds were screened *in silico* for their structural similarity to the GPR52 agonist c17. This screening provided a compound priority list of 400 predicted GPR52 ligands. These priority compounds were obtained and subsequently screened at 10 μM using a Glosensor cAMP assay in HEK293 cells expressing human GPR52. The primary screen showed 21 hit compounds activated GPR52 cAMP signaling at > 40% of the maximal response to the positive control agonist 4-(3-(3-fluoro-5-(trifluoromethyl) benzyl)-5-methyl-1H-1,2,4-triazol-1-yl)-2-methylbenzamide (FTBMT). Subsequent re-testing confirmed activities, and the five most active compounds were evaluated in concentration responses to determine potency (EC_{50}) and efficacy (E_{max}). All five compounds exhibited low micromolar potency (ranging from 1.6 to 4.0 μM) and were partial agonists when compared to FTBMT. Two promising validated compounds included 2-B3 (N-(5-{[3-(trifluoromethyl)phenyl]methyl}-1,3-thiazol-2-yl)cyclopropanecarboxamide) and 5-E1 (ethyl 2-benzyl-4-methyl-1,3-thiazole-5-carboxylate). Compound 2-B3 showed lower partial agonist activity (E_{max}= 39 ± 2%) with a potency (pEC_{50}) of 5.80 ± 0.07 [1.6 μM]. Compound 5-E1 showed moderate partial agonist activity (E_{max} = 71 ± 2%) and potency (pEC_{50}) of 5.47 ± 0.02 [3.4 μM]. 2-B3 was docked into the previously solved GPR52 crystal structure (PBD 6LI0) using AMDock program. 2-B3 docked into a similar binding site as the agonist c17, with potential hydrogen bonding at the ECL2 amino acid D188. Structural derivatives of agonist 2-B3 are being actively screened to define structure activity relationships important for GPR52 potency and efficacy. Taken together, this virtual screening with pharmacological validation provides a viable method for the discovery of ligands for orphan GPCRs. Compounds 2-B3 and 5-E1 are promising GPR52 agonist ligands amenable to further chemical optimization to expand ligand diversity for GPR52.

893

Discovery, Characterization, and Optimization of a Novel Positive Allosteric Modulator-Antagonist of the D3 Dopamine Receptor

Kir K. Snyder[1], Amy E. Moritz[2], Nora Madaras[3], Feijun Wang[4], Amber Kelley[4], Disha Gandhi[4], Emmanuel Akano[5], Laura Inbody[4], Kuo Lee[6], R. Benjamin Free[7], Lei Shi[6], Kevin Frankowski[4], David R. Sibley[8]

NIH[1] Molecular Neuropharmacology Section, NINDS/NIH[2] Duke Department of Pharmacology[3] UNC Eshelman School of Pharmacy[4] National Institute of Neurological Disorders & Str[5] Computational Chemistry and Molecular Biophysics Section, NIDA/NIH[6] NINDS/NIH[7] National Institutes of Health[8]

Dopamine receptors (DARs) are responsible for a plethora of physiologic functions, including cognition, mood, movement, and motivation. Not surprisingly, DARs play a role in the etiology and/or therapy of many neuropsychiatric disorders, including schizophrenia and substance use disorder (SUD). There are five DAR subtypes divided into two categories: D1-like (D1R and D5R) and D2-like (D2R, D3R, and D4R). Current antipsychotic medications are antagonists of the D2-like subfamily. However, the lack of

selectivity among these D2R-preferring antagonists frequently produce motor-related extrapyramidal side effects, often leading to a lack of compliance among patients. Compounds that selectively antagonize the D3R may lead to fewer side effects while providing effective attenuation of drug craving and/or psychotic symptoms, making the discovery of novel D3R-selective antagonists a priority. A challenge to this goal is posed by the high sequence homology between the D2R and D3R within their orthosteric binding sites. Our lab aims to overcome these selectivity challenges by identifying D3R negative allosteric modulators (NAMs), compounds that inhibit the D3R via binding to an allosteric site. To this end, we screened the NIH Molecular Libraries Program 400,000+ small molecule library and identified MLS6357 as a promising hit compound that exhibited selectivity for the D3R over the D2R in multiple signaling outputs, while displaying an allosteric mechanism of action. Interestingly, radioligand binding assays demonstrated that MLS6357 increases D3R affinity for agonists, indicating that this scaffold is a D3R positive allosteric modulator-antagonist (PAM-antagonist), a special class of NAMs that potentiate agonist-receptor binding while concomitantly decreasing agonist-stimulated receptor signaling. Iterative medicinal chemistry and functional assays were used to synthesize and characterize >100 analogs of MLS6357, with several compounds displaying several-fold increases in potency as antagonists in both β-arrestin recruitment and G-protein activation assays, compared to the parent compound MLS6357. Among them, analogs UNC8747 and UNC6869 also maintained global D3R-selectivity. Additionally, both UNC8747 and UNC6869 appeared to recapitulate the activity of MLS6357 as PAM-antagonists and exhibited brain penetrance at sufficient concentrations to occupy the D3R *in vivo*, making them promising candidates for *in vivo* behavioral testing. In addition, several other analogs displayed functional selectivity for inhibiting G-protein activation versus β-arrestin recruitment and vice versa. Site-directed mutagenesis approaches are being utilized to determine the allosteric binding site for this PAM-antagonist scaffold at the D3R. The development of a novel, potent PAM-antagonist with high selectivity for the D3R may provide a therapeutic advance for many neuropsychiatric conditions, including SUD.

894

Dissecting the novel anti-obesity mechanism of prostaglandin D$_2$ via DP1 receptor agonism utilizing mouse 3T3-L1 adipocytes as well as primary human subcutaneous adipocytes

Mehonaz Sultana, Sunil Kumar

St. John's University

Obesity poses a serious health threat globally with concomitant rise in dreaded health consequences such as diabetes, dyslipidemia, and cardiovascular complications. It becomes even more clinically challenging when there is no FDA-approved therapeutic agent available to treat obesity safely. The prevalence of obesity in United States has increased from 30.5% in 2000 to 41.9% in 2020, illustrating a growing population that could benefit from a potent/efficacious anti-obesity therapeutic. Our *in-vivo* study identified severe fatty liver disease in Lipocalin Prostaglandin D2 Synthase (L-PGDS) knockout mice kept on high fat diet. Briefly, L-PGDS functions as a prostaglandin synthase where it catalyzes the isomerization of PGH$_2$ to PGD$_2$. PGD$_2$ regulates its physiological function via two individual G-protein coupled receptors named DP1 and DP2. Interestingly, while studying lipid metabolism utilizing DP1 and DP2 receptor modulators in apoE−/− mice, DP1 receptor agonist (BW245C) group prevented significant weight gain despite keeping on high fat diet for 10 weeks. Moreover, DP1 receptor agonist group showed significantly increased total plasma bile acids compared to the control. This exciting finding prompted us to delve into investigating the anti-obesity mechanism of BW245C. DP1 receptor activation also induces intracellular cAMP levels in adipose tissue similar to bile acid receptor, TGR5 activation. This pathway stimulates energy expenditure in adipose tissue which eventually translates into weight loss. Therefore, to untangle this puzzle, we aimed to investigate the novel anti-obesity mechanism of DP1 receptor agonist, BW245C in mouse 3T3-L1 adipocytes as well as primary human subcutaneous adipocytes. The 3T3-L1 and primary human subcutaneous adipocytes are well-established models to study the process of adipogenesis, lipogenesis, lipolysis, oxidation of fatty acids and browning similar to the one observed in *in-vivo* setting. 3T3-L1 pre-adipocytes to adipocytes differentiation feasibility is established in our

lab.   Briefly, based on our preliminary results, differentiated 3T3-L1 adipocytes will be treated with sodium palmitate (250mM) to induce lipogenesis and with or without BW245C (0.001, 0.1, 1, 10, and 100 μM concentrations) for 24, 48 and 72 hrs. Change in adipocytes lipid accumulation will be measured as an experimental outcome which will be determined involving Oil Red O staining, cell lysate and supernatant triglyceride measurement and cyclic AMP release assay techniques. Further, sodium palmitate treated cell lysates will be subjected to measure adipogenesis and lipolysis related protein and mRNA expressions including uncoupling protein 1 (UCP1), CCAAT/enhancer-binding proteins α (C/EBPα); peroxisome proliferator-activated receptor γ (PPARγ); fatty acid-binding protein 4 (FABP4); acetyl-CoA carboxylase (ACC); fatty acid synthase (FAS); hormone-sensitive lipase (HSL) and adipose triglyceride lipase (ATGL). Obtained results will be recapitulated in primary human subcutaneous adipocytes. Once, we fully understand the role of DP1 receptor agonist in adipocytes, further detailed study will be carried out using ob/ob mice model on high fat diet in future. Collectively, dissecting a novel role of DP1 receptor agonist will possibly bring a potential future treatment of obesity.

895

Neuroprotection in C. Elegans Parkinson's Disease Models: Discovering Therapeutic Insights via RNAi and Small Molecule High Throughput Screening

Alexis A. Surtel[1], Emmanuel Akano[1], Patricia K. Dranchak[2], Carl T. Ash[1], Emily E. Anderson[1], Amy E. Moritz[1], R. Benjamin Free[1], Joseph P. Steiner[3], James Inglese[2], David R. Sibley[1]

Molecular Neuropharmacology Section, NINDS/NIH[1] Assay Development and Screening Technology Laboratory, NCATS/NIH[2] Neurotherapeutics Development Unit, NINDS/NIH[3]

Abstract Text Parkinson's disease (PD) is a prevalent neurodegenerative condition characterized by degeneration of dopaminergic neurons in the substantia nigra of the midbrain. This results in bradykinesia, tremors, rigidity, and other motor and non-motor deficits. The prevalence of PD is increasing, in part, due to the aging population. Despite this growing burden, the development of effective therapies to halt disease progression remains an unmet need. This challenge is due to gaps in our understanding of the molecular mechanisms underlying the disease and deficiencies of preclinical models in recapitulating all aspects of the pathobiology of PD. Consequently, deepening our understanding of pathobiology and discovering druggable targets remain a research priority. Herein, we describe assay development and optimization of a high throughput phenotypic screen in the roundworm *Caenorhabditis elegans* for discovery of novel druggable targets and genetic influencers of neurodegeneration and neuroprotection. We utilized two transgenic *C. elegans* strains expressing human PD-linked genes—one with mutant (A53T) alpha-synuclein (SNCA) and the other expressing mutant (G2019S) leucine-rich repeat kinase 2 (LRRK2). These strains exclusively express the PD-related transgenes and green fluorescent protein (GFP) in their dopaminergic neurons, facilitating the tracking of neurodegeneration through measurable changes in the GFP fluorescence. Using laser cytometry and high content imaging with worms growing in liquid culture within 384-well plates, we assessed the health of the dopamine neurons via GFP intensity, number of neurons, and area of green objects. We observed a 30-50% and 75-85% decrease in GFP intensity in the SNCA and LRRK2 worms, respectively, by day seven compared to wild-type controls lacking the PD genes but expressing GFP exclusively in the dopaminergic neurons. We crossed the worms to RNAi hypersensitive backgrounds carrying eri-1, rrf-3, and eri-1;lin-15B mutations to overcome the typical resistance to neuronal RNAi knockdown in *C. elegans*. We observed a robust RNAi knockdown in the control and mutant worms with a 50-75% knockdown on day seven with RNAi against GFP, ama-1, ceh-43, and unc-62 compared to empty vector control. RNAi specifically engineered against the LRRK2 transgene slows neurodegeneration in the LRRK2 mutant worms. Additionally, we have identified selective LRRK2 kinase inhibitors that confer neuroprotection in the LRRK2-carrying worms with promising properties to serve as controls for high throughput molecular

library screening. Further optimization studies are ongoing with the goal of conducting a screen for genes influencing neuroprotection in these models. Additionally, we plan to conduct a small molecule library screen for novel neuroprotective compounds using these PD models. These lines of inquiry may identify new molecules or potential druggable targets for novel therapeutics for influencing neurodegeneration and PD progression.

896

Impact of RGS10 on Microglial Cell Migration and Proliferation

Shwetal Talele[1], Shelley Hooks[2], Benita Sjogren[1]

Univ of California-Irvine[1] University of Georgia[2]

Regulator of G protein signaling 10 protein (RGS10) canonically functions as a GTPase activating protein (GAP) for $G\alpha_i$ subunits of heterotrimeric G proteins. In recent years, its non-canonical functions have been explored, particularly as it relates to negative regulation of neuroinflammation originating in microglia. During chronic neuroinflammation, which characterizes aging, Alzheimer's and Parkinson's disease, microglia polarize towards a pro-inflammatory state, leading to a build-up of inflammatory factors and neurodegeneration. RGS10 is silenced during microglial activation, contributing to prolonged inflammation. Reintroduction of RGS10 in RGS10$^{-/-}$ mice reduces expression of pro-inflammatory factors and protects neurons from neurodegeneration. However, the mechanisms by which RGS10 is regulated, its role in neuroinflammation and its non-canonical functions are unknown. To understand the function of RGS10 in resting microglia, we studied the transcriptomic landscape using RNA-Sequencing in the murine microglial cell line (BV-2; WT) and CRISPR generated RGS10 knockout BV-2 cells (RGS10 KO). A total of 5 replicates of each genotype were used. We found 1580 differentially expressed genes, of which 460 genes were upregulated and 1120 genes were downregulated in RGS10 KO cells compared to the BV-2 WT cells. Functional analysis was performed using gene ontology and processes like chemotaxis, migration, synapse organization and proliferation were found to be significantly enriched. KEGG pathway analysis revealed that the differentially expressed genes were enriched in pathways such as cell adhesion, cytokine-cytokine interaction, and Rap1 signaling. Following up on migration and cell adhesion, we found 66 cell migration genes and 31 cell adhesion genes. Genes such as *Itgal, itga9, itgb7, pecam1, F11r* and *Sell* were found to be overlapping between the two processes. Gene expression for the above genes was validated using RT-qPCR. RGS10 KO cells displayed enhanced migration at both 24 and 48 hours as compared to BV-2 WT cells. RGS10 KO cells also displayed enhanced cell proliferation, another enriched process identified by the RNA-Seq data. Thus, our data shows that apart from its canonical role as a GAP for $G\alpha_i$, RGS10 is also implicated in cell migration and cell proliferation. Further studies to understand the mechanism by which RGS10 modulates migration and cell proliferation are underway, including how the role of RGS10 impacts migration and cell proliferation under an inflammatory stimulus.

897

STRUCTURE ACTIVITY RELATIONSHIP (SAR) OF GJ079 COMPOUND TO DEVELOP NOVEL TREM-1 INHIBITORS IN THE MANAGEMENT OF GLOBAL-ISCHEMIA AND RELATED NEUROINFLAMMATION

Prerna Tiwari[1], Peter Abel[1], Gopal Jadhav[1], Vanessa Caldwell[2], Hyunha Kim[1], Rachael Urquhart[1], Jee-Yeon Hwang[1]

Creighton University[1], College of Saint Mary, Omaha, Nebraska[2]

Global cerebral ischemia (GCI), induced neurodegeneration and cognitive deficits affect 200,000 Americans each year. There is an urgent need for an effective therapeutic intervention in managing brain injury associated with GCI. The triggering receptor expressed on myeloid cells-1 (TREM-1), is upregulated in the development of neuroinflammatory diseases, and its inhibition shows protection. Our GCI rat model revealed TREM1 upregulation in post-ischemic hippocampal CA1 regions. TREM1 inhibition by known peptide LR12 and novel, GJ079 demonstrated neuroprotection against ischemic insult. Thus, TREM1 inhibition can be a new therapeutic approach to treat global ischemia. We identified N^4-(amino-substituted)-N-substitued-benzenesulfonamide pharmacophore (GJ079) hit from molecular docking of 80K molecules in hTREM-1 (PDB: 1SMO) crystal structure. We verified GJ079 affinity to TREM1 by surface plasmon resonance (SPR) analysis with Kd = 14.3 uM. However, we witnessed some solubility issues with GJ079. Notably, PLT137, a *fluro*-analog of GJ079 showed ~350 folds (Kd= 4.8 nm) affinity to TREM1 and better solubility. Thus, <u>we hypothesized that *structural modifications in GJ079 molecule can develop non-toxic, bioavailable and potent TREM1 inhibitors*</u>.

Aim: (A) To design SAR of the GJ079 to develop its novel analogs as potent TREM1 inhibitors with acceptable pharmacokinetic profiles. (B) To evaluate *in vitro* pharmacological (high throughput assay, and IC$_{50}$ determination) and solubility and toxicity profiles of novel TREM1 inhibitors.

A) In our findings the *para*-fluro alteration on the Phenyl ring of R^3 in GJ079 developed PLT134, which notably improves TREM1 affinity and solubility. Thus, **GJ079 structure is amenable to chemical modification (Fig 1)**. We will use focused SAR tactics (Fig 1) to obtain ~200+ analogs. We will (i) substitute R^1 position with isosteric 5-membered heterocycles (Pink). (ii) replace *"-X-Y-"* group with the isosteric group (dotted square). We will also place fluorine (F) on a-carbon to verify if <u>keto-enol tautomerism is tolerated</u>. (iii), substitute *phenyl* (R^3) with electrophilic, and electron-deficient functions. (iv), replace bulky group (R^2) with stereo equivalent aromatic or hetroaromatic substitutions. **B)** We will employ SPR screens to quantify binding affinities (Kds) of analogs for TREM1 and eliminate non-binding analogs. We will determine toxicity assays in primary hippocampal cultures. We will employ TREM1/DAP12 promoters stably expressed in HEK293 cells with lacZ reporter gene high throughput screening (HTS) assay to determine TREM1 inhibitory potential. We will also determine IC$_{50}$ of analogs. We anticipate identifying <u>nanomole inhibitory compounds</u>. The top 2% potent analogs will be assessed for TREM1 downstream signaling in primary hippocampal cultures.

We optimized a series of chemical reactions involving multi-step chemical synthesis.
We have synthesized:
14 molecules from N-substituted benzene sulfonamide series where R^1 =thiazole,
21 molecules with substitions at N^4-amino group.
3 molecules from the third series with an aromatic substitution at R^2 position.

<u>In conclusion</u>, PLT134 has shown improved solubility as well as ~350-fold increase of affinity to TREM 1 compared to GJ079. Currently, we are developing an *in vitro* cell assay to perform HTS for hit-to-lead optimization.
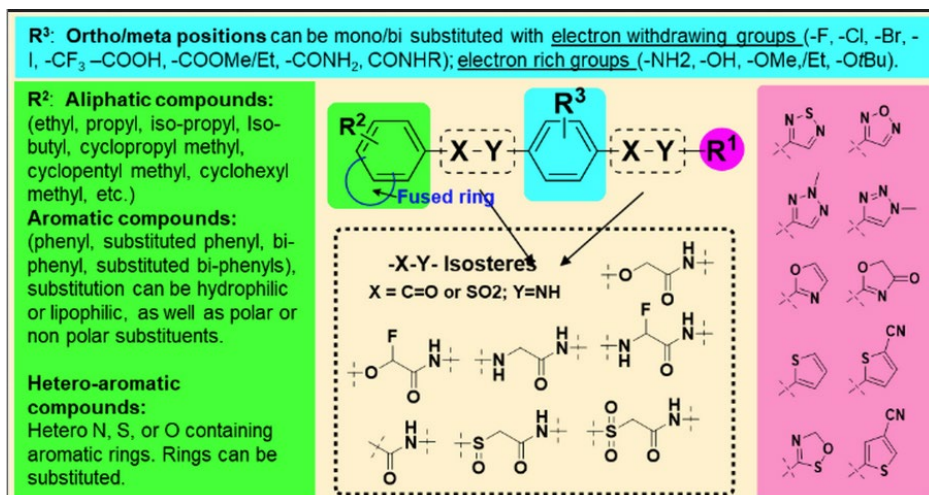
Figure 1 SAR of GJ079 hit compound.

898

Deuterated Buprenorphine Mitigates Fentanyl Effects in Pregnant Rats

Julia Tobacyk, Saki Fukuda, Brian Parks, Michael Berquist, Lisa Brents

University of Arkansas for Medical Sciences

During the 12-month period ending in April 2021, opioid-related deaths, primarily from fentanyl, reached an all-time high in the US, affecting up to 100,000 people annually. People undergoing medication-assisted treatment for **opioid use disorder (OUD)**, including pregnant women, often relapse to fentanyl use. The gold standard treatment for OUD during pregnancy is **buprenorphine (BUP)**, which improves maternal-fetal outcomes but causes **neonatal opioid withdrawal syndrome (NOWS)** in approximately 50% of newborns during their first weeks of life. We used a rat model to examine the effect of a novel drug, **deuterated buprenorphine (BUP-D2)**, on fentanyl-induced adverse effects in mothers and their neonates. We hypothesized that BUP-D2 would reduce fentanyl-related adverse effects in dams and neonates. Our preclinical model simulated the clinical scenario of fentanyl relapse while undergoing medication-assisted treatment with BUP or BUP-D2. Osmotic minipumps that continuously delivered vehicle (**veh**; 2% DMSO; 0.120 uL/day), 0.1 mg/kg/day BUP, or 0.1 mg/kg/day BUP-D2 for up to two weeks were subcutaneously implanted in pregnant Sprague-Dawley rats (dams) on gestational day **(GD)** 9. On GD 13-22, dams received daily s.c. fentanyl (100 μg/kg) or saline injections (1 mL/kg). We assessed post-injection oxygen saturation (O_2 sat.), catalepsy, and rectal temperature (temp.). Neonatal opioid withdrawal was precipitated by an i.p injection of naltrexone (**NTX**; 1 mg/kg) or saline 3-12 hours after delivery. Movement duration, a validated metric of NOWS, was determined using Noldus EthoVision XT. On GD 14, veh+fentanyl maximally induced catalepsy (i.e., to 30 sec cutoff) in all dams 15 min post-injection ($p<.0001$, vs veh+saline). Fentanyl-induced catalepsy was only partially blocked by BUP (21.25 ± 12.47, $p=.0322$), but fully blocked by BUP-D2 (10.95 ± 10.96, $p=.2046$). Veh+fentanyl decreased O_2 sat. by 28 ± 25.82% 15 min post-injection relative to pre-injection ($p= .0035$ vs veh+saline). BUP and BUP-D2 fully blocked the fentanyl-induced decrease in O_2 sat (102.0 ± 6.152 % and 100.7 ± 0.6140 % of pre-injection, respectively). Veh+fentanyl decreased temp. relative to veh+saline (35.84 ± 0.56 vs 36.58 ± 0.31 $p=.0172$) at 15 min post-fentanyl injection. Temp was not affected by BUP+ fentanyl (35.98 ± 1.15) or BUP-D2+fentanyl (36.20 ± 0.59). Lastly, NTX precipitated withdrawals in neonates that were prenatally exposed to BUP+fentanyl (females: 219.61 ± 71.54, $p=0.0229$; males: 172.72 ± 89.32, $p=0.0046$), but not neonates that were exposed to BUP-D2 + fentanyl (females: 91.46 ±59.7, $p=0.8740$; males: 102.67 ± 58.16, $p=0.9428$). This study is the first to assess effects of fentanyl combined with BUP

or BUP-D2 in pregnancy. Although BUP and BUP-D2 equally blocked fentanyl-induced respiratory depression in dams, our data suggest that BUP-D2 more effectively mitigated fentanyl-induced catalepsy and NOWS. This underscores the potential application of BUP-D2 as an improved OUD treatment during pregnancy.

899

Monensin and its derivatives increase MHC Class I and II presentations in breast cancer

Alicja Urbaniak[1], Marta Jędrzejczyk[2], Greta Klejborowska[2], Natalia Stępczyńska[2], Adam Huczyński[2], Bolni Marius Nagalo[1], Thomas Kelly[1], Alan J. Tackett[1]

University of Arkansas for Medical Sciences[1] Adam Mickiewicz University[2]

The recent approval of immune checkpoint inhibitors (ICIs) has revolutionized the treatment of metastatic breast cancer (BC). However, approximately 30% of patients remain unresponsive. The effectiveness of ICIs depends on the effective presentation of tumor-specific antigens by cancer cells. Consequently, augmenting this presentation holds the potential to enhance the efficacy of ICI treatment.
Monensin (MON), a naturally occurring ionophore antibiotic with anti-cancer properties, emerges as a promising candidate for drug repositioning. In the present study, we assessed the activity of ester and urethane derivatives of MON in cell monolayer and organoid models of both human and mouse BC. We identified several compounds with increased potency and selectivity against MDA-MB-231, MDA-MB-468, E0771, and 4T1 cell lines compared to the parent MON.

Further studies showed that both MON and its most potent derivatives increased Major Histocompatibility Complex (MHC) class I and II presentation. Additionally, these compounds significantly downregulated programmed death-ligand 1 (PD-L1) expression in BC cell lines.

The present findings suggest that MON is a potential model for new therapeutics, which can serve as single agents or be used in combination with existing ICIs for the treatment of metastatic BC.

900

Novel Mechanistic Physiologically Based Pharmacokinetic Model to Predict Renal Clearance and CYP2D6 Activity Across Pregnancy

Yue Wen, Nina Isoherranen

University of Washington

Pregnancy induces physiological changes that impact the pharmacokinetics (PK) of drugs. Interpretation and prediction of observed PK changes during pregnancy is challenging via static methods due to the interconnected dynamic alterations. For example, pregnancy results in an approximately 40% increase in cardiac output and kidney blood flow, leading to changes in renal clearance (CL$_r$) of drugs but also in distribution rates and hepatic clearance. Additionally, the increased activity of cytochrome P450 2D6

(CYP2D6) and 3A4 (CYP3A4) during pregnancy increases drug clearance resulting in altered pharmacological effects. Despite these known changes, there is a gap in systematic physiologically based pharmacokinetic (PBPK) modeling of pregnancy in simulating changes in CL_r mechanisms during pregnancy. This is important as CL_r is a major clearance pathway for may drugs used during pregnancy and urinary ratios are often used as markers of pregnancy mediated metabolic clearance changes. This study aims to comprehensively understand pregnancy-induced alterations in CL_r via PBPK modeling and to address the translation of urinary ratios of CYP2D6 substrates to quantitation of the induction of CYP2D6 activity during pregnancy.

Pregnancy-related physiological changes for the third trimester were collected from the literature. Existing literature suggests an elevation in urine pH during pregnancy and altered urine flow and water reabsorption. These changes were incorporated into a previously published mechanistic kidney model and a novel pregnancy-mechanistic kidney model was developed using Matlab Simulink. The pregnancy-mechanistic kidney model was incorporated into a full PBPK model, and a parent-metabolite PBPK model to simulate plasma concentration profiles for the selected drugs. A 100% induction in CYP2D6 activity was incorporated in the liver. The full model was validated fusing dextromethorphan (DEX) and its metabolite dextrorphan (DOR), metoprolol, clonidine, and atenolol as model drugs. These drugs were selected due to known changes in CL_r during pregnancy and CYP2D6-mediated metabolism. Drug-specific parameters were verified against observed CL_r in nonpregnant populations. Considering different physicochemical properties of the drugs such as pKa, permeability, and fraction unbound in plasma together with the model incorporated physiological changes during pregnancy, changes in CL_r and plasma concentrations-versus-time profiles were simulated.

The mechanistic kidney model was successfully developed with fold-error (predicted CL_r /observed CL_r) and absolute fold error consistently below 2 for the selected drugs for nonpregnant and pregnant populations. The observed alterations in maternal plasma concentration profiles of the model drugs and their metabolites were predicted within predefined acceptance criterion. In addition, the plasma and urinary DOR/DEX metabolic ratios were successfully simulated across pregnancy. Significant impact of altered urine pH was predicted for this metabolic ratio suggesting that changes in urine pH during pregnancy may confound use of urinary metabolic markers for assessment of liver CYP2D6 induction. The developed model provides a comprehensive approach to predicting drug disposition during pregnancy and can be applied to predict changes in CL_r for drugs that are renally cleared but have not been previously studied during pregnancy.

901

Analogs of α-conotoxin PnIC are selective for α7β2 over α7-only subtype nicotinic acetylcholine receptors

Paul Whiteaker[1], Andrew A. George[1], Sabin J. John[2], Linda M. Lucero[3], Jason B. Eaton[3], Ekta Jaiswal[3], Yiwei Cao[4], Wonpil Im[4], Joseph M. McIntosh[5]

Virginia Commonwealth University[1] University of Bath[2] Barrow Neurological Institute[3] Lehigh University[4] University of Utah[5]

Objective/Aim/Hypothesis: The objective of this work is to discover and characterize the first ligands able to identify selectively nicotinic acetylcholine receptors assembled from α7 and β2 subunits (α7β2-nAChR). Basal forebrain cholinergic neurons (BFCNs) express α7β2-nAChR. Elevated concentrations of oligomeric amyloid-β (associated with early Alzheimer's disease) appear to mediate BFCN neuronal dysfunction. Expression of α7β2-nAChR by additional important cholinergic and GABAergic neuronal circuits of the central nervous system has been observed. However, further studies are stymied by a lack of ligands that can positively identify α7β2-nAChR from the related and more widespread α7-only

homomeric nAChR subtype. This problem arises since α7-only- and α7β2-nAChR share identical agonist binding sites, located at α7/α7 subunit interfaces, that are the targets of most current ligands. We hypothesized that new α-conotoxin (α-Ctx) ligands may instead selectively inhibit α7β2-nAChR via α7/β2 subunit interfaces.

Design/Approach/Methods: Two-electrode voltage clamp (TEVC) electrophysiology was used to screen »500 novel α-Ctxs for selectivity towards α7β2- over α7-only-nAChR functionally expressed in *Xenopus* oocytes. Kinetics analysis was used to probe the subtype selectivity and mechanism of α-Ctx antagonism. Molecular dynamics (MD) simulations were used to identify amino-acid residues at putative α7/β2 subunit α-Ctx binding sites. Site-directed mutagenesis was used to probe these hypothesized sites. TEVC electrophysiology was also used to determine α-Ctx activity at non-α7 nAChR subtypes.

Results: We discovered α-CtxPnIC analogs that selectively antagonize α7β2- over α7-only-nAChR. Kinetics analysis showed that association rates were similar across α-CtxPnIC analogs, and between α7β2- and α7-only-nAChR subtypes. Slower disassociation from α7β2- *vs.* α7-only-nAChR mainly drove selectivity towards α7β2-nAChR. The α-CtxPnIC [S4R] and [L10Y] analogs were the most selective towards α7β2-nAChR (18- and 57-fold vs. α7-only-nAChR, respectively). MD identified two sets of β2 subunit residues at the putative α7/β2 subunit interface for α-CtxPnIC analogs that differed from those at the known α7/α7 subunit interface competitive agonist site. Mutating either set of β2 subunit residues to their α7 subunit equivalents partially reduced α-CtxPnIC [S4R] selectivity towards α7β2-nAChR. Activity of α-CtxPnIC analogs was generally low at non-α7-nAChR subtypes; data across analogs suggested approaches to decrease off-target affinity further.

Conclusions: We have identified the first ligands with selectivity towards α7β2-nAChR and proved a prototypical example of non-competitive antagonism by α-Ctxs. This discovery profoundly expands the scope of application of α-Ctx ligands (which have already provided important nAChR research and translational breakthroughs). Further development of α-CtxPnIC analogs will enhance α7β2-nAChR selectivity, providing opportunities for basic and translational scientific breakthroughs related to nAChR biology, Alzheimer's disease, and cholinergic contributions to cognition.

902

Pharmacologic Factors and Their Impact on Drug Elimination Half-Life

Mary Wilkerson[1], Danielle Moretti[1], Tarek Mahfouz[2], Lance Dillon[1]

Ohio Northern University[1], Ohio Northern University, Raabe College of Pharmacy[2]

The half-life of a drug is the time it takes for the amount in the body to be reduced by half and it indicates the length of time that a drug remains in the body to produce pharmacological response. Many factors determine how long the active form of a drug remains in the body with some relate to the human body (e.g. metabolizing enzymes) and others relate to the physicochemical properties of the drug itself (e.g. aqueous number of oxygens, number of nitrogens, solubility, lipophilicity …etc.). This research aims to identify what drug related variables correlate best with half-life and to develop a mathematical model with strong predictive qualities. Such a model can be used to predict the half-life of new chemical structures to facilitate the development of new, longer-lasting drugs. Chemical structures of 52 drugs belonging to five different drug classes whose experimental half-life have been reported in literature were classified based

on their pharmacological effect and their physicochemical properties were calculated. The data were fitted to different regression models to detect strong and statistically significant relations. No single physicochemical variable correlated significantly with half-life across all the drug families included in this study. However, each of the number of oxygens, the number of nitrogens, and the number of rotatable bonds correlates significantly with the half-life for two of the drug families. The opioid family had the highest number of variables that correlate strongly with half-life whereas the NSAIDs had the least.

903

Metabolism and clearance characterization of novel HBV RNase H inhibitors

Molly Woodson[1], M. Abdul Mottaleb[1], Ryan P. Murelli[2], Marvin Meyers[1], John E. Tavis[3]

Saint Louis University[1] City University of New York, Brooklyn College[2] Saint Louis University School of Medicine[3]

Hepatitis B Virus (HBV) chronically infects ~300 million people worldwide, resulting in > 880,000 deaths annually from HBV-associated liver complications. Current treatment employs a combination of nucleos(t)ide analogs and interferon-α. The NAs dominate therapy, however, in most patients, treatment cessation results in viremia recurrence, and thus lifelong treatment is required. HBV replicates by reverse transcription, which is catalyzed by the reverse transcriptase (RT) and ribonuclease H (RH) domains of the polymerase (P) protein. We have determined that the RH active site is an attractive drug target and have ~300 RH inhibitors within a growing library of >2500 experimental compounds. Inhibitors primarily belong to 3 chemotypes: The α-Hydroxytropolones (αHT), the *N*-hydroxypyridinediones (HPD), and the *N*-hydroxynapthyridinones (HNO), and while we have determined compounds within these chemotypes have sub-micromolar effective concentrations 50% (EC_{50}) with minimal toxicity in liver cell lines, we have never characterized them pharmacologically. Here we assess the metabolism and clearance parameters of the compounds with the best selectivity indexes (cytotoxicity/efficacy) in each chemotype to guide an ongoing medicinal chemistry campaign. To assess factors that affect a compound's rate of clearance, we measured the effect of plasma protein concentration on compound potency for 10 compounds in each chemotype by our established HBV replication inhibition assay with and without supplemental bovine serum albumin. We determined that the potency of 4 αHTs, 2 HPDs, and 1 HNO was significantly decreased in increased albumin levels. We next determined the half-life of 10 compounds from each chemotype by a microsome stability assay. All compounds tested with detectable analyte peaks by liquid chromatography tandem mass spectrometry had half-lives >30 min. To assess drug-drug interaction potential, 10 compounds from each chemotype were first screened at 10 µM against the 5 major CYP isoforms: 3A4, 2C19, 2C9, 1A2, and 2D6 in biochemical competitive inhibition assays and no compounds substantially inhibited any isoform (<50%). Finally, the potential to induce CYP3A4 expression was assessed for 2 compounds in each chemotype by reverse transcriptase qPCR, and we determined that CYP3A4 expression increased after incubation with both αHTs, 1 HPD, and 1 HNO at 10 µM for 72 hr. These data indicate that the most promising anti-HBV RNase H compounds have pharmacological characteristics that reflect approved drugs and inform future structure activity relationships during drug design.

904

Enhancement of ANGPTL4 exacerbates post-ischemic myocardial ferroptosis and cellular injury in diabetic conditions via impairing AKT/AMPK signaling

Weiyi Xia[1], Lin Xie[2], Zhiyi Li[2], Jiaqi Zhou[2], Jiajia Chen[2], Kaijia Han[2], Dongcheng Zhou[2], Yin Cai[1], Zhengyuan Xia[3]

Department of Health Technology and Informatics, The Hong Kong Polytechnic University[1] Department of Anesthesiology, Affiliated Hospital of Guangdong Medical University[2] Doctoral Training Platform for Research and Translation, BoShiWan, GuanChong Village, Hubei Province[3]

Background: Myocardial infarction as a result of ischemic heart disease is the primary cause of death in patients with type 2 diabetes mellitus (T2DM). Reperfusion therapy restores blood flow, but paradoxically exacerbates myocardial injury, known as ischemia/reperfusion injury (I/RI). Ferroptosis is an important type of cardiomyocyte death caused by infarction-reperfusion, especially in the later phase of reperfusion.

Research has shown that abnormal expression of the Angiopoietin-like protein 4(ANGPTL4) is associated with various pathological conditions, such as myocardial ischemia and diabetic cardiomyopathy. The role of ANGPTL4 in diabetic myocardial IRI and its potential interaction with myocardial cell ferroptosis in this pathology is unknown.

Methods: Male C57BL/6 mice were fed with a high-fat diet (HFD) for 6 weeks and received intraperitoneal injection of low dose streptozotocin to induce T2DM. In vivo diabetic myocardial I/R model was induced by occluding the left anterior descending (LAD) artery for 30 mins, followed by 2h reperfusion. Sham operations were performed by passing a silk thread under the LAD without occlusion. Infarct size was determined by using Evans blue/TTC staining, and cardiac function was determined by echocardiography. In vitro, The cardiac origin HL-1 cells were exposed to high glucose (HG) and palmitic acid (PAL) for 24 hours, followed by H/R (6 hours hypoxia followed by 12 hours reoxygenation) in the absence or presence of ANGPTL4 gene knockdown or AMPK gene overexpression.

Results: The result showed that ANGPTL4 increased significantly in the diabetic mouse myocardium after I/RI and in H/R-stimulated HL-1 cells, but cardiac levels of p-AMPK and p-AKT reduced as compared to non-diabetic control that was accompanied with reduced GPX4 protein expression and increased oxidative stress and ferroptosis. Knockdown of ANGPTL4 in HL-1 cells with ANGPTL4 siRNA significantly enhanced GPX4 protein expression, reduced ferroptosis as evidenced by reduced production of reactive substances, ferrous ion content and lipid peroxidation and attenuated H/R-induced cell injury that was concomitant enhanced protein levels of p-AMPK and p-AKT. Activation of Akt is known to protect against myocardial I/RI via inhibition of cell apoptosis, and activation of AMPK may be related to the inhibition of cell ferroptosis. Of note, overexpression of AMPK in HL-1 cells cultured under diabetic conditions with high glucose and palmitate reversed H/R induced reductions in p-Akt and GPX4, and significantly reduced post-hypoxic ferroptosis and cardiomyocyte injuries without significant impact on the increased post-hypoxic ANGPTL4 protein expression.

Conclusion: Findings of the current study are indicative that excessive enhancement of ANGPTL4 after myocardial I/RI in diabetic conditions may exacerbate post-ischemic myocardial injury via impairing P-AMPK/P-AKT signaling and that AMPK works downstream of ANGPTL4.

905

Chemical Analysis of Neuropeptide Y and Glutamate using Carbon Fiber Microelectrodes and Fast-Scan Cyclic Voltammetry

Alexander Zestos[1], Nadiah Alyamni[2], Cam Abdullaeva[1]

American University[1], Catholic University[2]

Neuropeptide Y (NPY) plays a great role and importance on feeding, satiety, obesity, and weight. Due to its complicated peptide structure, measuring this chemical quickly and achieving high biocompatibility is

difficult. Previous investigations have measured peptides by oxidizing amino acid residues like tyrosine using carbon fiber microelectrodes (CFMEs) and fast-scan cyclic voltammetry (FSCV). Here, we utilize the Modified Sawhorse Waveform (MSW) to identify Neuropeptide Y (NPY) by oxidizing tyrosine residues. The MSW enhances NPY measurement and sensitivity and selectivity by boosting efficient electron transfer kinetics compared to the triangle waveform used for dopamine detection. This method uses a holding potential of 1.2 V to achieve a limit of detection of 5 uM by etching and renewing the electrode surface, improving sensitivity and the ability to detect NPY and other monoamines simultaneously. When the MSW is applied onto CFMEs, it increases NPY selectivity over the triangle waveform, allowing for significant differentiation from other catecholamines including dopamine and serotonin. NPY was found to be adsorption controlled onto the surface of CFMEs. This sub-second and biocompatible measurement approach may improve the physiological measurement of NPY and reveal new insights. The successful identification of exogenously applied NPY in urine shows that this technology is suitable for biological studies and *in vivo* and *ex vivo* assessments. These findings demonstrate MSW's promise for quick subsecond and biocompatible NPY measurement and other larger neuropeptide assays. Through improved NPY quantification, we hope to better understand its physiological significance in vivo. Furthermore, we have also developed novel assays for the measurement of glutamate with CFMEs and FSCV. Glutamate is an important excitatory neurotransmitter and amino acid that serves as a biomarker for epilepsy and other neurological disorders. Currently, glutamate is not redox active at carbon electrode surface. We have utilized the enzyme Glutamate oxidase to modify CFMEs, which can metabolize glutamate to the redox active hydrogen peroxide. CFMEs were modified with glutamate oxidase to indirectly measure glutamate dynamics. These studies and future work will investigate the pharmacology of NPY and glutamate and will examine how certain drugs change extracellular levels of these molecules in real-time as potentially treatments for neurological disorders and states caused by the flux of these molecules.

906

SS-31 Attenuates Doxorubicin-induced Cardiomyoblast H9C2 Cell Senescence

Huiliang Zhang[1], Jiaojiao Fan[1], Shuoqiu Deng[1], Lixin Xie[1], Jinzi Wu[1], Christoph J. Mora[1], Peter S. Rabinovitch[2], Nancy Rusch[3]

University of Arkansas for Medical Sciences[1] University of Washington[2] Univ of Arkansas for Med Sci College of Med[3]

Abstract:
Background: Doxorubicin (DOX), an effective drug for many types of cancer, is associated with substantial cardiotoxicity. A 3-hour treatment of cardiomyoblast H9C2 cells with a low concentration of DOX (100 nM) can induce senescence-associated β-galactosidase (SA β-gal) staining, the gold standard of cell senescence. Here, we comprehensively characterized the phenotype of the DOX-induced senescent cardiomyocytes for the first time. We plan to use this cell model to search for effective treatments for DOX-induced cell senescence.

Methods and Results: Using SA β-gal staining and cell growth rate as readouts, we assessed the concentration-dependent effect of DOX on H9C2 cell senescence. The cells were treated with DOX for 3 hours and subsequently cultured for 3 days. We found that a 50 nM concentration of DOX induced ~ 50% SA β-gal staining and completely inhibited cell growth. The DOX-induced H9C2 cell senescence was further confirmed by several well-accepted senescence markers including cell hypertrophy, increased p16 and p21 expression, increased Senescence Associated Secretory Phenotype (SASP) markers, arrested cell cycle at S phase and G2 phase, and increased ROS production. Interestingly, we found that 50 nM DOX increased mitochondrial respiration. Translationally, we found that mitochondrial-targeted tetrapeptide SS-31 (elamipretide, 1 µM), which is in clinical trials for heart failure and other diseases associated with mitochondrial dysfunction, partially attenuated 50 nM DOX-induced SA β-gal staining from 51.4% to 35.8%. SS-31 also prevented increases of the p16, p21, and SASP markers and mitigated

mitochondrial ROS production. SS-31 also reversed the 50 nM DOX-induced elevation of mitochondrial respiration. However, 1 μM SS-31 failed to prevent the cell cycle arrest and cell growth retardation induced by 50 nM DOX.'

Conclusion: We determined that a 3-hour treatment with 50 nM DOX establishes a H9C2 cell senescence model. Treatment with mitochondrial-targeted SS-31 reverses the 50 nM DOX-induced cell senescence but not the cell cycle arrest. These data suggest that SS-31 is a promising drug to treat DOX-induced cardiomyocyte senescence.

Keywords: Doxorubicin; H9C2 cell; Senescence; Mitochondria; SS-31